

High-resolution UAS multispectral imaging for cultivar selection in grain sorghum breeding trials

by

Isaac Harrison Barnhart

B.S., Sterling College, 2017

A THESIS

submitted in partial fulfillment of the requirements for the degree

MASTER OF SCIENCE

Department of Agronomy
College of Agriculture

KANSAS STATE UNIVERSITY
Manhattan, Kansas

2020

Approved by:

Co-Major Professor
Dr. Ignacio A. Ciampitti

Approved by:

Co-Major Professor
Dr. Mithila Jugulam

Copyright

© Isaac Barnhart 2020

Abstract

As the global human population continues to increase, there is an increased responsibility on plant breeders to develop varieties with improved productivity. Current yearly yield improvement rates are not completely estimated to meet future demands, so new technologies that allow for rapid cultivar screening and selection in large-scale breeding trials are warranted. High-resolution imagery data collected with unmanned aerial systems (UAS) shows potential to greatly assist breeders. A crop that could greatly benefit from this technology is grain sorghum (*Sorghum bicolor* (L.) Moench). Grain sorghum is an important food, fuel, forage, and livestock feed source for many people across the world. In addition, it is well-suited to be grown in climates with limited precipitation, providing a means of food security for nations in such agro climatic regions. As global climate becomes increasingly warmer, more grain sorghum is predicted to be grown in areas that have traditionally grown with more water-dependent crops. To maximize productivity, sorghum not only needs to be selected for higher yielding cultivars, but also cultivars that can withstand abiotic stresses such as herbicide application and drought. Focusing on these two stresses, the objectives of this project were to: i) evaluate the effectiveness of UAS imagery in quantifying, detecting, and differentiating sorghum spectral response to herbicide, mesotrione, and ii) develop and evaluate a methodology to collect, process, extract, and compare UAS data to select for traits related to drought tolerance in grain sorghum. For the first objective, a field experiment was sown in the 2019 growing season (Ashland Bottoms, Manhattan, KS) consisting of a mesotrione tolerant and susceptible genotypes, and a commercial grain sorghum hybrid for comparison. Plots were sprayed with 0, 105, 420, and 840 g ae (acid equivalent) ha⁻¹ of mesotrione, and weekly flights were flown over the experiment up to 35 days after treatment (DAT). Ground-measured herbicide damage ratings were taken, and were

compared to vegetative indices (VIs) derived from the imagery. Results showed highly-significant relationships between VIs and ground ratings. For the second objective, an experiment with 20 commercial hybrids was planted in 2019 (Manhattan, KS). Flights were flown at the flowering (F), soft dough (SD), hard dough (HD), and physiological maturity (PM) growth stages. Ground-samples that were collected included whole plant biomass, leaf biomass, stem biomass, senescence scores, leaf area index, and final grain yield. Results showed that the near infrared (NIR) spectral band was the most significant to plant traits related to biomass, the green normalized difference vegetation index (GNDVI) was highly significant to yield, and the visible atmospheric resistant index (VARI) was the most related to both senescence at PM and senescence rates. A hierarchical clustering analysis showed that through all stages, significant differences among groups could be detected. These results suggest that multi-spectral imagery data collected via UAS could be very useful for sorghum breeders to differentiate between grain sorghum hybrids in large-scale breeding trials, particularly for breeders looking to increase herbicide tolerance in grain sorghum and to develop more drought-resistant cultivars.

Table of Contents

List of Figures	vii
List of Tables	ix
Acknowledgements	x
Dedication	xii
Chapter 1 - General Introduction	1
Grain Sorghum.....	1
Herbicide Tolerance.....	2
Post-Flowering Drought Tolerance	3
Remote Sensing for Crop Breeding	4
Thesis Objectives	6
References.....	8
Chapter 2 - Use of high resolution unmanned aerial systems imagery and machine learning to evaluate grain sorghum response to mesotrione	19
Abstract	19
Introduction.....	20
Materials and Methods.....	23
<i>Field Experiment</i>	23
<i>Image Acquisition</i>	24
<i>Image Processing</i>	25
<i>Machine Learning Classification</i>	26
<i>Ground Truth Measurements</i>	27
<i>Data Extraction</i>	27
<i>Statistical Analysis</i>	28
Results.....	28
<i>Classification Accuracy</i>	28
<i>Relation of Vegetative Indices to Ground Truth Injury</i>	29
Discussion.....	30
<i>Limitations</i>	33
Conclusions.....	35

References.....	36
Figures	43
Tables.....	48
Chapter 3 - Investigation of high-resolution UAS imagery for SG trait characterization in grain	
sorghum	52
Abstract.....	52
Introduction.....	53
Materials and Methods.....	57
<i>Field Study Information</i>	57
<i>Image Collection</i>	57
<i>Image Processing</i>	59
<i>Field Determinations</i>	60
<i>Data Processing, Extraction, and Exportation</i>	62
<i>Statistical Analysis</i>	63
Results.....	65
<i>Biomass, LAI, and yield traits</i>	65
<i>Senescence</i>	67
Discussion.....	68
<i>Limitations</i>	71
Conclusions.....	72
References.....	74
Figures	84
Tables.....	87
Chapter 4 - Conclusions and Further Direction	93
Conclusions.....	93
Further Direction.....	96

List of Figures

Figure 2.1 Location of the field trial in Manhattan, Kansas (US) evaluating 84G62, S-1, and G-2 spectral responses to mesotrione. The genotypes were planted in two rows, as denoted by the red rectangles. Plot numbers are denoted below each rectangle.....	43
Figure 2.2 View of individual plots consisting of sorghum rows and sub-plots. Sub-plots were indicated by two ground targets placed within the north end of each plot to identify the plants on which ground-truth injury ratings were taken. Sub-plot dimensions were approximately 1.5 m x 1 m. Border polygons were drawn over each sub-plot to allow for data extraction.....	44
Figure 2.3 Image collection, processing, and data extraction workflow.....	45
Figure 2.4 Methodology for vegetative indices (VI) data extraction based on the results of the image classification. (A) Original red-green-blue (RGB) sub-plot image; (B) each VI was computed from the original RGB images, creating a new raster layer for each VI; (C) RGB images were classified via supervised, pixel-based algorithms into leaves, shadows, and soil; and (D) each VI raster was combined with the classified image to create a new raster layer, allowing for VI data from only the sorghum leaves to be extracted for statistical analysis.....	46
Figure 2.5 ANOVA results for main effect models, genotype + rate. Means were separated using Tukey's HSD test at the 0.05 significance level.....	47
Figure 3.1 Overview of field study in Manhattan, Kansas. 20 sorghum genotype plots (indicated by the red boxes) were planted randomly within three blocks, indicated by the white squares.....	84
Figure 3.2 Workflow diagram of image collection, image processing, data extraction, and statistical analysis.....	85

Figure 3.3 Dendrogram produced by hierarchical clustering the mean GNDVI data for each of the genotypes, resulting in the formation of three distinct cluster groups. Hybrids are denoted by year of release..... 86

List of Tables

Table 2.1 Equations and common uses for vegetative indices used in this study.	48
Table 2.2 Overall accuracies for each algorithm on each measurement date.	49
Table 2.3 Results of the Dunn test indicating significant differences between mean overall classification accuracy percentages. No significant differences were found between the SVM-ML algorithms, but the RF algorithm was significantly less accurate than the others.	50
Table 2.4 Pearson correlation coefficients between vegetative indices and ground-measured visual injury ratings.....	51
Table 3.1 Correlation and Regression Coefficients for spectral bands and sampled biomass traits, LAI, and grain yield.	87
Table 3.2 Vegetation indices computed for biomass, LAI, and yield comparison.	88
Table 3.3 Correlation and regression coefficients for VIs and ground sampled biomass traits, LAI, and grain yield.	89
Table 3.4 Results of ANOVA and Tukey HSD test for significant differences in biomass traits, LAI, and grain yield in clusters defined by hybrid NIR spectral responses.	90
Table 3.5 RGB VIs computed for comparison with ground-measured senescence scores.	91
Table 3.6 Correlation and regression coefficients for RGB VIs and senescence scores.	92

Acknowledgements

I would like to sincerely thank Dr. Mithila Jugulam and Dr. Ignacio Ciampitti for all of their help, mentorship, and guidance in the development and execution of this project. I am incredibly thankful for the opportunity they provided for me to use UAS technology in my agronomic research. Thank you both for taking the time to invest in me and to help me grow in my career; I have sincerely enjoyed my time as a M.S. student. A special thanks also goes out to Dr. P.V. Vara Prasad for being on my committee and providing feedback to the manuscripts that we have sent him. All of this is very much appreciated.

A special thanks goes out to all of the people I have had the privilege of working with in the KSU Weed Physiology and Crop Production teams. Special thanks to Dr. Sushila Chauhaudri for taking the time to help guide me in my data analysis and for helping to put together the mesotrione summer experiment. Special thanks to Balaji Aravindhana Pandian for guiding me and introducing me to working with sorghum in the greenhouse. A special thanks to Dr. Ivan Cuvaca, Edinaldo Borgado, Chandrima Shyam, and Sathish Raj Rajendran for assisting me whenever I would have a question or need a hand with my field work. In addition, I would personally like to thank Mario Secchi for working so hard to help me get what I need in the lab, Luiz Mororosso for his help to introduce me to R and to answer my coding questions, and to Paula Demarco for working so faithfully and skillfully in order to collect samples from the field. To these kind people, and everyone else I have worked with in these labs, I would like to sincerely thank you for all of your help.

Lastly, but certainly not least, I would like to thank all the current and former members of the Kansas State Polytechnic UAS lab for being so knowledgeable, dedicated, and willing to help

with all things UAS related. Specifically Trevor Witt, Travis Balthazor, and Spencer Schrader for each of their assistance in my research endeavors.

Dedication

“And we know that all things work together for good to those who love God, to those who are called according to His purpose.” ~ Romans 8:28.

This thesis is dedicated first and foremost to God, who has truly been with me throughout this entire process. The time between leaving my Doctor of Physical Therapy program and beginning my agronomy graduate program was the hardest time I have ever been through, but He was with me the entire way.

This thesis also dedicated to my father, Dr. Richard Kurt Barnhart, former department head of KSU Aviation and who led the charge in beginning the KSU UAS program. Without his valiant efforts to begin this program, I would likely not have taken an interest in UAS. Your ingenuity and innovation has always inspired me, and to that, I say thank you. It is also dedicated to my mother, who has been my number one fan and supporter throughout my entire life, and to my sister, who I love very much.

I would also like to dedicate this to a professor at my undergraduate institution, Dr. Jonathan Conard, who convinced me to double-major in Biology. Without this degree, it would not have been possible to get a M.S. in agronomy. He has done so much for not only myself, but for every other student to ever have taken his courses. I hope this serves as a small token of my gratitude for all you’ve done.

Finally, I would like to dedicate this to my soon-to-be wife (two more weeks at the time of this writing!!), Claire. Thank you for taking such an interest in this project, and doing your absolute best to support it. I greatly look forward to our life together, and for all the adventures that we will share. I love you!

Chapter 1 - General Introduction

Grain Sorghum

Grain sorghum [*Sorghum bicolor* (L.) Moench] is a resilient C4 cereal crop that can yield well in environments where other crops may fail [1-2]. Originating from the sub-Saharan African region, it is a major food source for people within the region, but is traditionally used in the United States for animal feed, forage, and biofuel production [3, 6-7]. Sorghum is the fifth most produced grain crop in the world, trailing behind production of maize (*Zea mays*), rice (*Oryza sativa* L.), wheat (*Triticum aestivum*), and barley (*Hordeum vulgare*) [3-5]. Sorghum is well-adapted to precipitation-limited environments, and has been documented to produce grain with as little as 350-700 mm of annual rainfall [4, 8]. Because of this, grain sorghum is frequently grown in semi-arid environments [1, 9]; it has even been shown to have a distinct yield advantage in these environments [10].

As a whole, 80% of the human diet is plant-based, with cereal crops making up half of this percentage [11]. Crop production will have to be doubled in order to meet the projected global food demands in 2050 [12-14, 61-65], therefore, intensification of agriculture is projected as the end goal of many crop breeding programs throughout the world. Increasing in crop productivity can be achieved by developing crop varieties resilient to various environmental conditions including biotic and abiotic stresses via transferring stress-tolerant traits. As most crops encounter some form of yield-limiting biotic or abiotic stressors during their life cycles (such as heat stress, drought stress, nutrient stress, light competition, and saline soils) [16], breeding for stress tolerance becomes of the utmost importance for future crop intensification. For grain sorghum, the International Crops Research Institute for the Semi-Arid Tropics (ICRISAT) has placed a priority on breeding for a wide adaptability to biotic and abiotic stresses

[17] in order to increase crop yields in stressful environments. Although there are many stressors challenging sorghum production being addressed by breeders, this discussion will focus on sorghum tolerance to two specific abiotic stresses, i.e., herbicide and post-flowering drought.

Herbicide Tolerance

Weeds are considered to be one of the main biotic pestilences in crop production [18], because of how well they can compete with crops for water, nutrients, and solar radiation, etc. [19]. Managing weeds in grain sorghum continues to be a major problem for growers across the globe; for example, a recent survey in the United States determined that controlling weeds, especially post-emergence, was the top concern among growers [20]. Depending on the severity of infestation, sorghum yield losses due to weeds can be as high as 85%, [19, 21], which can tremendously reduce profitability for these cropping systems [22-23]. Common tactics to manage weeds include mechanical and cultural techniques such as reducing row spacing [24], increasing higher planting populations [24], inter-row cultivation [25], and tillage [26]. However, the use of herbicides is the most widely followed practice for weed control, especially with the increased adoption of no-till planting practices [27-29].

At early growth stages, sorghum does not compete well with weeds [30]. Effective weed control is therefore essential to avoid costly yield losses. However, weed control is further complicated in grain sorghum due to the limited number of herbicides available for use, as well as the rising number of resistant weed species to these herbicides [20, 31]. The majority of herbicide programs used in grain sorghum involve mostly pre-emergence (PRE) herbicides, as post-emergence (POST) options are limited [20, 30, 38]. Many POST herbicides currently labeled for use can cause crop injury, therefore leaving sorghum susceptible to damage from

other abiotic and biotic forces as well [28, 32-33]. Because of the relatively small acres of sorghum produced relative to other crops, lack of profit opportunities for chemical companies, and concerns of resistant gene transfers to close relatives such as Johnson grass (*Sorghum halepense*) and shattercane (*Sorghum bicolor*), herbicide-tolerant technology development for grain sorghum will continue to be slow [20]. This limitation can lead to overreliance on an already limited number of herbicides, which in turn can contribute to evolution of ever-increasing number of resistant weeds [34].

One method that has been proposed to increase herbicide options for growers involves selectively breeding for herbicide-tolerant traits [35-36]. This can be achieved by screening a wide collection of germplasm for herbicide tolerance, primarily for POST applications [35]. There are many benefits to such breeding programs. If new genotypes with elevated tolerance to herbicides compared to commercial hybrids are identified, these traits could eventually be transferred to agronomically-desirable germplasms to develop new hybrids. This could reduce the risk of yield losses by providing POST weed control and reducing crop injury [37] and provide more herbicide options for growers [35, 37]. Additionally, the risks of crop damage due to residual herbicide persistence could also be significantly reduced [36].

Post-Flowering Drought Tolerance

Since sorghum is usually the crop of choice where precipitation is limited; and because it is well-adapted to arid environments [39-40], it is an important food source for over 100 million people in Africa [60]. One of the reasons for this wide adaptation to such environments is that many sorghum genotypes have a characterized form of post-flowering drought stress known as the stay green (SG) trait [41-43]. Post-flowering drought stress, also known as “terminal

drought,” is detrimental and can cause severe yield losses in grain sorghum through inducing premature plant senescence [44-45]. However, sorghum genotypes with the SG trait continue grain filling under these stress conditions, and also have been observed to resist other factors affecting sorghum during moisture stress including lodging and various types of stem rot [46-51]. The SG trait extends green leaf functionality further into the latter growth stages, keeping the plant alive to continue the uptake of water and nutrients for grain filling [52]. Further, the SG trait not only also helps resist drought conditions, but also shows no yield penalties (compared to non-SG counterparts) when grown where excess rainfall is plentiful [53-54].

Since the 1970s, SG has become a major marketed feature in many commercial crops [55]. Because of such agronomic importance, many sorghum breeders continue to intensively select for this trait in breeding trials [43, 56]. To evaluate this trait, breeders typically irrigate the genotypes of interest until flowering, and then allow for moisture stress at post-flowering stages [43, 57]. Plants will then be evaluated for greenness retention, traditionally using various visual leaf scoring systems [57-59]. Certain crops such as maize and rice have been subjected to this SG breeding for more than 100 years, and have thus reached a point where no more SG improvements can be made with crop breeding [55]. However, sorghum has yet to reach this point [55], and as there are still more strides to be made in this realm, it can be assumed that SG breeding operations will continue for a foreseeable future.

Remote Sensing for Crop Breeding

Plant breeding is vital to maintain food security and adaption to changes to environmental factors [77]. As stated previously, current crop production must be doubled to meet projected demand by 2050. This means that crop yields must increase approximately 2.4% each year, but

current increases in crop production are only at 1.3% per year [61]. This poses a significant challenge to crop breeders. In order to meet these future needs, an increase in breeding efficiency, especially in terms of crop resilience to stress, is warranted [61]. Such traits controlling stress adaptation, plant growth, and yield are complex and controlled by many genes [66-68], adding to the challenges of phenotyping in breeding trials. As field-based phenotyping is crucial to improve crop genetics, breeders are sometimes tasked with phenotyping thousands of plots, despite traditional manual sampling methods being time-consuming, labor-intensive, and sometimes inaccurate [61, 63, 69-72]. Because of this, new methods are needed to enable plant breeders to rapidly phenotype large numbers of plots, which would help to identify the best progenies for a given breeding program.

Recently, plant breeders have begun to use remote sensing for phenotyping purpose. Remote sensing is defined as the process of detecting characteristics of an area by measuring its reflected and emitted radiation [73], and is frequently used to quantify changes in vegetation [74]. The driving factor that makes this possible is that photosynthetically active vegetation reflects near infrared radiation (NIR) light, whereas vegetation that is stressed reflects more visible radiation (especially the red region) [62, 66, 75]. This spectral reflectance information can then be used to compute vegetation indices, equations or ratios between any given electromagnetic reflectance regions, that have been shown to be related to vegetation parameters such as (but not limited to) plant biomass, canopy cover, final grain yields, and leaf area index [63, 66, 70, 76]. Platforms that have been used include autonomous ground vehicles, field scanning towers, piloted aircraft, blimps, unmanned aerial systems (UAS), and satellites [62-63, 80]. However, UAS are the platform of choice for crop breeding, as they have the ability to collect high spatial resolution imagery at relatively low operating costs [61-63, 69, 72, 77-78].

UAS and high-resolution aerial imaging have revolutionized crop phenotyping, as hundreds to thousands of plots are able to be photographed in a short time [65, 81]. This rapid and non-destructive method of extracting phenotypic information from breeding plots has helped greatly to improve the efficiency of crop breeding [63, 79]. As a whole, UAS are very versatile in the types of payload they can carry; these range from cost-effective red-green-blue (RGB) cameras, NIR cameras, thermal sensors, hyperspectral sensors, and Light Detection and Ranging (LiDAR) sensors [69, 76, 82]. Of these, most breeders have found that RGB and NIR cameras to have the most value, as they are relatively cost-effective and allow for rapid and effective assessment of breeding plots [62]. After radiometric calibration to convert camera digital numbers to reflectance values [63, 83], images collected from the UAS camera are combined to form an orthomosaic image, and can be exported to various GIS software for analysis. In most cases, areas of interest (plots) are defined, and vegetation is extracted from background noise using binary thresholding [84-85] or machine learning algorithms such as support vector machines, random forest, or maximum likelihood classification [83, 86-90]. Information can then be extracted and sent for further analysis.

Thesis Objectives

In grain sorghum breeding, UAS imagery has been shown useful for quantifying plant tillers and grain head numbers [91-92], determining leaf numbers and plant locations [93], plant height [94-95], biomass accumulation [96-98] and cold tolerance [99]. Although there is some information on the use of UAS to monitor herbicide tolerance and SG breeding in sorghum, there is much that can be contributed and improved on in these fields. In SG breeding trials, it has been determined that using UAS and vegetative indices such as the normalized difference red edge

(NDRE) index may be effective for monitoring sorghum senescence patterns [100], as significant differences between NDRE scores of SG and non-SG genotypes have been detected [101]. As these studies mainly evaluated the spectral change of the NDRE index over time, there is still more to be learned in terms of the relationship of UAS-derived data to traditional visual senescence scoring techniques. Numerous studies have been conducted using remote sensing platforms to detect herbicide injury (i.e. from drift) [102-104], but few have focused exclusively on identifying herbicide-tolerant genotypes in large-scale breeding operations.

The overall objective of this thesis was to evaluate the use of UAS as a tool to aid sorghum breeders in identification of herbicide tolerant and drought-resistant (SG) genotypes of grain sorghum in large-scale breeding trials. Thus, specific objectives of Chapter 2 and 3 of this thesis were:

Chapter 2:

- Develop and elaborate a methodology for sorghum breeders to extract and process data using user-friendly computer programs (Agisoft Metashape and ArcGIS Pro) to aid in speed of data processing.
- Test the methodology in a small-scale study evaluating sorghum tolerance to herbicide, mesotrione, with activity on broad spectrum of weeds.

Chapter 3:

- Develop a methodology for UAS data processing and extraction for SG trait evaluation using Agisoft Metashape and ArcGIS Pro.
- Investigate the relationship between various UAS-derived vegetative indices and ground-truth visual senescence measurements, biomass traits, and final grain yield.

References

1. Prasad, P.V.V.; Pisipati, S.R.; Mutava, R.N.; Tuinstra, M.R. Sensitivity of grain sorghum to high temperature stress during reproductive development. *Crop Sci.* **2015**, *48*, 1911-1917. doi: 10.2135/cropsci2008.01.0036
2. Ciampitti, I.A., Prasad, P.V.V., editors. *Sorghum: A State of the Art and Future Perspectives*. American Society of Agronomy, Wisconsin, United States. American Society of Agronomy, **2019**, volume 58.
3. Stefoska-Needham, A.; Beck, E.J.; Johnson, S.K.; Tapsell, L.S. Sorghum: An Underutilized cereal whole grain with the potential to assist in the prevention of chronic disease. *Food Rev. Int.* **2015**, *31*, 401-437. doi: 10.1080/87559129.2015.1022832
4. Mundia, C.W.; Secci, S.; Akamani, K.; Wang, G. A Regional comparison of factors affecting global sorghum production: the case of North America, Asia, and Africa's Sahel. *Sustainability* **2019**, *11*, 2135-2153. doi: 10.3390/su11072135
5. Zheng, L.; Guo, X.; He, B.; Sun, L.; Peng, Y.; Dong, S.; Liu, T.; Jiang, S.; Ramachandran, S.; Liu, C.; Jing, H. Genome-wide patterns of genetic variation in sweet and grain sorghum (*Sorghum bicolor*). *Genome Biol.* **2011**, *12*, R114. doi: 10.1186/gb-2011-12-11-r114
6. Rooney, L.W.; Awika, J.M. Overview of products and health benefits of specialty sorghums. *Cereal Food World* **2005**, *50*, 114-115.
7. Taylor, J.R.N.; Schober, T.J.; Bean, S.R. Novel food and non-food uses for sorghum and millets. *J. Cereal Sci.* **2006**, *44*, 252-271. doi: 10.1016/j.jcs.2006.06.009
8. Food Security Department. *Sorghum: Sorghum Post-harvest Operations*. In: Meija D, Lewis B, eds. INPhO-Post-Harvest Compendium, Natural Resources Institution, University of Greenwich: London, United Kingdom. **1999**. Available: <http://www.fao.org/3/a-ax443e.pdf>
9. Beheshti, A.R.; Behboodi fard, B. Dry matter accumulation and remobilization in grain sorghum genotypes (*Sorghum bicolor* L. Moench) under drought stress. *Aust. J. Crop Sci.* **2010**, *4*, 185-189.

10. Staggenborg, S.; Dhuyvetter, K.C.; Gordon, W.B. Grain sorghum and corn comparisons: yield, economic, and environmental responses. *Agron. J.* **2008**, 100, 1600-1604. doi: 10.2134/agronj2008.0129
11. Langridge, P.; Fleury, D. Making the most of 'omics' for crop breeding. *Trends Biotechnol.* **2010**, 29, 33-40. doi: 10.1016/j.tibtech.2010.09.006
12. Ortez-Amador, O.A. Study off Nitrogen Limitation and Seed Nitrogen Sources for Historical and Modern Genotypes in Soybean. M.Sc. Thesis, Kansas State University, Manhattan, Kansas, United States, **2018**. Available from: <https://krex.k-state.edu/dspace/handle/2097/38812>
13. Araus, J.L.; Cairns, J.E. Field high-throughput phenotyping: the new crop breeding frontier. *Trends Plant Sci.* **2014**, 19, 52-61. doi: 10.1016/j.tplants.2013.09.008
14. Tilman, D.; Balzer, C.; Hill, J.; Befort, B.L. Global food demand and the sustainable intensification of agriculture. *Proc. Natl. Acad. Sci. USA* **2011**, 108, 20260-20264. doi: 10.1073/pnas.1116437108
15. Rebetzke, G.J.; Condon, A.G.; Richards, R.A.; Farquhar, G.D. Selection for reduced carbon isotope discrimination increases aerial biomass and grain yield of rainfed bread wheat. *Crop Sci.* **2002**, 42, 739-745. doi: 10.2135/cropsci2002.0739
16. Pessarakli, M. *Handbook of Plant and Crop Physiology*, 2nd ed.; Marcel Dekker, Inc., New York, New York, United States, **2001**.
17. Reddy, B.V.S.; Ramesh, S.; Reddy, P.S. Sorghum breeding research at ICRISAT – goals, strategies, methods and accomplishments. *International Sorghum and millets Newsletter* **2004**, 45, 5-12.
18. Benaragama, D.I.; Shirliffe, S.J.; Johnson, E.N.; Duddu, H.S.; Syrovy, L.D. Does yield loss due to weed competition differ between organic and conventional cropping systems? *Weed Res.* **2016**, 56, 274-283. doi: 10.1111/wre.12213
19. Limon-Ortega, A.; Mason, S.C.; Martin, A.R. Production practices improve grain sorghum and pearl millet competitiveness with weeds. *Agron. J.* **1998**, 90, 227-232. doi: 10.2134/agronj1998.00021962009000020020x
20. Thompson, C.R.; Dille, J.A.; Peterson, D.E. Weed Competition and Management in Sorghum. In *Sorghum: A State of the Art and Future Perspectives*; Ciampitti, I.A., Prasad,

- P.V.V., eds.; American Society of Agronomy, Wisconsin, United States, 2019, Volume 58.
21. Okafor, L.I.; Zitta, C. The influence of nitrogen on sorghum weed competition in the tropics. *Trop. Pest Manage.* **1991**, *37*, 138-143. doi: 10.1080/09670879109371561
 22. Left uncontrolled, weeds would cost billions in economic losses every year. Available online: <https://www.ksre.k-state.edu/news/stories/2016/05/uncontrolled-weeds051216.html> (accessed on 1 May 2020).
 23. Dille JA, Stahlman PW, Thompson CR, Bean BW, Soltani N, Sikkema PH. Potential yield loss in grain sorghum (*Sorghum bicolor*) with weed interference in the United States. *Weed Technol.* **2020**. doi: 10.1017/wet.2020.12
 24. Grichar, W.J.; Besler, B.A.; Brewer, K.D. Effect of row spacing and herbicide dose on weed control and grain sorghum yield. *Crop Prot.* **2004**, *23*, 263-267. doi: 10.1016/j.cropro.2003.08.004
 25. Phillips, L.J.; Norman, M.J.T. The influence of inter-row and intra-row cultivation on the yield of grain sorghum at Katherine, N.T. *Aust. J. Exp. Agric.* **1962**, *2*, 204-208. doi: 10.1071/EA9620204
 26. Dickey, E.C.; Jasa, P.J.; Grisso, R.D. Long term tillage effects on grain yield and soil properties in a soybean/grain sorghum rotation. *J. Prod. Agric.* **1994**, *7*, 465-470. doi: 10.2134/jpa1994.0465
 27. Brown, D.W.; Al-Khatip, K.; Stahlman, P.W.; Loughin, T.M. Safening of metsulfuron grain sorghum injury with growth regulator herbicides. *Weed Sci.* **2004**, *52*, 319-325. doi: 10.1614/P2002-074
 28. Abit, M.J.M.; Al-Khatib, K. Absorption, translocation, and metabolism of mesotrione in grain sorghum. *Weed Sci.* **2009**, *57*, 563-566. doi: 10.1614/WS-09-041.1
 29. Sala, C.A.; Buelos, M.; Altieri, E.; Ramos, M.L. Genetics and breeding of herbicide tolerance in sunflower. *Helia* **2012**, *35*, 57-70. doi: 10.2298/HEL1257057S
 30. Besançon, T.E.; Riar, R.; Heinigen, R.W.; Weisz, R.; Everman, W.J. Weed control and crop tolerance with pyrasulfotole plus bromoxynil combinations in grain sorghum. *Int. J. Agron. Crop. Sci.* **2016**, *1*, 14-27.

31. Fromme, D.D.; Dotray, P.A.; Grichar, W.J.; Fernandez, C.J. Weed control and grain sorghum (*Sorghum bicolor*) tolerance to pyrasulfotole plus bromoxynil. *Intern. J. Agron.* **2012**, 2. doi: 10.1155/2012/951454
32. Abit, M.J.M.; Al-Khatib, K.; Regher, D.L.; Tuinstra, M.R.; Claassen, M.M.; Geier, P.W.; Stahlman, P.W.; Gordon, B.W.; Currie, R.S. Differential response of sorghum hybrids to foliar applied mesotrione. *Weed Technol.* **2009**, 23, 28-33. doi: 10.1614/WT-08-086.1
33. Horkey, K.T.; Martin, A.R. Evaluation of preemergence weed control programs in grain sorghum. Lincoln, NE: **2005** NCWSS Research Report-V.62, pp. 30-32. Available from: http://ncwss.org/proceed/2005/ResRep05/table_contents.html
34. Sutton, P.; Richards, C.; Buren, L.; Glasgow, L. Activity of mesotrione on resistant weeds in maize. *Pest Manag Sci.* **2002**, 58, 981-984. doi: 10.1002/ps.554
35. Leon, R.G.; Tillman, B.L. Postemergence herbicide tolerance variation in peanut germplasm. *Weed Sci.* **2015**, 63, 546-554. doi: 10.1614/WS-D-14-00128.1
36. Hartwig, E.E. Identification and utilization of variation in herbicide tolerance in soybean (*Glycine max*) breeding. *Weed Sci.* **1987**, 35, 4-8.
37. Harrison, H.F. Developing herbicide-tolerant crop cultivars: introduction. *Weed Sci.* **1992**, 6, 613-614. doi: 10.1017/S0890037X00035909
38. Regehr, D. Weed Control. In *Grain Sorghum Production Handbook*; Kansas State University Agricultural Experiment Station and Cooperative Extension Service, Manhattan, Kansas, United States, **1998**, pp. 10-11.
39. Jordan, D.R.; Hunt, C.H.; Cruickshank, A.W.; Borrell, A.K.; Henzell, R.G. The relationship between the stay-green trait and grain yield in elite sorghum hybrids grown in a range of environments. *Crop Sci.* **2012**, 52, 1153-1161. doi: 10.2135/cropsci2011.06.0326
40. Haussman, B.I.G.; Obilana, A.B.; Ayiecho, P.O.; Blum, A.; Schipprack, W.; Geiger, H.H. Yield and yield stability of four population types of grain sorghum in a semi-arid area of Kenya. *Crop Sci.* **2000**, 40, 319-329
41. Sanchez, A.C.; Subudhi, P.K.; Rosenow, D.T.; Nguyen, H.T. Mapping QTLs associated with drought resistance in sorghum (*Sorghum bicolor* L. Moench). *Plant Mol Biol.* **2002**, 48, 713-726. doi: 10.1023/a:1014894130270

42. Rosenow, D.T.; Quisenberry, J.E.; Wendt, C.W.; Clark, L.E. Drought tolerant sorghum and cotton germplasm. *Agr. Water Manage.* **1983**, 7, 207-222. doi: 10.1016/0378-3774(83)90084-7
43. Xu, W.; Rosenow, D.T.; Nguyen, H.T. Stay green trait in grain sorghum: relationship between visual rating and leaf chlorophyll concentration. *Plant Breeding* **2000**, 119, 365-367. doi: 10.1046/j.1439-0523.2000.00506.x
44. Yadav, R.S.; Hash, C.T.; Bidinger, F.R.; Devos, K.M.; Howarth, C.J. Genomic regions associated with grain yield and aspects of post-flowering drought tolerance in pearl millet across stress environments and tester background. *Euphytica* **2004**, 136, 265-277. doi: 10.1023/b:euph.0000032711.34599.3a
45. Kebede, H.; Subudhi, P.K.; Rosenow, D.T.; Nguyen, H.T. Quantitative trait loci influencing drought tolerance in grain sorghum (*Sorghum bicolor* L. Moench). *Theor. Appl. Genet.* **2001**, 103, 266-276. doi: 10.1007/s001220100541
46. Sanchez, A.C.; Subudhi, P.K.; Rosenow, D.T.; Nguyen, H.T. Mapping QTLs associated with drought resistance in sorghum (*Sorghum bicolor* L. Moench). *Plant Mol Biol.* **2002**, 48, 713-726. doi: 10.1023/a:1014894130270
47. Rosenow, D.T. Breeding sorghum for drought resistance. In: *Food Grain Production in Semi Arid Africa*. Menyoga, J.M., Bezuneh, T., Youdeowei, A., eds.; OAU-STRC/SAFGRAD, Ouagadougou, Burkina Faso; **1987**. pp 83-89.
48. Evangelista, C.C.; Tangonan, N.G. Reaction of 31 non-senescent sorghum genotypes to stalk rot complex in southern Philippines. *Trop Pest Manage.* **1990**, 36, 214-215. doi: 10.1080/09670879009371474
49. Subudhi, P.K.; Rosenow, D.T.; Nguyen, H.T. Quantitative trait loci for the stay green trait in sorghum (*Sorghum bicolor* L. Moench): consistency across genetic backgrounds and environments. *Theor. Appl. Genet.* **2000**, 101, 733-741. doi: 10.1007/s001220051538
50. Joshi, A.K.; Kumari, M.; Singh, V.P.; Reddy, C.M.; Kumar, S.; Rane, J.; Chand, R. Stay green trait: Variation, inheritance and its association with spot blotch resistance in spring wheat (*Triticum aestivum* L.). *Euphytica* **2006**, 153, 59-71. doi: 10.1007/s10681-006-9235-z

51. Reddy, P.S.; Patil, J.V. Genetic Enhancement of Rabi Sorghum: Adapting the Indian Durras. 1st ed. Elsevier Inc.; **2015**. doi: 10.1016/C2014-0-01532-8
52. Van Oosterom, E.J.; Jayachandran, R.; Bidinger, F.R. Diallel analysis of the stay-green trait and its components in sorghum. *Crop Sci.* **1996**, 6, 549-555. doi: 10.2135/cropsci1996.0011183X003600030002x
53. Harris, K.; Subudhi, P.K.; Borrell, A.; Jordan, D.; Rosenow, D.; Nguyen, H.; Klein, P.; Klein, R.; Mullet, J. Sorghum stay-green QTL individually reduce post-flowering drought-induced leaf senescence. *J. Exp. Bot.* **2007**, 58, 327-338. doi: 10.1093/jxb/erl225
54. Borrell, A.K.; Hammer, G.L.; Henzell, R.G. Does maintaining green leaf area in sorghum improve yield under drought? II. Dry matter production and yield. *Crop Sci.* **2000**, 40, 1037-1056. doi: 10.2135/cropsci2000.4041037x
55. Thomas, H.; Ougham, H. The stay-green trait. *J. Exp. Bot.* **2014**, 5, 3889-3900. doi: 10.1093/jxb/eru037
56. Duvick, D.N.; Smith, J.C.; Cooper, M. Long-Term Selection in a Commercial Hybrid Maize Breeding Program. In *Plant Breeding Reviews: Part 2: Long-term Selection: Crops, Animals, and Bacteria*. Janick, J., ed.; John Wiley & Sons, Inc., Volume 24, **2003**. doi: 10.1002/9780470650288.ch4
57. Reddy, B.V.S.; Ramaiah, B.; Kumar, A.A.; Reddy, P.S. Evaluation of sorghum genotypes for the stay-green trait and grain yield. *SAT eJournal – ICRISAT Open Access Journal* **2007**, 3. Available from: <http://citeseerx.ist.psu.edu/viewdoc/download?doi=10.1.1.496.5943&rep=rep1&type=pdf>
58. Bogard, M.; Jourdan, M.; Allard, V.; Martre, P.; Perretant, M.R.; Ravel, C.; Heumez, E.; Orford, S.; Snape, J.; Griffiths, S.; Gaju, O.; Foulkes, J.; Le Gouis, J. Anthesis date mainly explained correlations between post-anthesis leaf senescence, grain yield, and grain protein concentration in a winter wheat population segregating for flowering time QTLs. *J. Exp. Bot.* **2011**, 62, 3621-3636. doi: 10.1093/jxb/err061
59. Wanous, M.K.; Miller, F.R.; Rosenow, D.T. Evaluation of visual rating scales for green leaf retention in sorghum. *Crop Sci.* **1991**, 31, 1691-1694. doi: 10.2135/cropsci1991.0011183X003100060063x

60. Gebretsadik, R.; Shimelis, H.; Laing, M.D.; Tongoona, P.; Mandefro, N. A diagnostic appraisal of the sorghum farming system and breeding priorities in *Striga* infested agro-ecologies of Ethiopia. *Agric. Syst.* **2014**, *123*, 54-61. doi: 10.1016/j.agry.2013.08.008
61. Araus, J.L.; Cairns, J.E. Field high-throughput phenotyping: the new crop breeding frontier. *Trends Plant Sci.* **2014**, *19*, 52-61. doi: 10.1016/j.tplants.2013.09.008
62. Shakoor, N.; Lee, S.; Mockler, T.C. High throughput phenotyping to accelerate crop breeding and monitoring of diseases in the field. *Curr. Opin. Plant Bio.* **2017**, *38*, 184-192. doi: 10.1016/j.pbi.2017.05.006
63. Yang, G.; Liu, J.; Zhao, C.; Li, Z.; Huang, Y.; Yu, H.; Xu, B.; Yang, X.; Zhu, D.; Zhang, X.; Zhang, R.; Feng, H.; Zhao, X.; Li, Z.; Li, H.; Yang, H. Unmanned aerial vehicle remote sensing for field-based crop phenotyping: Current status and perspectives. *Front. Plant Sci.* **2017**, *8*. doi: 10.3389/fpls.2017.01111
64. Ray, D.K.; Mueller, N.D.; West, P.C.; Foley, J.A. Yield trends are insufficient to double global crop production by 2050. *PLoS ONE* **2013**, *8*, e66428. doi: 10.1371/journal.pone.0066428
65. Reynolds, M.; Langridge, P.; Physiological breeding. *Curr. Opin. Plant Bio.* **2016**, *31*, 162-171. doi: 10.1016/j.pbi.2016.04.005
66. Cabrera-Bosquet, L.; Crossa, J.; Von Zitzewitz, J.; Serret, M.D.; Araus, J.L. High-throughput phenotyping and genomic selection: the frontiers of crop breeding Converge. *J. Integr. Plant Biol.* **2012**, *54*, 312-320. doi: 10.1111/j.1744-7909.2012.01116.x
67. Li, Z.; Pinson, S.R.; Park, W.D.; Paterson, A.H.; Stansel, J.W. Epistasis for three grain yield components in rice (*Oryza sativa* L.). *Genetics* **1997**, *145*, 453-465.
68. Li, Z.K.; Luo, L.J.; Mei, W.H.; Wang, D.L.; Shu, Q.Y.; Tabien, R.; Zhong, D.B.; Ying, C.S.; Stansel, J.W.; Khush, G.S.; Paterson, A.H. Overdominant epistatic loci are the primary genetic basis of inbreeding depression and heterosis in rice. I. Biomass and grain yield. *Genetics* **2001**, *158*, 1737-1753.
69. Berni, J.A.J.; Zarco-Tejada, P.J.; Suarez, L.; Fereres, E. Thermal and narrowband multispectral remote sensing for vegetation monitoring from an unmanned aerial vehicle. *IEEE Trans. Geosci. Remote Sens.* **2009**, *47*, 722-738. doi: 10.1109/tgrs.2008.2010457

70. Rahaman, M.M.; Chen, D.J.; Gillani, Z.; Klukas, C.; Chen, M. Advanced phenotyping and phenotype data analysis for the study of plant growth and development. *Front. Plant Sci.* **2015**, *6*. doi: 10.3389/fpls.2015.00619
71. Li, W.; Niu, Z.; Chen, H.Y.; Li, D.; Wu, M.Q.; Zhao, W. Remote estimation of canopy height and aboveground biomass of maize using high-resolution stereo images from a low-cost unmanned aerial vehicle system. *Ecol. Indic.* **2016**, *67*, 637-648. doi: 10.1016/j.ecolind.2016.03.036
72. Tattaris, M.; Reynolds, M.P.; Chapman, S.C. A Direct Comparison of remote sensing approaches for high-throughput phenotyping in plant breeding. *Front. Plant Sci.* **2016**, *7*. doi: 10.3389/fpls.2016.01131
73. United States Geological Survey. What is remote sensing and what is it used for? Available online: https://www.usgs.gov/faqs/what-remote-sensing-and-what-it-used?qt-news_science_products=0#qt-news_science_products (accessed 6 May 2020)
74. Jones, H.G.; Vaughn, R.A. Remote Sensing of Vegetation: Principles, Techniques, and Applications. Oxford, NY: Oxford University Press; **2020**.
75. Karlovska, A.; Grīnfeldē, I.; Alsīņa, I.; Priedītis, G.; Rose, D. Plant Reflected Spectral Depending on Biological Characteristics and Growth Conditions. In Proceedings of the 7th International Scientific Conference Rural Development, Aleksandras Stulginskis University, Lithuania, 19-20 Nov. **2015**. doi: 10.15544/RD.2015.045
76. Zhang, C.; Kovacs, J.M. The application of small unmanned aerial systems for precision agriculture: A review. *Precis. Agric.* **2012**, *13*, 693-712. doi: 10.1007/s11119-012-9274-5
77. Chapman, S.C.; Merz, T.; Chan, A.; Jackway, P.; Hrabar, S.; Dreccer, M.F. Phenocopter: a low-altitude, autonomous remote-sensing robotic helicopter for high-throughput field-based phenotyping. *Agronomy* **2014**, *4*, 279-301. doi: 10.3390/agronomy4020279
78. Liebisch, F.; Kirchgessner, N.; Schneider, D.; Walter, A.; Hund, A. Remote, aerial phenotyping of maize traits with a mobile multi-sensor approach. *Plant Methods* **2015**, *11*. doi: 10.1186/s13007-015-0048-8
79. Yang, W.; Duan, L.; Cheng, G.; Xiong, L.; Liu, Q. Plant phenomics and high-throughput phenotyping: accelerating rice functional genomics using multidisciplinary technologies. *Curr. Opin. Plant Biol.* **2013**, *16*, 180-187. doi: 10.1016/j.pbi.2013.03.005

80. Sankaran, S.; Khot, L.R.; Espinoza, C.Z.; Jarolmasjed, S.; Sathuvalli, V.R.; Vandermark, G.J.; Miklas, P.N.; Carter, A.H.; Pumphrey, M.O.; Knowles, N.R.; Pavék, M.J. Low-altitude, high-resolution aerial imaging systems for row and field crop phenotyping: a review. *Eur. J. Agron.* **2015**, *70*, 112-123. doi: 10.1016/j.eja.2015.07.004
81. Mahlein, A. Plant disease detection by imaging sensors – parallels and specific demands for precision agriculture and plant phenotyping. *Plant Dis.* **2016**, *100*, 241-251. doi: 10.1094/PDIS-03-15-0340-FE
82. Wallace, L.; Lucieer, A.; Watson, C.; Turner, D. Development of a UAV-LiDAR system with application to forest inventory. *Remote Sens.* **2012**, *4*, 1519-1543. doi: 10.3390/rs4061519
83. Lu, B.; He, Y. Species classification using Unmanned Aerial Vehicle (UAV)-acquired high spatial resolution imagery in a heterogeneous grassland. *ISPRS J. Photogramm. Remote Sens.* **2016**, *128*, 73-85. doi: 10.1016/j.isprsjprs.2017.03.011
84. Otsu, N. A Threshold Selection Method from Gray-Level Histogram. *IEEE Trans. Syst. Man. Cybern. C. Appl. Rev.* **1979**, *9*, 62-66. doi: 10.1109/TSMC.1979.4310076
85. Han, L.; Yang, G.; Dai, H.; Xu, B.; Yang, H.; Feng, H.; Li, Z.; Yang, X. Modeling maize above-ground biomass based on machine learning approaches using UAV remote-sensing data. *Plant Methods* **2019**, *15*. doi: 10.1186/s13007-019-0394-z
86. Shafian, S.; Rajan, N.; Schnell, R.; Bagavathiannan, M.; Valasek, J.; Shi, Y.; Olsenholler, J. Unmanned aerial systems-based remote sensing for monitoring sorghum growth and development. *PLoS ONE* **2018**, *13*, e0196605. doi: 10.1371/journal.pone.0196605
87. Rodriguez-Galiano, V.F.; Ghimire, B.; Rogan, J.; Chica-Olmo, M.; Rigol-Sanchez, J.P. An assessment of the effectiveness of a random forest classifier for land-cover classification. *ISPRS J. Photogramm. Remote Sens.* **2012**, *67*, 93-104. doi: 10.1016/j.isprsjprs.2011.11.002
88. Belgiu, M.; Drăguț, L.; Random forest in remote sensing: A review of applications and future directions. *ISPRS J. Photogramm. Remote Sens.* **2016**, *114*, 24-31. doi: 10.1016/j.isprsjprs.2016.01.011
89. Su, L. Optimizing support vector machine learning for semi-arid vegetation mapping by using clustering analysis. *ISPRS J. Photogramm. Remote Sens.* **2009**, *64*, 407-413

90. Singh, S.K.; Srivastava, P.K.; Gupta, M.; Thakur, J.K.; Mukherjee, S. Appraisal of land use/land cover of mangrove forest ecosystem using support vector machine. *Environ. Earth Sci.* **2013**, *71*, 2245-2255. doi: 10.1007/s12665-013-2628-0
91. Guo, W.; Zheng, B.; Potgieter, A.B.; Diot, J.; Watanabe, K.; Noshita, K.; Jordan, D.R.; Wang, X.; Watson, J.; Ninomiya, S.; Chapman, S.C. Aerial imagery analysis – quantifying appearance and number of sorghum heads for applications in breeding and agronomy. *Front. Plant Sci.* **2018**, *9*, 1544. doi: 10.3389/fpls.2018.01544
92. Guo, W.; Potgieter, A.B.; Jordan, D.; Armstrong, R.; Lawn, K.; Kakeru, W.; Tao, D.; BangYou, Z.; Iwata, H.; Chapman, S.; Ninomiya, S. Automatic detecting and counting of sorghum heads in breeding field using RGB imagery from UAV. In *Abstracts and Full papers*, Proceedings of the CIGR-AgEng Conference, Aarhus, Denmark, 26-29 Jun **2016**.
93. Ribera, J.; He, F.; Chen, Y.; Habib, A.F.; Delp, E.J. Estimating Phenotypic Traits From UAV Based RGB Imagery. In Proceedings of the 22nd ACM SIGKDD International Conference on Knowledge Discovery and Data Mining, San Francisco, California, United States, **2016**.
94. Hu, P.; Chapman, S.C.; Wang, X.; Potgieter, A.; Duan, T.; Jordan, D.; Guo, Y.; Zheng, B. Estimation of plant height using a high throughput phenotyping platform based on unmanned aerial vehicle and self-calibration: example for sorghum breeding. *Eur. J. Agron.* **2018**, *95*, 24-32. doi: 10.1016/j.eja.2018.02.004
95. Watanabe, K.; Guo, W.; Arai, K.; Takanashi, H.; Kajiya-Kanegae, H.; Kobayashi, M.; Yano, K.; Tokunaga, T.; Fujiwara, T.; Tsutsumi, N.; Iwata, H. High-throughput phenotyping of sorghum plant height using an unmanned aerial vehicle and its application to genomic prediction modeling. *Front. Plant Sci.* **2017**, *8*, 421. doi: 10.3389/fpls.2017.00421
96. Masjedi, A.; Carpenter, N.R.; Crawford, M.M.; Tuinstra, M.R. Prediction of Sorghum Biomass Using Uav Time Series Data and Recurrent Neural Networks. In Proceedings of the 2019 IEEE/CVF Conference on Computer Vision and Pattern Recognition Workshops (CVPRW). Long Beach, California, United States, **2019**. pp. 2695-2702. doi: 10.1109/CVPRW.2019.00327
97. Zhang, Z.; Masjedi, A.; Zhao, J.; Crawford, M.M. Prediction of sorghum biomass based on image based features derived from time series of UAV images. In Proceedings of the

2017 IEEE International Geoscience and Remote Sensing Symposium (IGARSS), Fort Worth, Texas, United States, **2017**. pp 6154-6157. doi: 10.1109/IGARSS.2017.8128413

98. Masjedi, A.; Zhao, J.; Thompson, A.M.; Yang, K.; Flatt, J.E.; Crawford, M.M. Sorghum Biomass Prediction Using Uav-Based Remote Sensing Data and Crop Model Simulation. In Proceedings of the IGARSS 2018 – 2018 IEEE International Geoscience and Remote Sensing Symposium, Valencia, Spain, **2018**. pp. 7719-7722. doi: 10.1109/IGARSS.2018.8519034
99. Chiluwal, A.; Bheemanahalli, R.; Perumal, R.; Asebedo, A.R.; Bashir, E.; Lamsal, A.; Sebela, D.; Shetty, N.J.; Jagadish, S.V.K. Integrated aerial and destructive phenotyping differentiates chilling stress tolerance during early seedling growth in sorghum. *Field Crops Res.* **2018**, 227, 1-10. doi: 10.1016/j.fcr.2018.07.011
100. Potgieter, A.B.; Watson, J.; Eldridgex M.; Laws, K.; George-Gaeggli, B.; Hunt, C.; Borrell, A.; Mace, E.; Chapman, S.; Jordan, D.; Hammer, G.L. Determining Crop Growth Dynamics in Sorghum Breeding Trials Through Remote and Proximal Sensing Technologies. In Proceedings of the IGARSS 2018 – 2018 IEEE International Geoscience and Remote Sensing Symposium, Valencia, Spain, **2018**. pp. 8244-8247. doi: 10.1109/IGARSS.2018.8519296
101. Potgieter, A.B.; George-Jaeggli, B.; Chapman, S.C.; Laws, K.; Suárez Cadavid, L.A.; Wixted, J.; Watson, J.; Eldridge, M.; Jordan, D.L.; Hammer, G.L. Multi-spectral imaging from an unmanned aerial vehicle enables the assessment of seasonal leaf area dynamics of sorghum breeding lines. *Front. Plant. Sci.* **2017**, 8, 1532. doi: 10.3389/fpls.2017.01532
102. Henry, W.B.; Shaw, D.R.; Reddy, K.R.; Bruce, L.M.; Tamhankar, H.D. Remote sensing to detect herbicide drift on crops. *Weed Technol.* **2004**, 18, 358-368. doi: 10.1614/WT-03-098
103. Dicke, D.; Jacobi, J.; Büchse, A. Quantifying herbicide injuries in maize by use of remote sensing. In Proceedings 25th German Conference on Weed Biology and Weed Control, Braunschweig, Germany, 13-15 Mar **2012**, pp. 199-205. doi: 10.5073/jka.2012.434.024
104. Duddu, H.S.N.; Johnson, E.N.; Willenborg, C.J.; Shirtliffe, S.J.; High-throughput UAV image-based method is more precise than manual rating of herbicide tolerance. *Plant Phenomics* **2019**; doi: 10.34133/2019/6036453

Chapter 2 - Use of high resolution unmanned aerial systems imagery and machine learning to evaluate grain sorghum response to mesotrione

Abstract

Manual evaluation of crop injury to herbicides is time-consuming. Unmanned aircraft systems (UAS) and high-resolution multispectral sensors and machine learning classification techniques have the potential to save time and improve precision in the evaluation of herbicide injury in crops, including grain sorghum (*Sorghum bicolor* L. Moench). The objectives of this research were to (1) evaluate three supervised classification algorithms (support vector machine, maximum likelihood, and random forest) for categorizing high-resolution UAS imagery to aid in data extraction and (2) evaluate the use of vegetative indices (VIs) collected from UAS imagery as an alternative to traditional methods of visual herbicide injury assessment in mesotrione-tolerant grain sorghum breeding trials. An experiment was conducted in a randomized complete block design using a factorial treatment arrangement of three genotypes by four mesotrione doses. Herbicide injury was rated visually on a scale of 0 (no injury) to 100 (complete plant mortality). The UAS flights were flown at 9, 15, 21, 27, and 35 days after treatment. Results show the SVM algorithm to be the most consistently accurate, and high correlations ($r = -0.83$ to -0.94 ; $p < 0.0001$) were observed between the normalized difference vegetative index (NDVI) and ground-measured herbicide injury. Therefore we conclude that VIs collected with UAS coupled with machine learning image classification, has the potential to be an effective method of evaluating mesotrione injury in grain sorghum.

Abbreviations: UAS, unmanned aerial systems; VI, vegetative indices; SVM, support vector machine; NDVI, normalized difference vegetative index.

Introduction

Grain sorghum (*Sorghum bicolor* L. Moench) is an important crop with diverse uses throughout the world [1]. Sorghum is known to have originated from sub-Saharan Africa, where it has been used as a major food crop [2]. Grain sorghum has a vast genetic diversity with many genotypes possessing agronomically-desirable traits [3]. Traditionally, sorghum is used in the Western Hemisphere as animal feed; however, other uses include biofuel, forage production, and as a gluten-free alternative for human consumption [3-4]. In the United States, grain sorghum ranks the fifth-most important grain crop with 1.9 million hectares harvested in 2019 [5]. As sorghum is adapted to semi-arid regions of the world, it has been shown to have distinct yield advantages over corn (*Zea mays* L.) in such environments [6].

Weed competition is a common biotic pestilence that interferes with grain sorghum production. Prior research has demonstrated that infestations of weeds in grain sorghum can reduce yields ranging from 8 to 56%, depending on the type of weeds [7]. Despite other methods of weed control such as crop rotation and row cultivation, herbicides are the most common method of weed control in grain sorghum in the United States [7-8]. Several herbicides are registered for use in grain sorghum as pre (PRE)- or post (POST)-emergence treatments. For example, herbicides such as atrazine and mesotrione can be used as a PRE, and 2,4-D and dicamba as POST treatments [9]. Despite having several herbicides used for PRE treatments, the options for POST treatments are limited in grain sorghum, especially those used for grass weed

control. More options for POST grass control herbicides are needed for grain sorghum cropping systems.

The 4-hydroxyphenylpyruvate dioxygenase (HPPD)-inhibiting herbicides (e.g. mesotrione, tembotrione) are widely used for POST emergence grass weed control in corn [10] but not registered for POST use in grain sorghum because of crop injury [11]. These herbicides are used both as soil and foliar applied, and control a broad spectrum of grass and broadleaf species while providing soil residual activity for extended protection [10, 12-13]. These herbicides inhibit the HPPD enzyme in the plastoquinone biosynthesis pathway, leading to the depletion of plastoquinone levels. This results in the inhibition of carotenoids biosynthesis and subsequent plant death by photo-oxidation of chloroplasts. Because of this photo-oxidation, the main symptom after treatment with these herbicides is the bleaching of plant tissue, although additional symptoms including stunting of growth, leaf chlorosis and necrosis are also common in susceptible plants [8, 10]. HPPD-inhibiting herbicides are widely used as POST in corn, which can actively metabolize these herbicides into non-phytotoxic compounds [10].

Mesotrione is an HPPD-inhibitor in the triketone chemical family [14], and can be used as a pre-emergence treatment in grain sorghum. However, it has been shown to cause damage including 20% chlorosis in sorghum when applied POST [8, 15]. Recent research has identified grain sorghum genotypes with elevated tolerance to post-emergence applications of mesotrione with minimal crop damage [16]. These grain sorghum genotypes are valuable for the development of mesotrione-tolerant varieties in breeding programs. Although herbicide-tolerant traits could be quite useful for growers, implementing herbicide tolerance to grain sorghum breeding operations can be difficult. This is because several combinations of herbicides rates and genetic lines need to be fully investigated to quantify the data of herbicide injury level [17]. In

addition, previous methods to assess plant responses to herbicides, including visual scoring, portable chlorophyll sensors, and biomonitoring [18-20] are labor-intensive and time-consuming. New methods of evaluation of herbicide damage are warranted to support and hasten the screening large number of genotypes and populations in the breeding programs for the development of herbicide-tolerant technology in crops.

The use of high-resolution remote sensing techniques coupled with machine learning image classification algorithms is one of the promising methods for quantification of plant response to various biotic or abiotic stresses [21-22]. Image classification via remote sensing has been explored extensively, with the majority of platforms using either satellite, piloted aircraft, or unmanned aerial systems (UAS) [19, 23]. Images collected from these platforms can then be separated into distinct classes through various algorithms, allowing extraction of data from individual classes for external analysis [24-26]. A highly accurate set of image classification includes a supervised approach, which uses user-defined training samples to make these feature classifications [23, 27]. In addition to image classification, vegetative indices such as the normalized difference vegetation index (NDVI) can be computed, which have been shown to be useful in predicting plant parameters such as biomass, nitrogen status and chlorophyll content [28-30]. The quality of the data enhances with improved image resolution, making UAS a useful platform for collecting high-resolution remote sensing imagery in agricultural settings [31-34].

Proposed uses of UAS imagery in weed science, include weed pressure mapping, quantifying herbicide damage on non-target crops, herbicide applications, and site-specific weed management [32-33, 35-38]. However, very few studies have been carried out using UAS imagery to quantify herbicide injury in crops, specifically in grain sorghum. Therefore, the objectives of this study were to (1) determine the most suitable method of classifying high-

resolution UAS imagery in grain sorghum to aid in data extraction and (2) evaluate the use of UAS imagery as an alternative to traditional methods of assessing visual herbicide injury in grain sorghum.

Materials and Methods

Field Experiment

A field study was conducted in 2019 at the Kansas State University Ashland Bottoms Research Farm in Manhattan, Kansas (Figure 2.1). The soil type at the study location was a Reading silt loam with 2.42% organic matter and a pH of 6.07. A grain sorghum genotype (G-1) identified with tolerance to mesotrione [16] was planted along with a known mesotrione-susceptible genotype (S-1) and a Pioneer® (Corteva Agriscience, Wilmington, Delaware; USA) sorghum hybrid (84G62) for comparison. The experiment was arranged in a randomized complete block design (with three replications) with a two-way factorial arrangement of treatments, consisting of three genotypes and four herbicide rates. The genotypes were planted on June 8, 2019 at a rate of 175,000 seeds ha⁻¹, with a row spacing of 76 cm and a planting depth of 5 cm. The experiment plots were 2 m wide and 6.5 m long, consisting of four sorghum rows. The two middle rows consisted of each genotype (G-1, S-1, 84G62), and two outside border rows of Pioneer 84G62 were planted to act as a buffer between treatments. Mesotrione (Callisto® SC; Syngenta Crop Protection, LLC, Greensboro, North Carolina, USA) rates of 0, 105, 420, and 840 g ai ha⁻¹ were applied at the 3-4 leaf growth stage using a CO₂-pressurized backpack sprayer consisting of a four nozzle boom fitted with 110-02 flat-fan nozzles (TeeJet Spraying Systems Co., Wheaton, Illinois, USA) calibrated to deliver 187 L ha⁻¹ at 276 kPa.

Fertilizer applications followed the recommendations determined from a pre-plant soil test, and pests and diseases were controlled on an as-needed basis.

Image Acquisition

Prior to seedling emergence, 10 ground control points (GCPs) were placed within the experiment, and real-time kinematic (RTK) points were collected to aid in image processing. In addition to GCPs, each plot received two diagonally-placed ground targets indicating the sub-plots where ground-truth measurements were taken. Dimensions of the sub-plots were approximately 1.5 m x 1m. After processing, geo-centered border polygons could then be drawn over these sub-plots to allow for data extraction (Figure 2.2).

The Imagery was collected with a DJI Matrice 200 (DJI Inc., Shenzhen, China; <https://www.micasense.com/>) multi-rotor aircraft equipped with a Micasense RedEdge-MX multispectral camera (Micasense Inc., Seattle, Washington, USA; <https://www.micasense.com/>). The camera is capable of capturing five spectral bands of the visible and invisible electromagnetic spectrum (blue, 465-485 nm; green, 550-570 nm; red, 663-673 nm; red edge, 712-722 nm; near infrared, 820-860 nm) [40]. Each band is captured independently with a separate camera lens, and is capable of capturing images with a spatial resolution of 8 cm/pixel at an altitude of 120 m. To measure fluctuations in ambient lighting conditions, a down-welling light sensor (DLS) was included on the top of the aircraft.

Flights were flown 9, 15, 21, 27, and 35 days after treatment (DAT) for data collection. Flights were flown under clear, sunny conditions with no cloud cover. These conditions were selected to standardize lighting across all measurement dates, ensuring differences in data due to lighting conditions would be minimized. All flights were taken within ± 2.5 hours of solar noon

as recommended by the camera manufacturers. Radiometric calibration was performed using the calibration panel before and after each flight to ensure image quality. Each flight was flown at an altitude of 15 m and was flown using a pre-programmed GPS waypoint mapping mission using the DJI Pilot application. To ensure image quality, each flight was flown with an 80% front overlap and a 75% side overlap. The camera was set to capture images every 2 seconds to ensure adequate amounts of images were taken for processing. Images collected in flight were stored on an SD card and transferred to a desktop computer for further processing.

Image Processing

Data processing followed a workflow involving image orthomosaic generation in Agisoft Metashape (Agisoft LLC., St. Petersburg, Russia) and data extraction in ArcGIS Pro (ESRI Headquarters, Redlands, California, USA) (Figure 2.3). UAS images processed in Agisoft Metashape were processed with the slight modifications discussed in Holman et al. [39]: When aligning images and generating the sparse point cloud, alignment accuracy was set to high as opposed to ultra-high to reduce processing time and decrease levels of noise. When generating the dense point cloud, depth filtering was disabled to prevent any smoothing of the sorghum canopy. In addition, the quality of the dense point cloud was also set to high instead of ultra-high to reduce processing time. The resulting orthomosaic spatial resolution was between 1.1-1.3 cm/pixel for each of the 5 flight dates.

The image orthomosaic was exported to ArcGIS Pro for further data analysis. Ground targets within each plot were located, and sub-plots were defined. The sub-plots were then clipped from the original image, and vegetative indices (VIs) were computed on the sub-plots. The vegetative indices (VIs) computed were NDVI, enhanced normalized difference vegetation

index (ENDVI), simple ratio (SR), and enhanced vegetation index 2 (EVI2) (Table 2.1). These VIs were chosen for their close relations to plant greenness and canopy chlorophyll content [41].

Machine Learning Classification

A supervised classification approach was chosen over unsupervised methods because of the classification accuracy advantage over unsupervised methods [26-27]. Due to high image resolutions and standardized lighting conditions on each measurement date, we chose to use pixel-based classification algorithms, as opposed to other methods such as object based. After computing VI imagery, each sub-plot was classified into three categories: Sorghum leaves, shadows, and soil. To test for differences between accuracies in classification algorithms, we chose three different algorithms: support vector machine (SVM), random forest (RF), and maximum likelihood (ML). These three algorithms were chosen because they are all the options offered for pixel-based classifications in ArcGIS Pro. In order to classify the imagery, we followed a similar approach described by Tay et al. and Makanza et al. [47-48]. First, a classification scheme consisting of three categories was created. Twenty representative training samples were taken at random from the sub-plot, grouping similar pixels based on visual similarity and assigning them to each class. The training dataset and classification schema was then saved as a signature file and used to classify each sub-plot using each machine learning algorithm. In order to achieve maximum accuracy across each measurement day, this process was repeated with new representative training samples generated for each day. All algorithms were run with the default settings provided by ArcGIS Pro.

Ground Truth Measurements

Herbicide injury was assessed visually by using a scale of 0 (no visual injury) to 100 (complete plant mortality). Injury ratings were based on the presence of foliar bleaching, growth stunting, leaf chlorosis and tissue necrosis [8, 10, 49]. Ratings were taken within sub-plots so data from flights could be taken from the same plants in which the ratings were assigned. Each rating were taken ± 1 day of flight measurements.

Accuracy assessments were conducted on the classification methods by computing confusion matrices [50-51]. For each measurement day, 300 accuracy assessment points were generated via stratified random sampling. Each point was manually designated to the class to which it belonged, relative to the original orthomosaic image, creating ground reference points. When overlaid onto each classified raster, overall accuracy (OA) percentages were then computed by dividing the total number of correctly classified pixels by the total number of reference pixels. Accuracies at or above 85% were considered to be accurate classifications, which is a commonly-used target accuracy when classifying imagery [50]. For this study, we selected the most consistently-accurate algorithm across all 5 treatment dates to use for further data extraction (see results section).

Data Extraction

The process of data extraction from each sub-plot is shown in Figure 2.4. To prevent extraction from background features, data from each sub-plot was extracted using a conditional statement. Using the selected classified image, a conditional statement was built to allow for data from each computed VI to be extracted only from the sorghum plants. The average value of each VI was then extracted and exported for further analysis.

Statistical Analysis

All data were exported for analysis in R statistical program (R Core Team, Vienna, Austria; <https://www.R-project.org>). Data analysis was completed in two stages. First, statistical differences between mean overall classification accuracies (per algorithm) were tested with the Shapiro-Wilks test to verify assumptions of analysis of variance (ANOVA) [52]. The classification accuracy dataset failed to meet ANOVA assumptions and was therefore analyzed using the Kruskal-Wallis chi-squared goodness of fit test [53]. Significant differences between algorithms were found with a post-hoc analysis using the Dunn test [54]. Second, relationships between VIs and ground truth injury ratings were investigated and tested for significance with Pearson correlation coefficients [40, 48, 55-57]. Correlations were then used to detect differences in spectral values between genotypes and application rates. After identifying levels of significance, the VI with the highest significance scores was used in a two-way ANOVA to examine the effect of genotype and rate on spectral scores. Means were separated using a Tukey HSD post hoc test. All significance levels were set at $\alpha = 0.05$.

Results

Classification Accuracy

Overall classification accuracies ranged from 82 to 93% across algorithms (Table 2.2). The SVM was the most consistent across all dates with accuracies of 90% (27 DAT) to 92% (9 DAT). The algorithm with the most variability was ML, while the lowest accuracies were achieved with RF. The Kruskal-Wallis test revealed significant differences between groups (Chi-square = 7.41, p-value = 0.025), and the RF algorithm was found to be less accurate when

compared with SVM and ML (Table 2.3). Because SVM was consistently the most accurate classification algorithm, it was chosen to continue to extract data for further analysis. When comparing the overall accuracy means of each algorithm, all algorithms accurately classified the imagery into three established classes, as compared to the threshold of 85%. However, RF was found to be significantly less accurate than SVM and ML, indicating that RF may not be the best choice in supervised, pixel-based classifications for images of similar sorghum breeding trials.

Relation of Vegetative Indices to Ground Truth Injury

Significant negative correlations were observed across all measurement dates with each VI. High correlations were observed between UAS-based VI data and ground truth herbicide injury across all measurement dates (Table 2.4). The NDVI coefficients ($r = -0.94$ to -0.83) consistently displayed the highest correlations with visual injury symptoms on every measurement day. ENDVI ($r = -0.92$ to -0.82) and EVI2 ($r = -0.94$ to -0.82) correlations were very similar to NDVI values and thus were also very highly correlated with injury symptoms. The SR demonstrated the most variability in each measurement date ($r = -0.92$ to -0.70).

As NDVI was shown to be the most consistently related to mesotrione injury, it was chosen for the ANOVA analysis. Across all treatment dates, there was no significant interaction effect between genotype and rate (data not shown). Despite this, the main effect models demonstrated significant differences, with the results of the post-hoc test shown in Figure 2.5. When looking at the main effects model for genotypes, the NDVI response for the G-1 genotype across all mesotrione doses was not statistically different from the commercial hybrid response until 35 DAT. However, in all cases, the NDVI values for the G-1 genotype and commercial hybrid were statistically different from the S-1 genotype, which was to be expected given the S-1

susceptibility to mesotrione. For the rate main effect model, plants treated with 0 and 105 g ae ha⁻¹ were not statistically different from one another on each measurement date, indicating that a low dose of mesotrione did not significantly injure the lines used in this study. Interestingly, on the 27 and 35 DAT, it appeared that the plots treated with a higher rate of mesotrione (420 and 840 g ai ha⁻¹) started to recover from their injuries, but were always significantly lower than the control and 105 g ae ha⁻¹ dose.

Discussion

UAS imagery has been used to monitor various agronomic traits, including plant response to stress [48]. Supervised machine learning algorithms are commonly used to classify remote sensing imagery, and have been shown to be highly accurate in terms of overall classification accuracies [24, 58]. However, their effectiveness in classifying vegetation from background noise in breeding trials, especially for herbicide-tolerant trait development has not yet been explored. Our current research shows that machine learning algorithms, most notably the SVM algorithm, could be an effective method of extracting VI values from grain sorghum treated with different rates of mesotrione (Table 3).

Key to this finding is the use of high-resolution UAS imagery coupled with small plot sizes across uniform lighting conditions. Within each plot, there were three classes identified in each classification schema: leaves, shadows, and soil. A stark contrast between pixel brightness values occurred throughout each of the classes, allowing for the SVM algorithm to effectively segregate each class throughout the plots with high accuracy percentages. We expect that this classification schema could be used in grain sorghum to assess injury of other HPPD-inhibitor herbicides, such as tembotrione, because similar classes would be expected, regardless of the

location of study or genotypes. As pixel-based classifications were studied, we did not compare these results with other methods of segregating vegetation from background noise, including using the Otsu algorithm [59] for binary thresholding and object based image analysis. Further research for vegetation classification in screening for herbicide tolerance studies should compare classification accuracies of pixel-based, object-based, and binary thresholding algorithms.

The classification method chosen for this study was supervised, which are often more accurate than unsupervised in some situations [27]. One of the main benefits of unsupervised classifications is that large areas of land can be classified in a very short period of time [60]. In situations where there are large numbers of classes to assign to the image, an unsupervised approach would be preferred as a supervised approach would be very time-consuming. However, as demonstrated by our study, segregating sorghum vegetation in herbicide breeding trials does not require a large number of classes or training samples. It can therefore be accomplished in a relatively short period of time. As supervised classification algorithms can accurately identify features within these breeding trials, more research is needed to compare supervised classifications with unsupervised classifications in herbicide tolerance trials to see if statistically significant differences exist between overall accuracies.

Using the NDVI values and an ANOVA, it was observed that differences in spectral values existed for genotypes with respect to mesotrione application rates. The ability to detect spectral responses of plots treated with mesotrione could aid in quickly assessing the variable responses of multiple sorghum genotypes to mesotrione treatment. To be useful for sorghum breeders, differences in plant responses to mesotrione must be detected by the camera and able to be seen after data extraction. Our data shows that the Micasense camera was able to detect significant differences among genotype responses, which could allow breeders to know which

genotypes are responding to herbicide treatment. This prevents a large-scale manual assessment of the entire operation, leading to reduced time, labor, and resources to achieve the desired objective.

It should be noted that all VIs showed the strongest correlations on 9 and 15 DAT, and showed slightly weaker correlations for the rest of the measurement days. This is most likely because reductions in chlorophyll due to herbicide injury were clearly visible on the canopy early during the experiment, but were overshadowed by new growth as the growing season progressed. As a result, injury symptoms were still visible during ground truth ratings but were not visible to the camera. As healthy plants absorb light in the visible spectrum and reflect near infrared (NIR) energy, higher NDVI values are observed with healthier plants, whereas lower NDVI values are recorded as plant health declines [36]. This explains the negative correlations, as plants injured by mesotrione applications experienced a loss of green pigmentation. Previous research suggested that the genotype G-1 is more tolerant to mesotrione than Pioneer 84G62 or S-1 [16] used in this research. In this research, the similar response of G-1 and Pioneer 84G62 to mesotrione application can be explained because of the bleaching symptoms due to mesotrione application were not directly classified with machine learning algorithms due to spectral similarities with soil values. Instead, the reduction in leaf greenness showed to be sufficient in determining correlations with ground truth injury ratings.

VI have been successfully correlated with herbicide injury involving chlorophyll pigmentation loss in previous research. Huang et al. [61] found that NDVI values were highly related to cotton (*Gossypium hirsutum* L.) injury from aerial applications of glyphosate, with very strong correlations observed between increased frequencies of spray drift droplets and NDVI values. Dicke et al. [35] found reductions in NDVI values in plots treated with

sulfonylurea herbicides as well as significant correlations between NDVI values and corn yield, suggesting that low NDVI values in herbicide-damaged plots can be used as predictor of final yield. Duddu et al. [62] reported strong correlations between the optimized soil adjusted vegetation index (OSAVI) and visual injury ratings of faba beans (*Vicia faba* L.) treated with 9 different herbicide tank mixtures. Faba bean visual injury ratings were based on visible growth reduction and tissue chlorosis. Our data is consistent with these findings in that the increase in herbicide foliar injury is strongly related to changes in VI scores. As a final recommendation for future studies, relationships between UAS data and other herbicide modes of action should be determined to investigate how useful UAS would be for determining grain sorghum tolerance to other herbicides.

Herbicide injury in grain sorghum breeding trials is traditionally been assessed with visual injury ratings, which can be prone to error due to variations among evaluators. For trials consisting of thousands of grain sorghum plots, traditional injury assessment methods would take many hours or days to complete. Alternatively, UAS imagery can be taken in as little as 20-25 minutes, and while the data extraction methodology may seem to take a long time, the methodology can actually be completed quickly once the process is established.

Limitations

Limitations of this study are centered on the lack of use of more number of herbicides, genotypes tested and geographic restrictions. As there was only one herbicide used in this study, it remains to be determined if tolerance/susceptibility to other herbicides could be detected with UAS. Mesotrione injury was well-detected due to foliar bleaching symptoms, resulting from the destruction of phyto-oxidation of chloroplasts. This resulted in stark differences between treated

and untreated plants, which were able to be detected with the camera due to differences in chlorophyll pigmentation loss. As other herbicides do not directly result in stark pigmentation losses (i.e. auxins), the ability to detect sorghum responses to these herbicides remains to be determined.

Additional limitations involve use of genotypes that are not bred similarly for cultivation. While Pioneer 84G62 is a commercially grown hybrid with desirable agronomic traits, the genotypes G-1 and S-1 represent sorghum diversity panel which do not possess agronomically suitable traits. The other limitation includes, use of only one year data at one geographic location. This experiment was conducted in one field (Manhattan, KS), and has only been replicated across one year. This methodology remains to be tested across multiple years/locations to determine the robustness of detecting differences in mesotrione tolerance. Further studies should determine UAS injury characterization across multiple locations and growing conditions.

Although significant spectral difference existed between certain genotypes and rates of herbicide applications, the differences were not as pronounced as would be expected between mesotrione tolerant and susceptible genotypes. A likely explanation can be found in precipitation patterns. Rainfall was plentiful for the 2019 growing season in central KS, enabling adequate growth and development for all sorghum lines studied. This further demonstrates the need for additional replications across different geographic regions, as greater spectral differences between tolerant and susceptible genotypes could potentially be observed in different growing conditions.

Conclusions

This study suggests that VIs collected from high-resolution imagery, coupled with image classification, may be a useful tool for sorghum breeders to quantify the degree of mesotrione injury in grain sorghum. Across all measurement dates, a supervised, pixel-based SVM classifier was shown to be accurate and consistent when classifying imagery into sorghum leaves, shadows, and soil. The high correlation between VI data and ground-measured injury scores indicates that high-resolution multispectral imagery is able to detect reductions in chlorophyll due to mesotrione injury. As NDVI values were shown to be the most correlated to herbicide injury, we have demonstrated that the most widely-used VI in agriculture is capable of detecting these changes. Therefore, cost-effective NDVI sensors of varying types could potentially be used to measure mesotrione injury or possibly other herbicide injury symptoms that can be quantifiable. To add, this methodology does not focus on labeling specific genotypes/hybrids as “tolerant” or “susceptible;” rather, it provides sorghum breeders with a means of discovering genotypes (based on spectral responses) for further evaluation.. In a breeding trial with thousands of plots, we anticipate that this could reduce time and efforts required to discover herbicide tolerant sorghum genotypes. With further testing, this methodology could help to increase genotype selection, and could ultimately help to decrease the time it takes to deliver new herbicide-tolerant technologies to sorghum growers around the world.

References

1. Stefoska-Needham, A; Beck, E.J.; Johnson, S.K.; Tapsel, L.C. Sorghum: An underutilized cereal whole grain with the potential to assist in the prevention of chronic disease. *Food Rev. Int.* **2015**, 31, 401-437. doi: 10.1080/87559129.2015.1022832
2. Ongom, P. Association mapping of gene regions for drought tolerance and agronomic traits in sorghum. Ph.D. dissertation, Purdue University, West Lafayette, Indiana, United States, **2015**. Available from: <https://docs.lib.purdue.edu/dissertations/AAI10190817/>
3. Rooney, L.W.; Awika, J.M. Overview of products and health benefits of specialty sorghums. *Cereal Food World* **2005**, 50, 109-115.
4. Taylor, J.R.N.; Schober, T.J.; Bean, S.R. Novel food and non-food uses for sorghum and millets. *J. Cereal Sci.* **2006**, 44, 252-271. doi: 10.1016/j.jcs.2006.06.009
5. United States Department of Agriculture National Agricultural Statistics Site Service. Charts and Maps. Available online: https://www.nass.usda.gov/Charts_and_Maps/A_to_Z/in-sorghum.php (Accessed 2 April **2020**).
6. Staggenborg, S.; Dhuyvetter, K. C.; Gordon, W.B. Grain sorghum and corn comparisons: yield, economic, and environmental responses. *Agron J.* **2008**, 100, 1-21. doi: 10.2134/agronj2008.0129
7. Brown, D.W.; Al-Khatip, K.; Stahlman, P.W.; Loughin, T.M. Safening of metsulfuron grain sorghum injury with growth regulator herbicides. *Weed Sci.* **2004**, 52, 319-325. doi: 10.1614/P2002-074
8. Abit, M.J.M.; Al-Khatib, K. Absorption, translocation, and metabolism of mesotrione in grain sorghum. *Weed Sci.* **2009**, 57, 563-566. doi: 10.1614/WS-09-041.1
9. Regehr D. Weed Control. In *Grain Sorghum Production Handbook*; Vanderlip, R., Roozeboom, K., Fjell, D., Shroyer, J., Kok, H., Regehr, D., Whitney, D., Rogers, D.H., Alam, M., Jardine, D., Brooks, H.L., Taylor, R.K., Harner III, J.P., Langemeier, L.N.; Kansas State University Agricultural Experiment Station and Cooperative Extension Service: Manhattan, KS, United States, **1998**. pp. 10-11.

10. Mitchell, G.; Bartlett, D.W.; Fraser, T.E.M.; Hawkes, T.R.; Holt, D.C.; Townson, J.K.; Wichert, R.A. Mesotrione: a new selective herbicide for use in maize. *Pest Manag. Sci.* **2001**, *57*, 120-128. doi: 10.1002/1526-4998(200102)57:2<120::AID-PS254>3.0.CO;2-E
11. Abit, M.J.M.; Al-Khatib, K.; Currie, R.S.; Stahlman, P.W.; Geier, P.W.; Gordon, B.W.; Olson, B.L.S.; Claassen, M.M.; Regehr, D.L. Effect of postemergence mesotrione application timing on grain sorghum. *Weed Technol.* **2010**, *24*, 85-90. doi: 10.1614/WT-09-067.1
12. Singh, V.P.; Guru, S.K.; Kumar, A.; Banga, A.; Tripathi, N. Bioefficacy of tembotrione against mixed weed complex in maize. *Indian J. Weed Sci.* **2012**, *44*, 1-5.
13. Stephenson, D.O.; Bond, J.A.; Landry, R.L.; Edwards, H.M. Weed management in corn with postemergence applications of tembotrione or thien carbazon: tembotrione. *Weed Technol.* **2015**, *29*, 350-358. doi: 10.1614/WT-D-14-00104.1
14. Williams, M.M.; Pataky, J.K. Genetic basis of sensitivity in sweet corn to tembotrione. *Weed Sci.* **2008**, *56*, 364-370. doi: 10.1614/WS-07-149.1
15. Horky, K.T.; Martin, A.R. Evaluation of preemergence weed control programs in grain sorghum. Lincoln, NE: **2005** NCWSS Research Report-V.62, 30 p. Available from: http://ncwss.org/proceed/2005/ResRep05/table_contents.html
16. Jugulam, M.; Varanasi, A.; Thompson, C.R.; Prasad, P.V.V. Characterization of HPPD-inhibitor-tolerant sorghum genotypes. In: Sorghum in the 21st century, Cape Town, South Africa (abstract P27), 9-12 April **2018**
17. Leon, R.G.; Tillman, B.L. Postemergence herbicide tolerance variation in peanut germplasm. *Weed Sci.* **2015**, *63*, 546-554. doi: 10.1614/WS-D-14-00128.1
18. Felsot, A.S.; Bhatti, M.A.; Mink, G.I.; Reisenauer, G. Biomonitoring with sentinel plants to assess exposure of nontarget crops to atmospheric deposition of herbicide residues. *Environ. Toxicol. Chem.* **1996**, *15*, 452-459. doi: 10.1002/etc.5620150407
19. Sea, W.B.; Sykes, N.; Downey, P.O. An assessment of the physiological response of weeds to herbicide application. *Plant Prot. Q.* **2013**, *28*, 132-138.
20. Weber, J.F.; Kunz, C.; Peteinatos, G.; Santel, H.J.; Gerhards, R. Utilization of chlorophyll fluorescence imaging technology to detect plant injury by herbicides in sugar beet and soybean. *Weed Technol.* **2017**, *31*, 523-535. doi: 10.1017/wet.2017.22

21. Barton, C.V.M. Advances in remote sensing of plant stress. *Plant Soil* **2012**, 354, 41-44. doi: 10.1007/s11104-011-1051-0
22. Singh, A.; Ganapathysubramanian, B.; Singh, A.K.; Sarkar, S. Machine learning for high-throughput stress phenotyping in plants. *Trends Plant Sci.* **2016**, 21, 110-124. doi: 10.1016/j.tplants.2015.10.015
23. Peña, J.M.; Gutiérrez, P.A.; Hervás-Martínez, C.; Six, J.; Plant, R.E.; López-Granados, F. Object-based image classification of summer crops with machine learning methods. *Remote Sens.* **2014**, 6, 5019-5041. doi: 10.3390/rs6065019
24. Otukei, J.R.; Blaschke, T. Land cover change assessment using decision trees, support vector machines and maximum likelihood classification algorithms. *Int. J. Appl. Earth Obs.* **2010**, 12, S27-S31. doi: 10.1016/j.jag.2009.11.002
25. Smith, A. Image segmentation scale parameter optimization and land cover classification using the Random Forest algorithm. *J. Spat. Sci.* **2010**, 55, 69-79. doi: 10.1080/14498596.2010.487851
26. Thai, L.; Hai, T.S.; Thuy, N.T. Image Classification using support vector machine and artificial neural network. *Int. J. Inf. Tech. Comput. Sc.* **2012**, 5, 32-38. doi: 10.5815/ijitcs.2012.05.05
27. Bah, M.D.; Hafiane, A.; Canals, R. Deep learning with unsupervised data labeling for weed detection in line crops in UAV images. *Remote Sens.* **2018**, 10, 1690. doi: 10.3390/rs10111690
28. Kulbacki, M.; Segen, J.; Knieć, W.; Klempous, R.; Kluwak, K.; Nikodem, J.; Kulbacka, J.; Serester, A. Survey of drones for agriculture automation from planting to harvest. In Proceedings of the 2018 IEEE 22nd International Conference on Intelligent Engineering Systems, Las Palmas de Gran Canaria, Spain, **2018**; pp. 353-358. doi: 10.1109/INES.2018.8523943
29. Milas, A.S.; Romanko, M.; Reil, P. Abeyasinghe, T.; Marambe, A. The importance of leaf area index in mapping chlorophyll content of corn under different agricultural treatments using UAV images. *Int. J. Remote Sens.* **2018**, 39, 5415-5431. doi: 10.1080/01431161.2018.1455244

30. Näsi, R.; Viljanen, N.; Kaivosoja, J.; Hakala, T.; Pandžić, M.; Markelin, L.; Honkavaara, E. Assessment of various remote sensing technologies in biomass and nitrogen content estimation using an agricultural test field. *Int. Arch. Photogramm. Remote Sens. Spatial Inf. Sci.* **2017**, XLII-3/W3, 137-141. doi: 10.5194/isprs-archives-XLII-3-W3-137-2017
31. De Castro, A.I.; Torres-Sánchez, J.; Peña, J.; Jiménez-Brenes, F.M.; Csillik, O.; López-Granados, F. An automatic random forest-OBIA algorithm for early weed mapping between and within crop rows using UAV imagery. *Remote Sens.* **2018**, 10, 285. doi: 10.3390/rs10020285
32. López-Granados, F.; Jurado-Expósito, M.; Peña-Barragán, J.M.; Torres, L.G. Using remote sensing for identification of late-season grass weed patches in wheat. *Weed Sci.* **2006**, 54, 346-353. doi: 10.1614/WS-05-54.2.346
33. Rasmussen, J.; Nielsen, J.; Garcia-Ruiz, F.; Christensen, S.; Streibig, J.C. Potential uses of small unmanned aircraft systems (UAS) in weed research. *Weed Res.* **2013**, 54, 242-248. doi: 10.1111/wre.12026
34. Torres-Sánchez, J.; López-Granados, F.; De Castro, A.I.; Peña-Barragán, J.M. Configuration and specifications of an unmanned aerial vehicle (UAV) for early site specific weed management. *PLoS ONE* **2013**, 8, e58210. doi: 10.1371/journal.pone.0058210
35. Dicke D, Jacobi J, Buchse A. Quantifying herbicide injuries in maize by use of remote sensing. In Proceedings of the 25th German Conference on Weed Biology and Weed Control, Braunschweig, Germany, **2012** Mar 13-15; pp. 199-205. doi: 10.5073/jka.2012.434.024
36. Henry, W.B.; Shaw, D.R.; Reddy, K.R.; Bruce, L.M.; Tamhankar, H.D. Remote sensing to detect herbicide drift on crops. *Weed Technol.* **2004**, 18, 358-368. doi: 10.1614/WT-03-098
37. Louargant, M.; Villette, S.; Jones, G.; Vigneau, N.; Paoli, J.N.; Gée, C. Weed detection by UAV: simulation of the impact of spectral mixing in multispectral images. *Precis. Agric.* **2017**, 18, 932-951. doi: 10.1007/s11119-017-9528-3
38. Prince Czarnecki, J.M.; Samiappan, S.; Wasson, L.; McCurdy, J.D.; Reynolds, D.B.; Williams, W.P.; Moorhead, R.J. Applications of unmanned aerial vehicles in weed science. In Proceedings of the 11th European Conference on Precision Agriculture;

Edinburgh, United Kingdom, **2017** Jul 16-20; Edinburgh, United Kingdom; International Society of Precision Agriculture; pp. 807-811. doi: 10.1017/S2040470017001339

39. Holman, F.H.; Riche, A.B.; Michalski, A.; Castle, M.; Wooster, M.J.; Hawkesford, M. High throughput field phenotyping of wheat plant height and growth rate in field plot trials using UAV based remote sensing. *Remote Sens.* **2016**, 8, 1031. doi: 10.3390/rs8121031
40. Li, J.; Shi, Y.; Veeranampalayam-Sivakumar, A.; Schachtman, D.P. Elucidating sorghum biomass, nitrogen and chlorophyll contents with spectral and morphological traits derived from unmanned aircraft system. *Front Plant Sci.* **2018**, 9, 1406. doi: 10.3389/fpls.2018.01406.
41. Garcia, I.A. UAS multispectral imaging for detecting plant stress due to iron chlorosis in grain sorghum. M.Sc. Thesis, Texas A&M University – Corpus Christi, Corpus Christi, Texas, United States, **2018**. Available from: <https://tamucc-ir.tdl.org/handle/1969.6/87102>
42. Gago, J.; Douthe, C.; Coopman, R.E.; Gallego, P.P.; Ribas-Carbo, M.; Flexas, J.; Escalona, J.; Medrano, H. UAVs challenge to assess water stress for sustainable agriculture. *Agr. Water Manage.* **2015**, 153, 9-19. doi: 10.1016/j.agwat.2015.01.020
43. Rouse, J.; Haas, R.; Schell, J.; Deering, D. Monitoring Vegetation Systems in the Great Plains with ERTS. In Proceedings from the NASA Goddard Space Flight Center 3d ERTS-1 Symposium. **1974**, 1, 309-317.
44. Rasmussen, J.; Ntakos, G.; Nielsen, J.; Svensgaard, J.; Poulsen, R.N.; Christensen, S. Are vegetation indices derived from consumer-grade cameras mounted on UAVs sufficiently reliable for assessing experimental plots? *Eur. J Agron.* **2016**, 74, 75-92. doi: 10.1016/j.eja.2015.11.026
45. Stenberg, P.; Rautiainen, M.; Manninen, T.; Voipio, P.; Smolander, H. Reduced simple ratio better than NDVI for estimating LAI in Finnish pine and spruce stands. *Silva Fenn.* **2004**, 38, 3-14. doi: 10.14214/sf.431
46. Jiang, Z.; Huete, A.R.; Didan, K.; Miura, T. Development of a two-band enhanced vegetation index without a blue band. *Remote Sens. Environ.* **2008**, 112, 3833-3845. doi: 10.1016/j.rse.2008.06.006

47. Tay, J.Y.; Erfmeier, A.; Kalwij, J.M. Reaching new heights: can drones replace current methods to study plant population dynamics? *Plant Ecol.* **2018**, 219, 1139-1150. doi: 10.1007/s11258-018-0865-8
48. Makanza, R.; Zaman-Allah, M.; Cairns, J.E.; Magorokosho, C.; Tarekegne, A.; Olsen, M.; Prasanna, B.M. High-throughput phenotyping of canopy cover and senescence in maize field trials using aerial digital canopy imaging. *Remote Sens.* **2018**, 10, 330. doi: 10.3390/rs10020330
49. Tate, T.M.; Meyer, W.A.; McCullough, P.E.; Yu, J. Evaluation of mesotrione tolerance levels and [¹⁴C]mesotrione absorption and translocation in three fine fescue species. *Weed Sci.* **2019**, 67, 497-503. doi: 10.1017/wsc.2019.39
50. Foody, G.M. Local characterization of thematic classification accuracy through spatially constrained confusion matrices. *Int. J. Remote Sens.* **2005**, 26, 1217-1228. doi: 10.1080/01431160512331326521
51. Lewis, H.G.; Brown, M. A generalized confusion matrix for assessing area estimates from remotely sensed data. *Int. J. Remote Sens.* **2001**, 22, 3223-3235. doi: 10.1080/01431160152558332
52. Wright, S.D.; Shrestha, A.; Hutmacher, R.B.; Banuelos, G.; Hutmacher, K.A.; Rios, S.I.; Dennis, M.; Wilson, K.A.; Avila, S.J. Glufosinate safety in WideStrike® Acala cotton. *Weed Technol.* **2014**, 8, 104-110. doi: 10.1614/WT-D-13-00039.1
53. Kruskal, W.H.; Wallis, W.A. Use of ranks in one-criterion variance analysis. *J. Am. Stat. Assoc.* **1952**, 47, 583-621. doi: 10.2307/2280779
54. Dunn, O.J. Multiple comparisons using rank sums. *Technometrics* **1964**, 6, 241-252. doi: 10.1080/00401706.1964.10490181
55. Han, L.; Yang, G.; Dai, H.; Xu, B.; Yang, H.; Feng, H.; Li, Z.; Yang, X. Modeling maize above-ground biomass based on machine learning approaches using UAV remote-sensing data. *Plant Methods* **2019**, 15, 10. doi: 10.1186/s13007-019-0394-z
56. Hassan, M.A.; Yang, M.; Rasheed, A.; Jin, X.; Xia, X.; Xiao, Y.; He, Z. Time-series multispectral indices from unmanned aerial vehicle imagery reveal senescence rate in bread wheat. *Remote Sens.* **2018**, 10, 809. doi: 10.3390/rs10060809

57. Schirrmann, M.; Giebel, A.; Gleiniger, F.; Pflanz, M.; Lentschke, J.; Dammer, K.H. Monitoring agronomic parameters of winter wheat crops with low-cost UAV imagery. *Remote Sens.* **2016**, *8*, 706. doi: 10.3390/rs8090706
58. Noi, P.T.; Kappas, M. Comparison of random forest, k-nearest neighbor, and support vector machine classifiers for land cover classification using Sentinel-2 imagery. *Sensors (Basel)* **2017**, pii: E18. doi: 10.3390/s18010018
59. Otsu, N. A. Threshold selection method from gray-level histograms. *IEEE Trans. Syst. Man. Cybern. Syst.* **1979**, *9*, 62-66. doi: 10.1109/TSMC.1979.4310076
60. Enderle, D.I.M.; Weih, R.C. Integrating supervised and unsupervised classification methods to develop a more accurate land cover classification. *J. Ark. Acad. Sci.* **2005**, *59*, 65-73.
61. Huang, Y.; Thomson, S.J.; Ortiz, B.V.; Reddy, K.N.; Ding, W.; Zablotowicz, R.M.; Bright, J.R. Airborne remote sensing assessment of the damage to cotton caused by spray drift from aerially applied glyphosate through spray deposition measurements. *Biosyst. Eng.* **2010**, *107*, 212-220. doi: 10.1016/j.biosystemseng.2010.08.003
62. Duddu, H.S.; Johnson, E.N.; Willenborg, C.J.; Shirtliffe, S.J. High-throughput UAV image-based method is more precise than manual rating of herbicide tolerance. *Plant Phenomics* **2019**, pii: 6036453. doi: 10.34133/2019/6036453

Figures

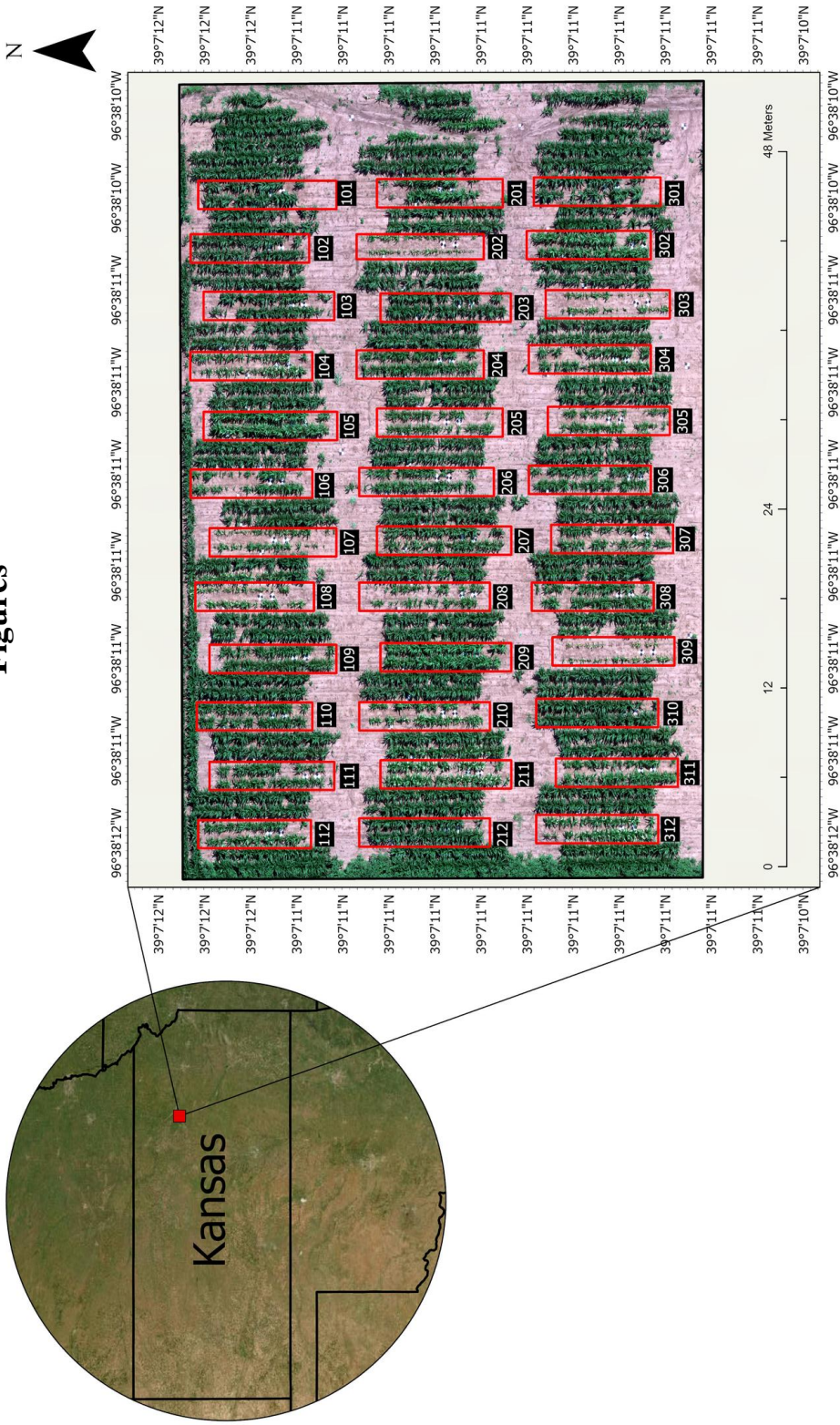


Figure 2.1 Location of the field trial in Manhattan, Kansas (US) evaluating 84G62, S-1, and G-2 spectral responses to mesotriene. The genotypes were planted in two rows, as denoted by the red rectangles. Plot numbers are denoted below each rectangle.

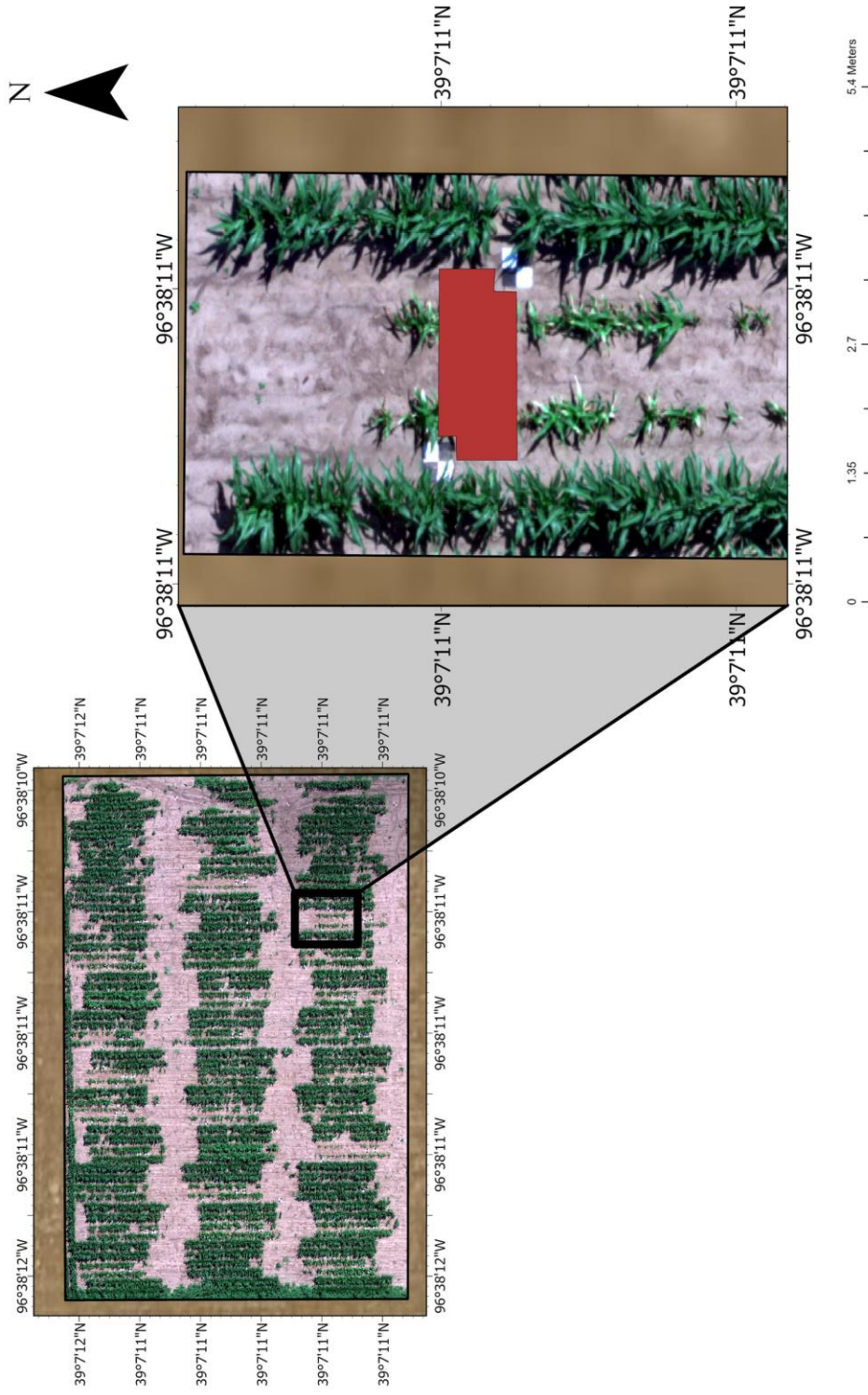


Figure 2.2 View of individual plots consisting of sorghum rows and sub-plots. Sub-plots were indicated by two ground targets placed within the north end of each plot to identify the plants on which ground-truth injury ratings were taken. Sub-plot dimensions were approximately 1.5 m x 1 m. Border polygons were drawn over each sub-plot to allow for data extraction.

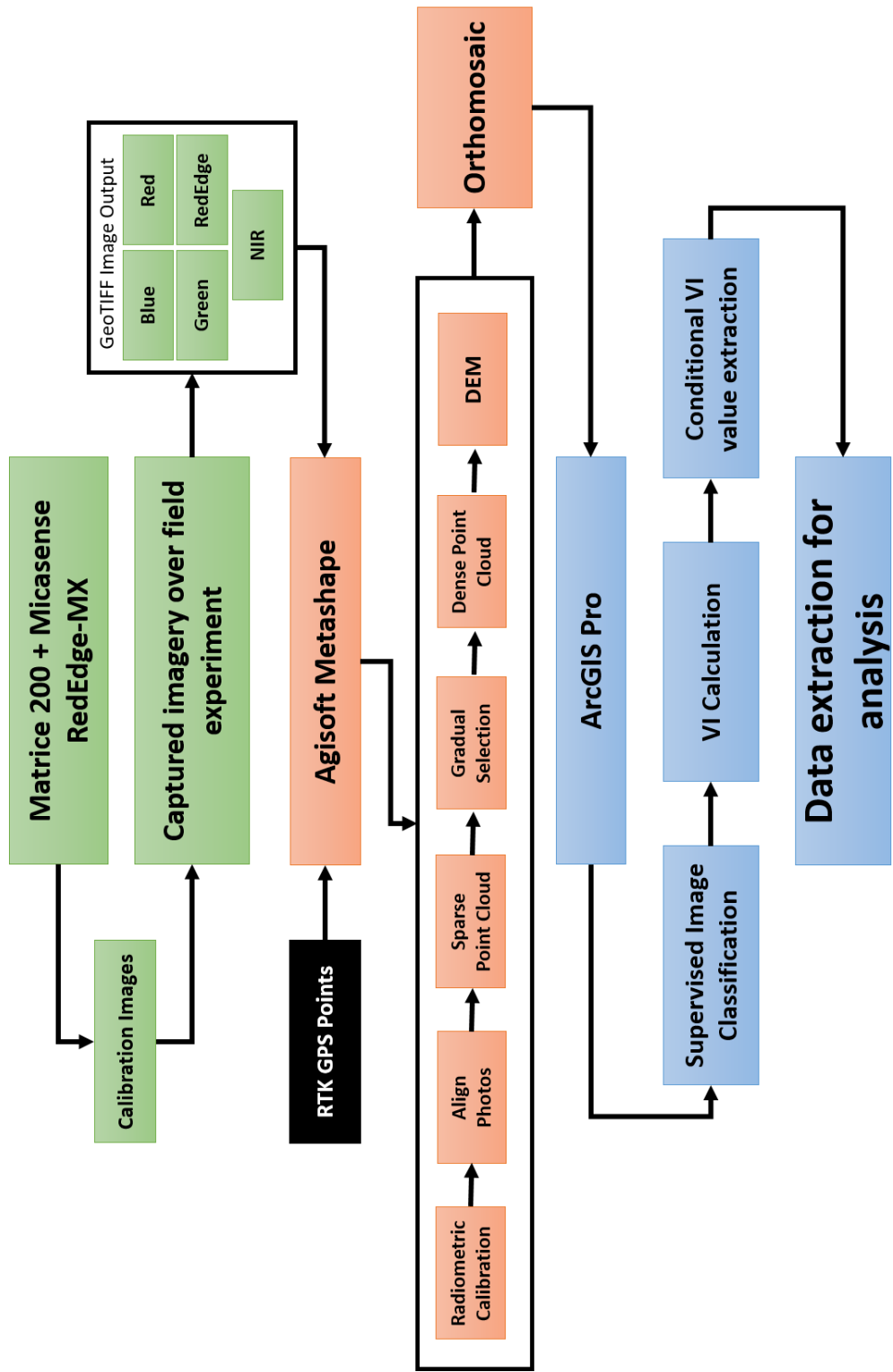


Figure 2.3 Image collection, processing, and data extraction workflow.

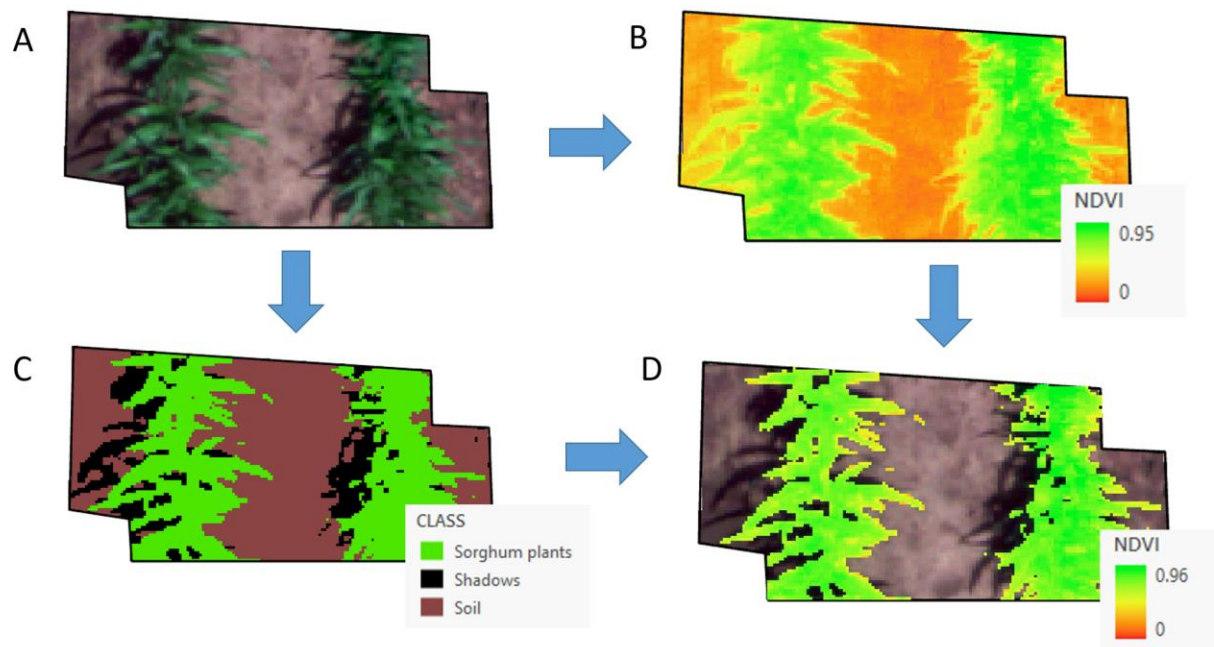


Figure 2.4 Methodology for vegetative indices (VI) data extraction based on the results of the image classification. (A) Original red-green-blue (RGB) sub-plot image; (B) each VI was computed from the original RGB images, creating a new raster layer for each VI; (C) RGB images were classified via supervised, pixel-based algorithms into leaves, shadows, and soil; and (D) each VI raster was combined with the classified image to create a new raster layer, allowing for VI data from only the sorghum leaves to be extracted for statistical analysis.

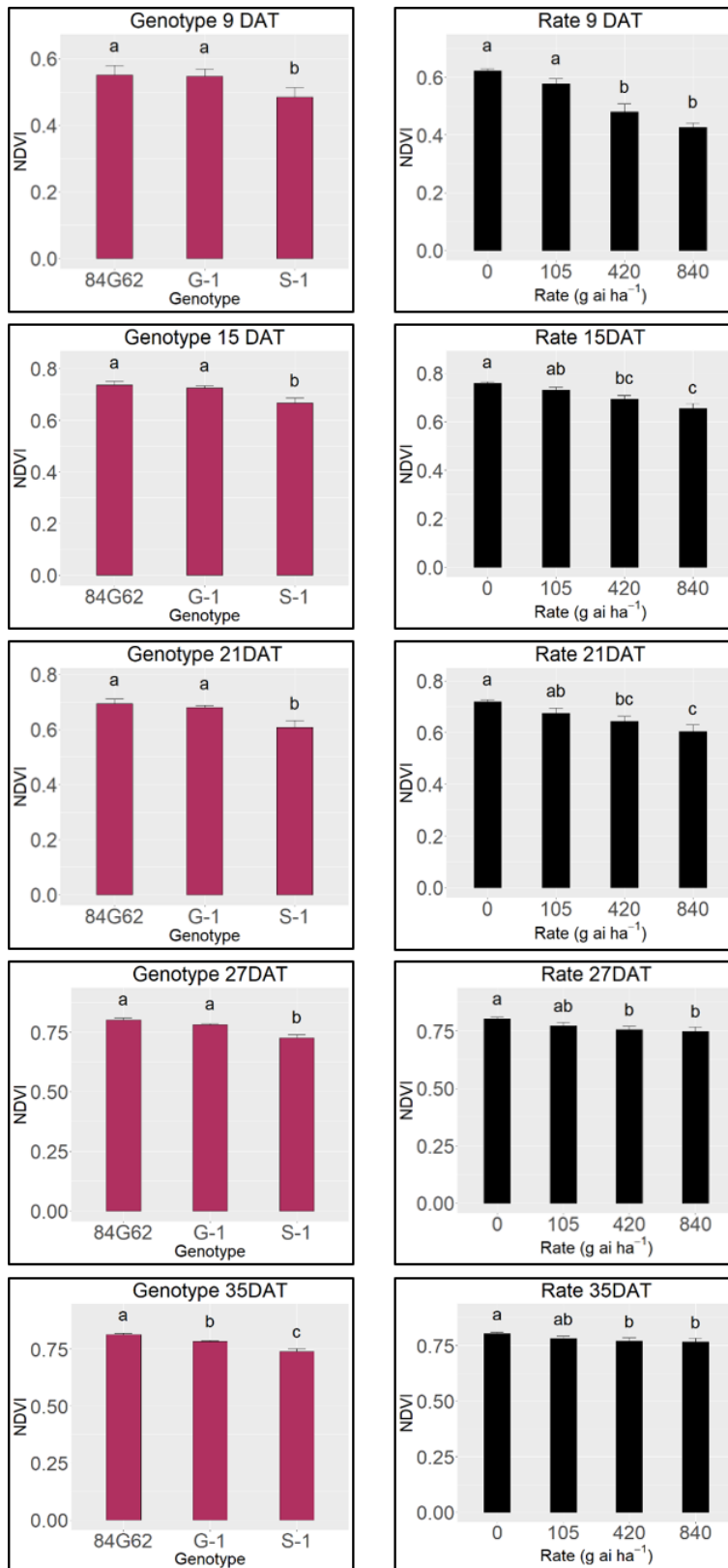


Figure 2.5 ANOVA results for main effect models, genotype + rate. Means were separated using Tukey's HSD test at the 0.05 significance level.

Tables

Table 2.1 Equations and common uses for vegetative indices used in this study.

Vegetative Index	Formula	Use	Reference
NDVI	$\frac{\rho\text{NIR}-\rho\text{R}}{\rho\text{NIR}+\rho\text{R}}$	Green biomass, chlorophyll	[40, 42-44]]
ENDVI	$\frac{((\rho\text{NIR}+\rho\text{G})-(2\times\rho\text{R}))}{((\rho\text{NIR}+\rho\text{G})+(2\times\rho\text{R}))}$	Chlorophyll content	[41, 44]
SR	$\frac{\rho\text{NIR}}{\rho\text{R}}$	Chlorophyll, leaf area index	[45]
EVI2	$2.5\times\frac{\rho\text{NIR}-\rho\text{R}}{\rho\text{NIR}+(2.4\times\rho\text{R})+1}$	Chlorophyll, canopy cover	[41, 43, 46-47]

Acronyms: NDVI, normalized difference vegetation index; ENDVI, enhanced normalized difference vegetative index; SR, simple ratio; EVI2, enhanced vegetation index 2. ρ denotes spectral reflectance.

Table 2.2 Overall accuracies for each algorithm on each measurement date.

DAT	Algorithm		
	SVM	RF	ML
9	92	88	85
15	91	82	92
21	91	87	93
27	90	87	92
35	91	82	90

Acronyms: DAT, days after treatment; SVM, support vector machine; RF, random forest; ML, maximum likelihood.

Table 2.3 Results of the Dunn test indicating significant differences between mean overall classification accuracy percentages. No significant differences were found between the SVM-ML algorithms, but the RF algorithm was significantly less accurate than the others.

Algorithm	P-value	Significance
ML-RF	0.02	*
ML-SVM	0.94	ns
RF-SVM	0.02	*

Acronyms: SVM, support vector machine; RF, random forest; ML, maximum likelihood. * indicates significant differences at the 0.05 level.

Table 2.4 Pearson correlation coefficients between vegetative indices and ground-measured visual injury ratings.

VI	9 DAT		15 DAT		21 DAT		27 DAT		35 DAT	
	r	p-value								
NDVI	-0.94	< 0.0001	-0.91	< 0.0001	-0.85	< 0.0001	-0.83	< 0.0001	-0.83	< 0.0001
ENDVI	-0.92	< 0.0001	-0.90	< 0.0001	-0.84	< 0.0001	-0.83	< 0.0001	-0.82	< 0.0001
EVI2	-0.94	< 0.0001	-0.90	< 0.0001	-0.84	< 0.0001	-0.81	< 0.0001	-0.82	< 0.0001

Acronyms: NDVI, normalized difference vegetation index; ENDVI, enhanced normalized difference vegetation index; EVI2, enhanced vegetation index 2; SR, simple ratio; DAT, days after treatment.

Chapter 3 - Investigation of high-resolution UAS imagery for SG trait characterization in grain sorghum

Abstract

Grain sorghum (*Sorghum bicolor* (L.) Moench) is a very important crop to the world's semi-arid regions, as it is able to produce grain and biomass yields in precipitation-limited environments. Many genotypes have a characterized form of drought resistance known as the stay-green (SG) trait, enabling sorghum plants to resist post-flowering drought stress that can severely reduce yields. Breeding for SG sorghum lines is considered very important for sorghum breeders around the world, but selecting for SG traits currently relies on methods that are labor-intensive and time-consuming. Using unmanned aerial systems (UAS) capable of capturing high-resolution imagery offers a solution for reducing the time and energy required to select for these traits. A field study was conducted in Manhattan, Kansas (United States) where 20 Pioneer[®] sorghum hybrids were planted in a randomized complete block design with three replications per hybrid. Imagery was collected with a DJI[®] Matrice 200[™] equipped with a MicaSense[®] RedEdge-MX[™] multispectral camera. Flight altitude was 30 m, and flights were collected under clear, sunny skies within ± 2.5 hours of solar noon. Ground-measured data included visual senescence ratings, fresh and dry plant biomass, leaf area index (LAI), and final grain yield. After correlation and regression analysis, results indicated significant relationships with the near infrared (NIR) spectral band with fresh and dry plant biomass samples, the green normalized difference vegetation index (GNDVI) scores at flowering were the most related to final grain yield, and the visible atmospherically resistant index (VARI) was the most related to visual senescence scores. Significant spectral band/vegetative indices were clustered into groups, and

significant differences were found between various traits. From this study, we have developed a methodology for SG sorghum growers to collect, process, and extract data for more efficient identification of traits of interest.

Introduction

In the year 2050, the human population is expected to rise from 7 to 10 billion people, consequently increasing global demand for food [1]. In order to meet these increasing demands, current global crop production will need to be at least doubled [2]. Even though there are nearly 200 species of plants are used for wide-scale human consumption, there are growing concerns that current farming practices and crop cultivars will not be capable of meeting these demands [1]. For major crops including corn (*Zea mays*), rice (*Oryza sativa* L.), and wheat (*Triticum aestivum*), displayed an annual yield of improvement from 0.8 to 1.2%, but this yield trend must be doubled to meet future demands [1, 3]. In addition, several regions around the world have experienced yield losses due to stresses brought by a warming climate [4], further complicating the goal of increasing yields. To address these challenges, crop breeders must select for cultivars for increased yield potential while simultaneously displaying stability against environmental stressors such as drought and temperature stress [5].

One crop that shows potential to contribute to and diversify human diets is grain sorghum (*Sorghum bicolor* (L.) Moench) [1]. Grain sorghum is a C4 crop that is an important food source for many people in Africa, Asia, and Central America [6]. Globally, it is the fifth most important cereal crop, after wheat, corn, rice, and barley (*Hordeum vulgare*) [7-9], and is also valued for its use for forage and biofuel production [10]. Since it is known to have originated in sub-Saharan Africa [11-12], it is well-adapted to semi-arid and arid regions of the world, making it a crop of

choice in areas with limited precipitation [6, 9]. Despite having distinct economic and yield advantages over corn in drier environments [13-14], sorghum is still considered to be well-below its yield potential [15]. This is partially because grain sorghum is widely-considered to be difficult to process into products for human consumption, so as a result, most grain sorghum grown in developed countries is exported and used as animal feed [15]. However, as many areas in the world are predicted to become warmer and drier due to climate change, it is estimated that more regions will adapt to this by growing more grain sorghum for human consumption [15]. Being well-suited for arid environments, sorghum is considered a crop that will help with the goal of global food security under future climate changes [10, 16].

One way sorghum breeders are looking to combat yield losses is to select for cultivars tolerant to abiotic stress, particularly in terms of drought tolerance [17-18]. All stresses considered, one of the most relevant stressors to sorghum is post-flowering drought stress, often known as “terminal drought” [7]. This type of stress severely limits grain filling during later growth stages, impacting the duration of this period and thus severely reducing grain yields. Many genetic lines of crops, including grain sorghum, have a characterized form of drought tolerance during post-flowering growth stages known as the non-senescence or “stay-green” (SG) trait [13, 19]. Grain sorghum genotypes with the SG trait continue to fill their grain under drought, and also exhibit tolerance to several factors that affect grain sorghum under moisture stress such as stem rot and lodging [13, 20-24]. In addition to yield retention, the SG trait is valuable for biomass production in regions where water is limited [25-26], allowing farmers in these regions to produce more above-ground biomass for forage and biofuel production. Due to these advantages, many breeders consider the SG trait of much agronomic importance, and has been and continues to be subjected to intensive selection in crop breeding trials [27].

With all of these predicted changes to world population and climate patterns, there is an increasing amount of pressure on farmers and crop breeders to improve crop cultivars [28]. As concerns arise regarding cultivar improvements beginning to plateau [1], new technologies are needed to boost the speed of cultivar selection in breeding trials. Technology that is capable of screening thousands of lines for a desired trait is essential for this process [29]. These technologies can be even more important when screening for SG traits, which can be very labor-intensive and time-consuming if scored with traditional methods (i.e. using visual leaf scoring systems or SPAD meters) [23, 30-31]. For this purpose, many breeders have turned to screening large trials with remote sensing methods, utilizing non-destructive approaches to measure reflected electromagnetic radiation from plants [32]. Through identifying changes in both the visible and invisible spectral bands, information regarding vegetation health and productivity can be detected and quantified [33]. In addition, these individual bands can be combined into vegetative indices (VIs), which have been shown to be successful in estimating traits such as (but not limited to) plant biomass [34], leaf area index (LAI) [35], leaf senescence [36], and final grain yield [37].

Because remote sensing platforms such as satellites may not currently provide the resolution necessary for screening individual cultivars, unmanned aerial systems (UAS) equipped with consumer-grade cameras have been shown to be useful for obtaining very high-resolution imagery for agricultural purposes [38]. In addition, UAS platforms are considered relatively inexpensive [39], and have recently become more accessible not only in cost but in easiness to use for data processing for both farmers and research programs [36]. Our hypothesis is that high-resolution UAS multispectral imagery is an effective alternative to time-consuming ground evaluation and selection of traits of interest in sorghum SG breeding trials.

Spectral data have been used to explain senescence in previous studies, as they have been deemed useful in the prediction of green leaf area during senescence [40]. In most vegetative remote sensing applications, healthy vegetation is sensed by detecting the quantity of NIR wavelengths emitted as a result of cellular refraction [41]. In cases of vegetative senescence, NIR reflectance does not significantly decrease; instead, the degradation of chlorophyll results in the decrease of green electromagnetic reflectance and the rise of red electromagnetic reflectance [42]. There is seldom a major change observed in the relation of green leaf area to NIR reflectance, but the relation between red reflectance and green leaf area changes substantially [43]. In many studies, there is an emphasis on quantifying red edge reflectance, as reductions in this region have been shown to be related to reductions in chlorophyll during senescence [35, 40, 43-45]. However, since there are significant spectral fluctuations across the entire visible electromagnetic spectrum [45], vegetative indices quantifying the change of green light reflectance to the change of red light reflectance are thought to also be able to quantify vegetative senescence.

In this paper, we explore the relationship between ground-sampled plant traits and cluster groups found by hierarchical clustering of individual spectral bands and VIs, focusing on characterizing sorghum senescence patterns, fresh and dry above-ground biomass, and grain yield. In an effort to encourage more SG sorghum breeding programs to utilize this technology, we have proposed a methodology to assist sorghum breeders in image collection, processing, data extraction, and analysis to locate plots with these traits of interest. For the purposes of this study, we have investigated as to whether or not significant differences can be detected from the clusters formed in this methodology. In addition, we have tested the relevancy of using individual spectral bands and red-green-blue (RGB) VIs versus VIs based on the invisible

electromagnetic spectrum by developing regression models comparing ground-sampled plant traits to spectral data.

Materials and Methods

Field Study Information

This study was conducted at the Corteva Agriscience (Corteva Agriscience, Wilmington, Delaware, USA; www.corteva.com) grain sorghum nursery in Manhattan, Kansas (39°9'13.69" N, 96°40'1.2" W). The soil type is classified as a Reading silt loam with a slope between 0-2%. Twenty Pioneer® sorghum hybrids with different released years were planted in a randomized complete block design at a density of 13 plants m⁻². Sorghum genotypes were Pioneer hybrids spanning six decades of genetic selection (from 1963 until 2017). Each hybrid was replicated three times for a total of 60 plots. The hybrids were planted on June 8, 2019 in blocks with 8 rows 5.3 m in length, with a row spacing of 0.76 m. Fertility and pest control measures were taken when necessary to ensure plant health throughout the season. Figure 3.1 illustrates the layout of the experiment.

Image Collection

Image collection, processing, and data extraction followed a framework presented in Figure 3.2. To collect aerial imagery, the UAS used for this study was a DJI Matrice 200 (DJI, Shenzhen, China; www.dji.com) outfitted with a MicaSense RedEdge-MX multispectral camera (MicaSense, Seattle, Washington, USA; www.micasense.com). The Matrice 200 design includes

a DJI SkyPort integration kit, allowing the sensor to be quickly mounted on the camera gimbal. The RedEdge-MX sensor is a five-banded multispectral sensor, able to simultaneously capture 5 narrow bandwidths on both the visible and invisible electromagnetic spectrum [blue, 465-485 nm; green, 550-570 nm; red, 663-673 nm; red edge (RE), 712-722 nm; near infrared (NIR), 820-860 nm]. The camera is capable of capturing a spatial resolution of 8 cm pixel⁻¹ at an altitude of 122 m, and is equipped with a downwelling light sensor (DLS) to detect changes in ambient lighting conditions during flight.

Prior to flights, ground control points (GCPs) were set around the perimeter of the study, and real time kinematic (RTK) GPS points were taken at each target. Throughout the growing season, 4 flights were flown in accordance to grain sorghum growth stage, primarily focusing on the reproductive period of the crop: Flowering, soft dough, hard dough, and physiological maturity. To ensure lighting conditions were the same for all flights, each mission was flown under clear, sunny conditions within ± 2.5 hours of solar noon. Due to close proximity to Class D airspace, flight altitude was limited to 30 m, with a forward and side overlap set to 80% to ensure clear image orthomosaic production. Missions were planned and uploaded to the aircraft using the DJI Pilot application, with all missions conducted as GPS waypoint mapping missions. Waypoint missions produce flight plan of GPS points with altitude, flight area, and overlap settings factored into it, creating points to which the aircraft will travel to during flight. The RedEdge-MX camera was set to collect imagery every 2 seconds to ensure that enough images would be collected for processing. Following recommendations from the manufacturer, gain (ISO) and exposure (i.e. shutter speed and aperture) were left at an automatic setting, allowing for the camera to self-adjust these settings for the conditions of the flights.

In order to assess image data quality, the signal-to-noise ratio (SNR) was computed. The SNR is an important parameter of remote sensing imagery, determining the quality of imagery that the camera is capable of collecting [46]. The SNR is commonly estimated by computing the mean pixel value to the standard deviation of a homogeneous area [46-47]. To test this, 4 Masonite boards with dimensions of 0.61m x 0.61m were painted with a flat white, flat black, flat brown, and Italian Olive color. Each color was chosen to replicate certain homogeneous features that would be found within a sorghum field (white representing maximum reflectance values, black for shadows, brown for soil, and Italian Olive for vegetation). Images of the boards were captured on a sunny day under the same conditions as the flights, and the ratio was computed for each band. After converting each ratio to decibels (dB), each band's SNR (over each panel) was averaged to produce an overall SNR, which was found to be 26 dB. Cameras over 20dB are considered high-quality research cameras [46, 48], so we therefore determined that the camera is capable of collecting suitable imagery for this study.

Image Processing

To process the images, we used Structure-from-Motion (SfM) photogrammetry. This technique allows for the production of 3-D surface models and orthomosaic image generation by processing a series of overlapping images [49]. The main steps in processing the imagery included image orthorectification, data extraction, and exportation for statistical analysis. Images taken via UAS were saved on an onboard SD card as 16-bit TIFF files and were tagged with GPS coordinates. UAS images were uploaded into Agisoft Metashape (Agisoft LLC, St. Petersburg, Russia; www.agisoft.com) where images were layered into multispectral images. Radiometric calibration converting digital numbers into reflectance values was conducted using a MicaSense

calibration panel. These images were then aligned by matching common features shared between photos, and a series of tie points were then computed into a sparse point cloud. RTK points were then placed onto each GCP to provide ground-reference points for more accurate alignment. A dense point cloud was then computed, followed by a digital elevation model, and finally an orthomosaic photo was produced. The end orthomosaic was produced as an unsigned 16-bit image, with the range of pixel values in each band ranging from 0 to 65,536 [50]. This process was repeated for each flight during this study. Each orthomosaic had a spatial resolution between 2.2 – 2.3 cm/pixel, and were then exported to ArcGIS Pro (ESRI inc., Redlands, California, USA; www.esri.com/en-us/arcgis/products/arcgis-pro/resources) for further analysis.

Field Determinations

Plant traits specifically related to biomass were chosen to be sampled through a destructive sampling process. These traits include fresh and dry aboveground whole plant biomass at varying growth stages during the reproductive period. Plant fractions were separated in leaves and stem during vegetative stages; and leaves, stem, and panicle (plus grain) during the reproductive stages. In addition, LAI at each sampling stage was measured, along with end-of-season yields.

Fresh biomass samples were taken at the flowering, soft dough, and physiological maturity growth stages, in the 3rd and 4th row of each plot. At each stage, all above-ground sorghum biomass within a 0.45 meters (m) length was sampled. Fresh weight of the samples was recorded, with subsequent partitioning of leaves, stems, and panicles. To determine LAI, 3 plants were chosen at random from the sampled plants, and each leaf from these plants was measured with a Licor 3100C leaf area meter (LICOR[®], Lincoln, Nebraska, United States;

www.licor.com). To obtain dry biomass measurements, all samples were oven-dried at 65° C until constant weight was achieved. At physiological maturity, rows 6 and 7 were machine harvested for final grain yield. Fresh and dry biomass measurements were adjusted to grams (g) m⁻², LAI to leaf area m⁻², and grain yield to kilograms (kg) hectare (ha)⁻¹.

For senescence, a sub-sample of 5 consecutive plants were set aside for ground-truth measurements in each plot. These plants were set aside in the 7th row of each plot. Leaf senescence was defined as the decrease in green color due to the breakdown of leaf chloroplasts [51], resulting in a certain percentage of leaf greenness loss for any given measurement stage. Each leaf on each plant was scored visually for leaf senescence on a scale of 100 (no visible senescence) to 0 (complete leaf mortality). Measurements were taken at soft dough, hard dough, and physiological maturity, and were made within 1-2 days of the flights to allow for comparisons in each growth stage. Measurements were taken from the 1st 8 leaves of the canopy, with the flag leaf being the first leaf measured. To ensure leaf senescence was measured from maximum leaf greenness to maturity, an additional set of ground measurements were taken at F, and only leaves that scored 100 at this stage were used for analysis. This proved effective, as almost all of the first 8 leaves showed no signs of senescence.

Prior to flights, elevated ground targets with dimensions of 0.3 m x 0.3 m were placed between the 5th and 6th row of each plot indicating the location of the ground-measured plants. Targets were placed exactly one row to the north of the plants to avoid casting shadows that would impede UAS data collection. In all cases, the width of the targets corresponded to the length of the measured plants, allowing for their locations to be identified when extracting data from the imagery.

Data Processing, Extraction, and Exportation

From the original orthomosaic data, image background noise was then removed via image classification. A supervised, pixel-based classification was chosen to allow the greatest user input in order to define classes. Each image was classified into four classes: sorghum leaves, shadows, soil, and grain heads. The only exception to this classification schema was the imagery collected at the F stage, which was classified as leaves, shadows, and soil because grain heads were not yet distinguishable from vegetation. As larger numbers of training samples are expected to increase supervised classification accuracies [52], 20 representative training sample polygons for each class were collected from each image. Separate training samples were generated for each orthomosaic to increase classification accuracies. A support vector machine algorithm was chosen for the classification, and a new raster image was created. Accuracy assessments were conducted using a stratified random sampling procedure with 500 total points. Accuracies for sorghum leaf classifications ranged between 88% and 95% correct for any given flight stage, indicating that vegetation was accurately classified when compared to a threshold of 85% [53].

After classification, each spectral band was extracted from the original orthomosaic. As outlined by Potgieter et al. [36], each band was extracted and was normalized between 0 and 1. To establish plot boundaries, shape-file polygons were drawn around both the whole plots and designated senescence plants, and data were extracted from each region. The average pixel value for each spectral band was extracted, and VIs were computed based on significant findings of spectral bands (see results section). Each band/VI was extracted with a conditional statement, allowing for only data to be extracted from the 'leaves' class to mask data from background features. The data were then exported for statistical analysis.

Statistical Analysis

Statistical analysis was conducted using R (R Core Team, Vienna, Austria; <https://www.R-project.org/>). To analyze spectral band relationships between biomass, yield, and LAI, simple correlation and regression analyses were used. The coefficient of determination (R^2) and root mean square error (RMSE) were also determined to verify the performance of the regression models [38]. For bands that were observed to be consistently significant, VIs were computed that composed of these bands to further investigate the relationships with ground-sampled data. From this data, either spectral bands or VIs were chosen for further analysis based on correlation and regression coefficient values. Hierarchical clustering was then used to cluster the significant spectral data into three distinct groups, based on Euclidean distance between clusters. To determine if significant differences existed in ground-sampled traits as defined by each cluster group, a one-way analysis of variance (ANOVA) was conducted using the mean of each cluster, comparing the effect of cluster groups on plant traits. A Tukey HSD test [54] was used to separate means from each cluster group.

To analyze senescence patterns, both correlation and simple regression analyses were used to determine the relation of spectral data to senescence scores at each growth stage. Each leaf that was scored for senescence was averaged into a “plant” score, with each plant score was averaged to form a “plot” score. The mean spectral band/VI score was correlated and regressed against the mean plot scores to determine significant relationships. In the same manner, the relationship between spectral data and post-flowering senescence rates was determined. Senescence rates were determined by subtracting the mean senescence score at maturity from mean scores at flowering, and spectral change rates were determined in the same manner [40]. As previously, hierarchical clustering using the R base package was used to divide each hybrid

into 3 groups based on spectral responses, and a 1-way ANOVA (comparing the effect of cluster on senescence/senescence rates) and Tukey HSD test conducted to determine significant differences in ground-measured scores. For all analyses, the ANOVAs and mean separations were computed using the “car” [55] and “agricolae” [56] R packages, respectively. All significance levels were set at $\alpha = 0.05$.

Results

Biomass, LAI, and yield traits

A variety of significant and non-significant results resulted from the correlation and regression analyses of the 5 spectral bands and field-measured plant traits (Table 3.1). The NIR band was seen to be the most consistently related to these traits across all growth stages. Weak to moderate relationships were observed between the NIR band and fresh biomass traits ($r = 0.36 - 0.61$; $r^2 = 0.10 - 0.37$; $RMSE = 0.01 - 0.02$). Most notably, the highest relationships were seen with fresh leaf biomass at each stage ($r = 0.51 - 0.61$; $r^2 = 0.26 - 0.37$). Weak to no significant relationships were observed with dry biomass at flowering, but total, stem, and leaf dry biomass were significantly related to the NIR band at the soft dough and maturity stages ($r = 0.30 - 0.46$; $r^2 = 0.09 - 0.21$). For LAI, weak correlations were observed between the blue and NIR bands at flowering, but were not significantly related at any other stage. As the blue band was significantly related to certain fresh and dry biomass traits for flowering and soft dough, these relationships were not statistically advantageous over the NIR band.

To investigate this further, the blue, green, red, and NIR band was chosen to create VIs to further investigate these relationships. The blue normalized difference vegetation index (BNDVI), green NDVI (GNDVI), NDVI, simple ratio (SR) and enhanced vegetation index (EVI) were all computed (Table 3.2). Results shown in Table 3.3 indicate significant relationships between the EVI and fresh biomass traits across all measured growth stages, ($r = 0.28 - 0.50$, $r^2 = 0.08 - 0.25$, $RMSE = 0.02 - 0.04$), with the exception of leaf fresh biomass at soft dough. In addition, significant relationships with fresh biomass traits were observed with the GNDVI at flowering ($r = 0.39$, $r^2 = 0.15 - 0.16$, $RMSE = 0.01$), and with the SR at M ($r = 0.29 - 0.34$, $r^2 = 0.09 - 0.11$, $RMSE = 0.43 - 0.44$). Total, leaf, and stem dry biomass was significant

for the EVI ($r = 0.31 - 0.39$, $r^2 = 0.10 - 0.15$, $RMSE = 0.03$) and SR ($r = 0.30 - 0.33$, $r^2 = 0.09 - 0.11$, $RMSE = 0.43 - 0.44$) at maturity. As a whole, it was determined that the NIR band was more consistently significant with biomass traits than the VIs, so it was selected for further analysis.

For each growth stage, the mean NIR band value for each hybrid was hierarchically clustered, and each hybrid was divided into three groups (1-3). The mean ground-sampled trait for each cluster group was then analyzed via ANOVA and separated with the Tukey HSD test for traits found significant in the previous correlation and regression analyses (Table 3.4). Within the assigned clusters, significant differences were seen with fresh and dry leaf biomass for all growth stages. No comparisons were made with total and stem dry biomass at flowering because it was not significantly related with NIR data at flowering, and no significant differences were seen between groups at soft dough or physiological maturity. For both total and stem fresh biomass, significant differences were only seen between groups at maturity. LAI mean separations at flowering revealed no significant differences, with no further comparisons made due to insignificant relationships with NIR data.

As demonstrated in table 4, it was discovered that the GNDVI ($r = 0.39 - 0.56$, $r^2 = 0.15 - 0.31$, $RMSE = 0.01 - 0.02$) and the SR ($r = 0.30 - 0.56$, $r^2 = 0.09 - 0.32$, $RMSE = 0.44 - 0.48$) were the most related to final grain yields throughout the post-flowering grow stages. As multispectral data taken at flowering has been found to be the most correlated to final grain yield in previous grain sorghum studies [38, 62], the GNDVI was used for further analysis since it was found to be the most related to yield at flowering in our study ($r = 0.56$, $r^2 = 0.31$, $RMSE = 0.01$). The mean GNDVI scores for each hybrid was clustered and divided into three distinct groups (Figure 3.3). Through the ANOVA to determine yield differences, we found no significant

differences between clusters ($F = 0.001$, $p = 0.97$). To determine if there were significant differences among yield that the cluster groups may have overlooked, an additional 1-way ANOVA was conducted to test the effect of hybrid on yield without clustering. No significant yield differences were found among the hybrids in this study ($F = 1.70$, $p = 0.09$).

Senescence

During data analysis, it was discovered that the panel we used to calibrate the images was highly reflective. There was a very high level of saturation in the NIR band in the boundaries drawn around the senescence plants, but there was very little saturation in the RGB bands. Therefore, VIs were computed using the RGB bands, including the excess green index (ExG), normalized difference index (NDI), excess green minus excess red index (ExGR), visible atmospherically resistant index (VARI), and the green leaf index (GLI) (Table 3.5).

When regressing the individual bands, there were no statistical differences observed with ground-truth scores (data not shown). However, significant relationships were discovered when regressing the RGB VIs chosen for this study (Table 3.6). At maturity, the most significant VIs were the NDI ($r = 0.57$, $r^2 = 0.33$, $RMSE = 0.03$), VARI (0.60 , $r^2 = 0.36$, $RMSE = 0.05$) and GLI ($r = 0.48$, $r^2 = 0.23$, $RMSE = 0.03$), with the VARI being selected for further cluster analysis. Dividing the resulting dendrogram into 3 groups, the ANOVA analysis showed no statistical differences between clusters ($F = 0.53$, $p = 0.47$). Similarly, an ANOVA analysis comparing the effect of hybrid on senescence scores at maturity showed no statistical differences amongst scores at physiological maturity ($F = 1.41$, $p = 0.18$). In the same manner, senescence and VI change rates were analyzed, and the VARI was again found to be the most significantly related to post-flowering senescence rates ($r = 0.42$, $r^2 = 0.18$, $RMSE = 0.05$). ANOVA analysis showed

no difference among clusters ($F = 0.21$, $p = 0.65$), and ANOVA analysis comparing the effect of hybrid on senescence rate revealed no significant differences in senescence rates in hybrids used for this study ($F = 1.88$, $p = 0.05$).

Discussion

We have introduced a methodology for sorghum researchers to follow in order to collect, process, extract, and analyze multispectral data for more efficient screening of large-scale grain sorghum breeding plots for traits associated with SG. As UAS have become a more cost-effective method of obtaining very high spatial resolution imagery for such evaluations [69], there is a need for specific methodologies to be developed for sorghum breeders to use this technology for rapid identification of the SG trait. If breeders are able to screen thousands of breeding lines quickly and effectively for this trait, improvements to current grain sorghum hybrids needed to sustain future demands can potentially be made in a much shorter period of time.

When compared to non-SG grain sorghum lines, SG sorghum lines have been related to increased yield and biomass production under heat and water stress [70]. In our methodology, we were able to find significant differences in fresh and dry biomass traits among cluster groups, as defined by the NIR band. While RGB and NIR data is most frequently combined to produce VIs, the NIR band has been already reported to be significantly correlated with above-ground sorghum biomass [71]. In this study, clear differences between fresh and dry leaf biomass cluster groups were observed for each measurement date, a result that was not surprising given that sorghum leaves were highly visible to the camera. Because the hybrids used in this study were not specifically chosen due to known differences in biomass traits, further research is needed to

validate this methodology for robustness in determining differences in each trait measured for this study. In addition, VI correlation and regression coefficients in this study were much lower than what has been previously reported for sorghum fresh biomass [71-72], LAI [38], and dry biomass [72].

Our results demonstrated that at flowering, yield was best predicted with the GNDVI. As the GNDVI has been shown to be a strong predictor of crop yield in previous works [73-77], these results were not surprising. The GNDVI has been shown to be sensitive to plant chlorophyll concentrations [78-79], which has been found to be directly related to end-of-season grain yields [80-81]. Previous studies have found that spectral data taken at flowering have produced the highest correlations with sorghum final grain yield [38, 62], which is why we chose to determine clusters with spectral data from this growth stage. Despite a trend of historical yield improvement for the hybrids used in this study [82], hybrids in this study were not selected specifically for yield differences. Therefore, further work should be conducted among hybrids with known yield differences to determine if clusters are able to detect significant differences.

In terms of quantifying senescence and senescence rates, our results indicate that RGB imagery alone may be useful in quantifying and characterizing grain sorghum senescence at maturity. In many cases, UAV RGB imagery may be desired over multispectral sensors due to their comparably lower costs [83]. In terms of evaluating for the SG trait, grain sorghum greenness at PM has been labeled as a very good indicator of SG, and has been successfully used to select for drought tolerance in previous sorghum breeding trials [31, 84]. In our study, the highest linear relationships between RGB VI data and senescence scores were observed at maturity. As sorghum plants do not typically completely senesce unless terminated by external factors such as freezing temperatures [85], senescence patterns are considerably less pronounced

when compared to annual crops such as corn and soybeans. This is probably the main reason why sorghum senescence was not well detected at soft dough and hard dough stages in our study. Many studies have previously used VIs such as the normalized difference red edge (NDRE) index to evaluate crop senescence rates by evaluating the spectral differences from flowering to maturity [36, 40, 86]. Although we did observe the VARI to be significantly related to post-flowering senescence rates, we did not observe significant differences in hybrid senescence rates. As none of the hybrids in this study have not been previously observed to have differing senescence rates, further work should be investigated to determine if significant differences in both senescence scores by growth stage and post-flowering senescence rates can be differentiated using this methodology.

In situations where very dense vegetation canopies are present, it can be difficult to get accurate VI data with the NIR band. This is because of a well-documented phenomenon involving the “leveling off” or saturation of reflected NIR in dense vegetative canopies [67, 87], making it difficult to detect changes in plant chlorophyll in these scenarios. In canopies with percent vegetation fractions greater than 50%, the NDI and VARI have been shown to be more linearly related to vegetation than indices using NIR reflectance [66]. In sorghum breeding trials with very dense canopies, the NDI or VARI could be useful in detecting rates of senescence at physiological maturity. In environments with limited precipitation, canopy sizes are usually smaller and saturation is not perceived as a problem [88]. As the SG trait is generally assessed in these environments, further research is needed to evaluate senescence detection for these VIs under such conditions.

The likely explanation for our low correlation and regression coefficients with biomass, LAI, and yield can be traced back to the problems we experienced with the calibration panel. As

the panel was highly reflective, most of our NIR data was highly saturated, depending on the flight date. This issue also prevented us from investigating VIs that have been previously related to senescence (i.e. NDRE). We anticipate that stronger relationships could be detected in future research if proper calibration equipment is used for radiometric calibration. Additionally, as one of the specific goals for this study was to develop a methodology that could be used by SG breeders, we focused on this and did not have any hybrids that were known to have the SG trait. To use UAV imagery effectively in large-scale sorghum breeding trials, the ability to distinguish between senescence rates of SG and non-SG plots is very important. Further research should be conducted to evaluate this methodology's ability to distinguish differences in sorghum hybrids based on the known presence or absence of the SG trait. Key to analyzing all traits in this study is the use of hierarchical clustering to select hybrids of interest. In breeding trials with thousands of hybrid plots, a cluster analysis can be used to group hybrids with spectral similarities, allowing for hybrids of interest to be investigated with ground-truth evaluation. In theory, this would eliminate the need to investigate every plot, which has the potential to save time, money, labor, and other resources. If subjected to further testing, this methodology shows potential for greatly assisting sorghum breeders looking for traits associated with SG.

Limitations

Within this study, there are some limitations that should be discussed. First, in terms of the senescence patterns, there were minor variations observed in the field among senescence patterns in the hybrids used for this study. As demonstrated by Potgieter et al. [36], sorghum lines with different rates of SG-induced senescence should be more easily evaluated for screening SG senescence. As SG delays in senescence are best observed under drought stress [9,

84], it is possible that SG senescence patterns were not able to be observed due to plentiful rainfall in the 2019 growing season. Future studies using this methodology should be done in precipitation-limited conditions in order to obtain maximum SG expression. This can be done in controlled environments such as using rain shelters to simulate these conditions. More studies in more locations are necessary to further investigate this methodology for SG evaluation.

In order to collect visual senescence scores, the top 8 leaves of the canopy were estimated based on percentage of senescence, and the average of these scores were used to compare with extracted spectral data. A different method to calculate leaf senescence should be evaluated with the data collected from this study. In addition, the UAS depth of detection into the sorghum canopy remains to be studied. As each leaf was measured, it remains possible to perform a sensitivity analysis to determine if leaves closer to the top of the canopy would result in significant relationships with spectral data.

Due to the highly-reflective panel used for radiometric calibration, a high saturation of our data was observed. Because of this saturation, we were unable to obtain highly significant relationships between NIR-based VIs and ground-measured plant traits. Future corrections on this methodology should involve the use of a less-reflective calibration panel, which would help to prevent said saturation.

Conclusions

This study presents a methodology to improve grain sorghum characterization in regard to biomass, yield, and senescence characterization using a consumer-available UAS camera. Results in this study shows potential that through hierarchical clustering of sorghum spectral responses, it is possible to group hybrids with significant differences in various measured traits.

The NIR band was found significantly related to various biomass traits, including fresh/dry total biomass and leaf biomass. For senescence evaluation, the VARI was observed to have the strongest relation with senescence scores at physiological maturity, as well as post-flowering senescence changes. As this methodology has led to the extraction of significant spectral relationships with biomass, grain yield, and senescence scores, we anticipate that with further evaluation, this methodology could greatly assist sorghum breeders in locating genotypes of interest in large-scale sorghum SG breeding trials.

References

1. Voss-Fels, K.P.; Stahl, A.; Hickey, L.T. Q&A: modern crop breeding for future food security. *BMC Biol.* **2019**, *17*. doi: 10.1186/s12915-019-0638-4
2. Ortez-Amador, O.A. Study of Nitrogen Limitation and Seed Nitrogen Sources for Historical and Modern Genotypes in Soybean. M.Sc. Thesis, Kansas State University, Manhattan, Kansas, United States, **2018**.
3. Li, H.; Rasheed, A.; Hickey, L.T.; He, Z. Fast-forwarding genetic gain. *Trends Plant Sci.* **2018**, *23*, 184-186. doi: 10.1016/j.tplants.2018.01.007
4. Challinor, A.J.; Watson, J.; Lobell, D.B.; Howden, S.M.; Smith, D.R.; Chhetri, N. A meta-analysis of crop yield under climate change and adaptation. *Nat. Clim. Change* **2014**, *4*, 287-291. doi: 10.1038/nclimate2153
5. Hall, A.E.; Ziska, L.H. Crop Breeding Strategies for the 21st Century. In *Climate Change and Global Crop Productivity*, 1st ed.; Reddy, K.R., Hodges, H.F., Eds.; CABI Publishing: New York, USA, **2000**; pp 407-423.
6. Stefoska-Needham, A.; Beck, E.J.; Johnson, S.K.; Tapsell, L.C. Sorghum: An Underutilized Cereal Whole Grain with the Potential to Assist in the Prevention of Chronic Disease. *Food Rev. Int.* **2015**, *31*, 401-437.
7. Harris, K.; Subudhi, P.K.; Borrell, A.; Jordan, D.; Rosenow, D.; Nguyen, H.; Klein, P.; Klein, R.; Mullet, J. Sorghum stay-green QTL individually reduce post-flowering drought-induced leaf senescence. *J. Exp. Bot.* **2007**, *58*, 327-338. doi: 10.1093/jxb/erl225
8. Kassahun, B.; Bidinger, F.R.; Hash, C.T.; Kuruvinashetti, M.S. Stay-green expression in early generation sorghum [*Sorghum bicolor* (L.) Moench] QTL introgression lines. *Euphytica*, **2010**, *172*, 351-362. doi: 10.1007/s10681-009-0108-0
9. Jordan, D.R.; Hunt, C.H.; Cruickshank, A.W.; Borrell, A.K.; Henzell, R.G. The relationship between the stay-green trait and grain yield in elite sorghum hybrids grown in a range of environments. *Crop Sci.* **2012**, *52*, 1153-1161. doi: 10.2135/cropsci2011.06.0326
10. Turner, M.F.; Heuberger, A.L.; Kirkwood, J.S.; Collins, C.C.; Wolfrum, E.J.; Broeckling, C.D.; Prenni, J.E.; Jahn, C.E. Non-targeted metabolomics in diverse sorghum breeding lines indicates primary and secondary metabolite profiles are associated with plant

- biomass accumulation and photosynthesis. *Front. Plant Sci.* **2016**, 7, 953-969. doi: 10.3389/fpls.2016.00953
11. Thomas, H.; Howarth, C.J. Five ways to stay green. *J. Exp. Bot.* **2000**, 51, 329-337. doi: 10.1093/jexbot/51.suppl_1.329
 12. Ongom, P. Association mapping of gene regions for drought tolerance and agronomic traits in sorghum. Ph.D. dissertation, Purdue University, West Lafayette, Indiana, United States, 2015
 13. Sanchez, A.C.; Subudhi, P.K.; Rosenow, D.T.; Nguyen, H.T. Mapping QTLs associated with drought resistance in sorghum (*Sorghum bicolor* L. Moench). *Plant Mol. Biol.* **2002**, 48, 713-726. doi: 10.1023/a:1014894130270
 14. Staggenborg, S.; Dhuyvetter, K.C.; Gordon, W.B. Grain sorghum and corn comparisons: yield, economic, and environmental responses. *Agron. J.* **2008**, 100, 1600-1604. doi: 10.2134/agronj2008.0129
 15. Mundia, C.W.; Secchi, S.; Akamani, K.; Wang, G. A regional comparison of factors affecting global sorghum production: the case of north america, asia and africa's sahel. *Sustainability-Basel* **2019**, 11, 2135-2152. doi: 10.3390/su11072135
 16. Teferra, T.F.; Awika, J.M. Sorghum as a healthy global food security crop: opportunities and challenges. *Cereal Food. World* **2019**, 64. doi: 10.1094/CFW-64-5-0054
 17. Joint FAO/IAEA Programme; Nuclear Techniques in Food and Agriculture. Sorghum Mutation Breeding for Improving Tolerance to Abiotic Stresses brought about by Climate Change. Available online: <http://www-naweb.iaea.org/nafa/news/pbg-sorghum-mutation.html> (accessed on 2 July **2020**)
 18. Digest Project. Breeding Sorghum for Improved Resistance to Biotic and Abiotic Stresses and Enhanced End. Available online: <http://crsps.net/resource/breeding-sorghum-for-improved-resistance-to-biotic-and-abiotic-stresses-and-enhanced-end-use-characteristics-for-southern-africa/> (accessed on 2 July **2020**)
 19. Rosenow, D.T.; Quisenberry, J.E.; Wendt, C.W.; Clark, L.E. Drought tolerant sorghum and cotton germplasm. *Agr. Water Manage.* **1983**, 7, 207-222. doi: 0.1016/0378-3774(83)90084-7

20. Rosenow, D.T. Breeding sorghum for drought resistance. In *Food Grain Production in Semi Arid Africa*; Menyoga, J.M., Bezuneh, T., Youdeowei, A., Eds.; OAU-STRC/SAFGRAD, Ouagadougou, Burkina Faso, **1987**, pp. 83-89
21. Evangelista, C.C.; Tangonan, N.G. Reaction of 31 non-senescent sorghum genotypes to stalk rot complex in southern Philippines. *Trop. Pest Manage.* **1990**, 36, 214-215. doi: 10.1080/09670879009371474
22. Subudhi, P.K.; Rosenow, D.T.; Nguyen, H.T. Quantitative trait loci for the stay green trait in sorghum (*Sorghum bicolor* L. Moench): consistency across genetic backgrounds and environments. *Theor. Appl. Genet.* **2000**, 101, 733-741. doi: 10.1007/s001220051538
23. Joshi, A.K.; Kumari, M.; Singh, V.P.; Reddy, C.M.; Kumar, S.; Rane, J.; Chand, R. Stay green trait: variation, inheritance and its association with spot blotch resistant in spring wheat (*Triticum aestivum* L.). *Euphytica* **2007**, 153, 59-71. doi: 10.1007/s10681-006-9235-z
24. Tao, Y.Z.; Henzell, R.G.; Jordan, D.R.; Butler, D.G.; Kelly, A.M.; McIntyre, C.L. Identification of genomic regions associated with stay green in sorghum by testing RILs in multiple environments. *Theor. Appl. Genet.* **2000**, 100, 1225-1232. doi: 10.1007/s001220051428
25. Thomas, H.; Ougham, H. The stay-green trait. *J. Exp. Bot.* **2014**, 65, 3889-3900. doi: 10.1093/jxb/eru037
26. Clifton-Brown, J.C.; Lewandowski, I.; Bangerth, F.; Jones, M.B. Comparative responses to water stress in stay-green, rapid- and slow senescing genotypes of the biomass crop, *Miscanthus*. *New Phytol.* **2002**, 154, 335-345. doi: 10.1046/j.1469-8137.2002.00381.x
27. Duvick, D.N.; Smith, J.S.C.; Cooper, M. Long-Term Selection in a Commercial Hybrid Maize Breeding Program. In *Plant Breeding Reviews Part 2: Long-term Selection: Crops, Animals, and Bacteria*; Janick, J., Ed.; John Wiley & Sons, Inc., **2004**, pp. 109-149
28. Edgerton, M.D. Increasing Crop Productivity to Meet Global Needs for Feed, Food, and Fuel. *Plant Physiol.* **2009**, 149, 7-13. doi: 10.1104/pp.108.130195
29. Shakoor, N.; Lee, S.; Mockler, T.C. High throughput phenotyping to accelerate crop breeding and monitoring of diseases in the field. *Curr. Opin. Plant Biol.* **2017**, 38, 184-192. doi: 10.1016/j.pbi.2017.05.006

30. Bogard, M.; Jourdan, M.; Allard, V.; Martre, P.; Perretant, M.R.; Ravel, C.; Heumez, E.; Orford, S.; Snape, J.; Griffiths, S.; Gaju, O.; Foulkes, J.; Le Gouis, J. Anthesis date mainly explained correlations between post-anthesis leaf senescence, grain yield, and grain protein concentration in a winter wheat population segregating for flowering time QTLs. *J. Exp. Bot.* **2011**, 62, 3621-3636. doi: 10.1093/jxb/err061
31. Wanous, M.K.; Miller, F.R.; Rosenow, D.T. Evaluation of Visual Rating Scales for Green Leaf Retention in Sorghum. *Crop Sci.* **1991**, 31, 1691-1694. doi: 10.2135/cropsci1991.0011183X003100060063x
32. Araus, J.L.; Cairns, J.E. Field high-throughput phenotyping: the new crop breeding frontier. *Trends Plant Sci.* **2014**, 19, 52-61. doi: 10.1016/j.tplants.2013.09.008
33. Buitrago, M.F.; Skidmore, A.K.; Groen, T.A.; Hecker, C.A. Connecting infrared spectra with plant traits to identify species. *ISPRS J. Photogramm.* **2018**, 139, 183-200. doi: 10.1016/j.isprsjprs.2018.03.013
34. Lu, D. The potential and challenge of remote sensing-based biomass estimation. *Int. J. Remote Sens.* **2006**, 27, 1297-1328. doi: 10.1080/01431160500486732
35. Garrigues, S.; Lacaze, R.; Baret, F.; Morisette, J.T.; Weiss, M.; Nickeson, J.E.; Fernandes, R.; Plummer, S.; Shabanov, N.V.; Myneni, R.B.; Knyazikhin, Y.; Yang, W. Validation and Intercomparison of global Leaf Area Index products derived from remote sensing data. *J. Geophys. Res.* **2008**, 113, G02028. doi: 10.1029/2007JG000635
36. Potgieter, A.B.; George-Jaeggli, B.; Chapman, S.C.; Laws, K.; Cadavid, L.A.S.; Wixted, J.; Watson, J.; Eldridge, M.; Jordan, D.R.; Hammer, G.L. Unmanned aerial vehicle enables the assessment of seasonal leaf area dynamics of sorghum breeding lines. *Front. Plant Sci.* **2017**, 8, 1532. doi: 10.3389/fpls.2017.01532
37. Shanahan, J.F.; Schepers, J.S.; Francis, D.D.; Varvel, G.E.; Wilhelm, W.W.; Tringe, J.M.; Schlemmer, M.R.; Major, D.J. use of remote sensing imagery to estimate corn grain yield. *Agron. J.* **2001**, 93, 583-589. doi: 10.2134/agronj2001.933583x
38. Shafian, S.; Rajan, N.; Schnell, R.; Bagavathiannan, M.; Valasek, J.; Shi, Y.; Olsenholler, J. Unmanned aerial systems-based remote sensing for monitoring sorghum growth and development. *PLoS ONE* **2018**. doi: 10.1371/journal.pone.0196605

39. Zhang, C.; Kovacs, J.M. The application of small unmanned aerial systems for precision agriculture: a review. *Precis. Agric.* **2012**, *13*, 693-712. doi: 10.1007/s11119-012-9274-5
40. Hassan, M.A.; Yang, M.; Rasheed, A.; Jin, X.; Xia, X.; Xiao, Y.; He, Z. Time-series multispectral indices from unmanned aerial vehicle reveal senescence rate in bread wheat. *Remote Sensing* **2018**, *10*, 809. doi: 10.3390/rs10060809
41. Di Bella, C.M.; Paruelo, J.M.; Becerera, J.E.; Bacour, C.; Baret, F. Effect of senescent leaves on NDVI-based estimates of fAPAR: Experimental and modelling evidences. *Int. J. Remote Sens.* **2004**, *25*, 5415-5427. doi: 10.1080/01431160412331269724
42. Curran, J.P. Multispectral remote sensing for the estimation of green leaf area index. *Phil. Trans. R. Soc. Lond. A.* **1983**, *309*, 257-270. doi: 10.1098/rsta.1983.0039
43. Gitelson, A.; Merzlyak, M.N. Spectral reflectance changes associated with autumn senescence of *Aesculus hippocastanum* L. and *Acer platanoides* L. leaves. spectral features and relation to chlorophyll estimation. *J. Plant Physiol.* **1994**, *143*, 286-292. doi: 10.1016/S0176-1617(11)81633-0
44. Belanger, M.J.; Miller, J.R.; Boyer, M.G. Comparative relationships between some red edge parameters and seasonal leaf chlorophyll concentrations. *Int. J. Remote Sens.* **1995**, *21*, 16-21. doi: 10.1080/07038992.1995.10874592
45. Boyer, M.; Miller, J.; Belanger, M.; Hare, E.; Wu, J. Senescence and spectral reflectance in leaves of northern pin oak (*Quercus palustris* Muenchh.). *Remote Sens. Environ.* **1988**, *25*, 71-87. doi: 10.1016/0034-4257(88)90042-9
46. Lu, B.; He, Y. Species classification using Unmanned Aerial Vehicle (UAV)-acquired high spatial resolution imagery in a heterogeneous grassland. *ISPRS J. Photogramm.* **2017**, *128*, 73-85. doi: 10.1016/j.isprsjprs.2017.03.011
47. Hruska, R.; Mitchell, J.; Anderson, M.; Glenn, N.F. Radiometric and geometric analysis of hyperspectral imagery acquired from an unmanned aerial vehicle. *Remote Sens.* **2012**, *4*, 2736-2752. doi: 10.3390/rs4092736
48. Johnson, D.H. Signal-to-noise ratio. *Scholarpedia* **2006**, *1*, 2088. doi: 10.4249/scholarpedia.2088

49. Westoby, M.J.; Brasington, J.; Glasser, N.F.; Hambrey, M.J.; Reynolds, J.M. ‘Structure-from-Motion’ photogrammetry: A low-cost, effective tool for geoscience applications. *Geomorphology* **2012**, 179, 300-314. doi: 10.1016/j.geomorph.2012.08.021
50. Overview of histograms and how they are used in Atlas. Available online: <https://support.micasense.com/hc/en-us/articles/224896827-Overview-of-histograms-and-how-they-are-used-in-Atlas> (accessed on 9 April **2020**)
51. Lim, P.O.; Kim, H.J.; Nam, H.G. Leaf senescence. *Annu. Rev. Plant Biol.* **2007**, 58, 115-136. doi: 10.1146/annurev.arplant.57.032905.105316
52. Perumal, K.; Bhaskaran, R. SVM-based effective land use classification system for multispectral remote sensing images. *IJCSIS* **2009**, 6, 95-107.
53. Foody, G.M. SVM-based effective land use classification system for multispectral remote sensing images. *Int. J. Remote Sens.* **2005**, 26, 1217-1228. doi: 10.1080/01431160512331326521
54. Haynes, W. Tukey’s test. In *Encyclopedia of Systems Biology*; Dubitzky, W., Wolkenhauer, O., Cho, K.H., Yokota, H., Eds.; Springer, New York, New York, United States, **2013**.
55. Fox, J.; Weisberg, S. *An {R} Companion to Applied Regression*, 3rd edition. Sage, Thousand Oaks, California, United States, **2019**.
<https://socialsciences.mcmaster.ca/jfox/Books/Companion/>
56. agricolae: Statistical Procedures for Agricultural Research. Available online: <https://cran.r-project.org/web/packages/agricolae/index.html> (Accessed 10 July **2020**)
57. Van der Merwe, D.; Price, K.P. Harmful algal bloom characterization at ultra-high spatial and temporal resolution using small unmanned aircraft systems. *Toxins* **2015**, 7, 1065-1078. doi: doi.org/10.3390/toxins7041065
58. Basso, M.; Stocchero, D.; Henriques, R.V.B.; Vian, A.L.; Bredemeier, C.; Konzen, A.A.; de Freitas, E.P. Proposal for an embedded system architecture using a GNDVI algorithm to support uav-based agrochemical spraying. *Sensors* **2019**, 19. doi: 10.3390/s19245397
59. Rouse, J.; Haas, R.; Schell, J.; Deering, D. Monitoring vegetation systems in the great plains with ERTS. In *Third Earth Resources Technology Satellite-1 Symposium, Volume*

I: Technical Presentations, section A; Freden, S.C., Mercanti, E.P., Becker, M.A., eds.; NASA, **1974**, pp. 309-317.

60. Sternberg, P.; Rautiainen, M.; Manninem, T.; Voipio, P.; Smolander, H. Reduced simple ratio better than ndvi for estimating lai in finnish pine and spruce stands. *Silva Fenn.* **2004**, 38, 3-14. doi: 10.14214/sf.431
61. Ali, S.M.; Salman, S.S. Estimating the yield of rice farms in southern iraq using landsat images. *Int. J. Sci. Eng. Res.* **2015**, 6, 1607-1614. doi: 10.13140/RG.2.1.3121.6806
62. Yang, C.; Everitt, J.H. Relationships between yield monitor data and airborne multirate multispectral digital imagery for grain sorghum. *Precis. Agric.* **2002**, 3, 373-388. doi: 10.1023/A:1021544906167
63. Zhao, B.; Zhang, J.; Yang, C.; Zhou, G.; Ding, Y.; Shi, Y.; Zhang, D.; Xie, J.; Liao, Q. Rapeseed seedling stand counting and seeding performance evaluation at two early growth stages based on unmanned aerial vehicle imagery. *Front. Plant Sci.* **2018**, 9, 1362. doi: 10.3389/fpls.2018.01362
64. Woebbecke, D.M.; Meyer, G.E.; Von Bargen, K.; Mortensen, D.A. Color indices for weed identification under various soil, residue, and lighting conditions. *T. ASAE.* **1995**, 38, 259-269.
65. Meyer, G.E.; Neto, J.C. Verification of color vegetation indices for automated crop imaging applications. *Comput. Electron. Agr.* **2008**, 63, 282-293. doi: 10.1016/j.compag.2008.03.009
66. Gitelson, A.A.; Kaufman, Y.J.; Stark, R.; Rundquist, D. Novel algorithms for remote estimation of vegetation fraction. *Remote Sens. Environ.* **2002**, 80, 76-87. doi: 10.1016/S0034-4257(01)00289-9
67. Zhang, J.; Virk, S.; Porter, W.; Kenworthy, K.; Sullivan, D.; Schwartz, B. Applications of unmanned aerial vehicle based imagery in turfgrass field trials. *Front. Plant Sci.* **2019**, 10, 279. doi: 10.3389/fpls.2019.00279
68. Louhaichi, M.; Borman, M.M.; Johnson, D.E. Spatially located platform and aerial photography for documentation of grazing impacts on wheat. *Geocarto Int.* **2001**, 16, 65-70. doi: 10.1080/10106040108542184

69. Holman, F.H.; Riche, A.B.; Michalski, A.; Castle, M.; Wooster, M.J.; Hawkesford, M.J. High throughput field phenotyping of wheat plant height and growth rate in field plot trials using uav based remote sensing. *Remote Sens.* **2016**, *8*, 1031. doi: 10.3390/rs8121031
70. Borrell, A.K.; Hammer, G.L.; Henzell, R.G. Does maintaining green leaf area in sorghum improve yield under drought? ii. dry matter production and yield. *Crop Sci.* **2000**, *40*, 1037-1048. doi: 10.2135/cropsci2000.4041037x
71. Sui, R.; Hartley, B.E.; Gibson, J.M.; Yang, C.; Thomasson, J.A.; Searcy, S.W. High-biomass sorghum yield estimate with aerial imagery. *J. Appl. Remote Sens.* **2011**, *5*, 053523. doi: 10.1117/1.3586795
72. Li, J.; Shi, Y.; Veeranampalayam-Sivakumar, A.N.; Schachtman, D.P. Elucidating sorghum biomass, nitrogen and chlorophyll contents with spectral and morphological traits derived from unmanned aircraft system. *Front. Plant Sci.* **2018**, *9*, 1406. doi: 10.3389/fpls.2018.01406
73. Shanahan, J.F.; Schepers, J.S.; Francis, D.D.; Varvel, G.E.; Wilhelm, W.W.; Tringe, J.M.; Schlemmer, M.R.; Major, D.J. Use of remote-sensing imagery to estimate corn grain yield. *Agron. J.* **2001**, *93*, 583-589. doi: 10.2134/agronj2001.933583x
74. Rahman, M.M.; Robson, A.J. A novel approach for sugarcane yield prediction using landsat time series imagery: a case study on Bundaberg region. *Advances in Remote Sensing* **2016**, *5*, 93-102. doi: 10.4236/ars.2016.52008
75. Pradhan, S.; Bandyopadhyay, K.K.; Joshi, D.K. Canopy reflectance spectra of wheat as related to crop yield, grain protein under different management practices. *J. Agrometeorol.* **2012**, *14*, 21-25.
76. Yang, C.; Everitt, J.H.; Bradford, J.M. Using multispectral imagery and linear spectral unmixing techniques for estimating crop yield variability. *T. ASABE.* **2007**, *50*, 667-674. doi: 10.13031/2013.22658
77. Moges, S.M.; Raun, W.R.; Mullen, R.W.; Freeman, K.W.; Johnson, G.V.; Solie, J.B. Evaluation of green, red, and near infrared bands for predicting winter wheat biomass, nitrogen uptake, and final grain yield. *J. Plant Nutr.* **2005**, *27*, 1431-1441. doi: 10.1081/PLN-200025858

78. Kayad, A.; Sozzi, M.; Gatto, S.; Marinello, F.; Pirotti, F. Monitoring within-field variability of corn yield using sentinel-2 and machine learning techniques. *Remote Sens.* **2019**, *11*, 2873. doi: 10.3390/rs11232873
79. Gitelson, A.A.; Kaufman, Y.J.; Merzlyak, M.N. Use of a green channel in remote sensing of global vegetation from EOS- MODIS. *Remote Sens. Environ.* **1996**, *58*, 289-298.
80. Ramesh, K.; Chandrasekaran, B.; Balasubramanian, T.N.; Bangarusamy, U.; Sivasamy, R.; Sankaran, N. Chlorophyll dynamics in rice (*Oryza sativa*) before and after flowering based on SPAD (chlorophyll) meter monitoring and its relation with grain yield. *J. Agron. Crop Sci.* **2002**, *188*, 102-105. doi: 10.1046/j.1439-037X.2002.00532.x
81. Gonçalves da Silva, M.A.; Muniz, A.S.; Mannigel, A.R.; Porto, S.M.A.; Marchetti, M.E.; Nolla, A.; Grannemann, I. Monitoring and evaluation of need for nitrogen fertilizer topdressing for maize leaf chlorophyll readings and the relationship with grain yield. *Braz. Arch. Biol. Technol.* **2011**, *54*, 665-674. doi: 10.1590/S1516-89132011000400004
82. Demarco, P.A.; Mayor, L.; Tamagno, S.; Fernandez, J.A.; Prasad, P.V.V.; Rotundo, J.L.; Messina, C.D.; Ciampitti, I.A. Physiological changes across historical sorghum hybrids released during the last six decades. *Kansas Agr. Exp. St. Res. Rep.* **2020**, *6*, doi: 10.4148/2378-5977.7925
83. Makanza, R.; Zaman-Allah, M.; Cairns, J.E.; Magorokosho, C.; Tarekegne, A.; Olsen, M.; Prasanna, B.M. High-throughput phenotyping of canopy cover and senescence in maize field trials using aerial digital canopy imaging. *Remote Sens.* **2018**, *10*, 330. doi: 10.3390/rs10020330
84. Borrell, A.K.; Hammer, G.L.; Douglas, A.C.L. Does maintaining green leaf area in sorghum improve yield under drought? i. leaf growth and senescence. *Crop Sci.* **2000**, *40*, 1026-1037. doi: 10.2135/cropsci2000.4041026x
85. Regehr, D. Preharvest desiccants for sorghum. In *Grain Sorghum Production Handbook*, Kansas State University Agricultural Experiment Station and Cooperative Extension Service, Manhattan, Kansas, United States, **1998**, pp. 23-24.
86. Potgieter, A.B.; Watson, J.; Eldridgex M.; Laws, K.; George-Gaeggli, B.; Hunt, C.; Borrell, A.; Mace, E.; Chapman, S.; Jordan, D.; Hammer, G.L. Determining crop growth dynamics in sorghum breeding trials through remote and proximal sensing technologies. In Proceedings of the IGARSS 2018 – 2018 IEEE International Geoscience and Remote

Sensing Symposium, Valencia, Spain, **2018**. pp. 8244-8247. doi:
10.1109/IGARSS.2018.8519296

87. Gitelson, A.A. Wide dynamic range vegetation index for remote quantification of biophysical characteristics of vegetation. *J. Plant Physiol.* **2004**, 161, 165-173. doi: 10.1078/0176-1617-01176
88. Montazeaud, G.; Karatoğma, H.; Öztürk, I.; Romut, P.; Ecartot, M.; Crossa, J.; Özer, E.; Özdemir, F.; Lopes, M.S. Predicting wheat maturity and stay-green parameters by modeling spectral reflectance measurements and their contribution to grain yield under rainfed conditions. *Field Crop. Res.* **2016**, 196, 191-198. doi: 10.1016/j.fcr.2016.06.021

Figures

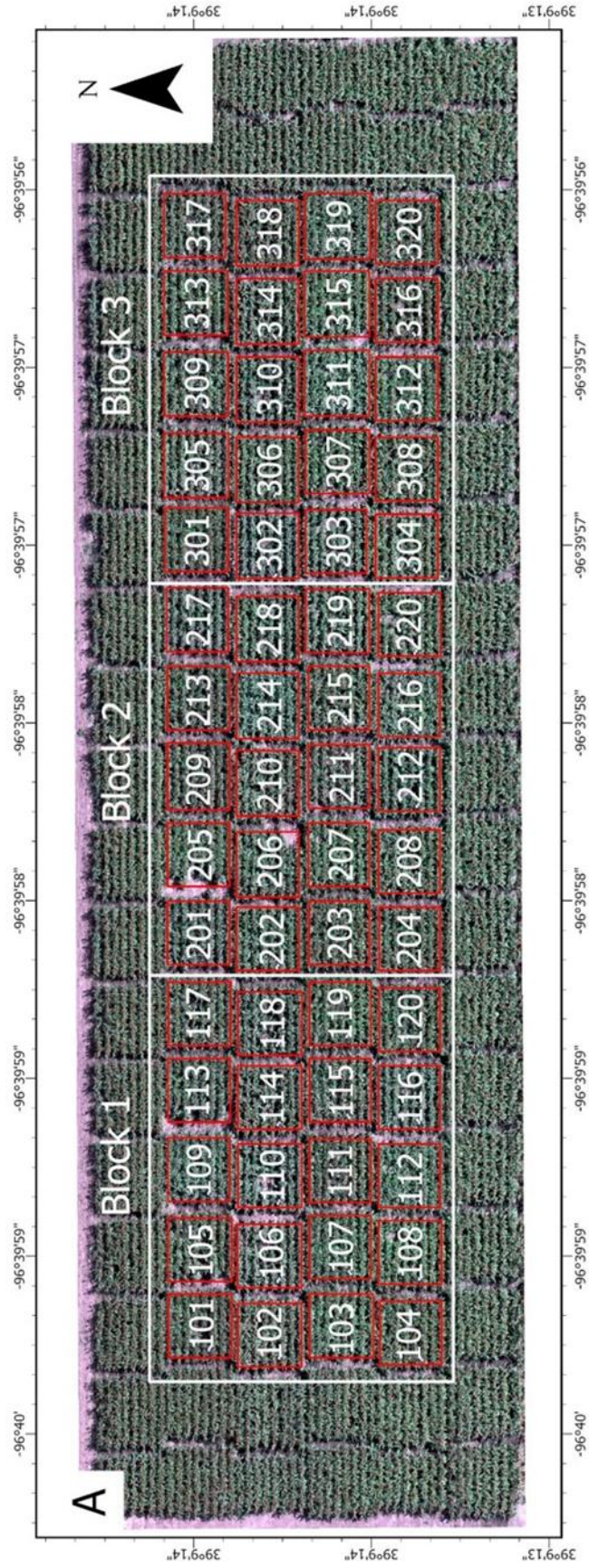


Figure 3.1 Overview of field study in Manhattan, Kansas. 20 sorghum genotype plots (indicated by the red boxes) were planted randomly within three blocks, indicated by the white squares.

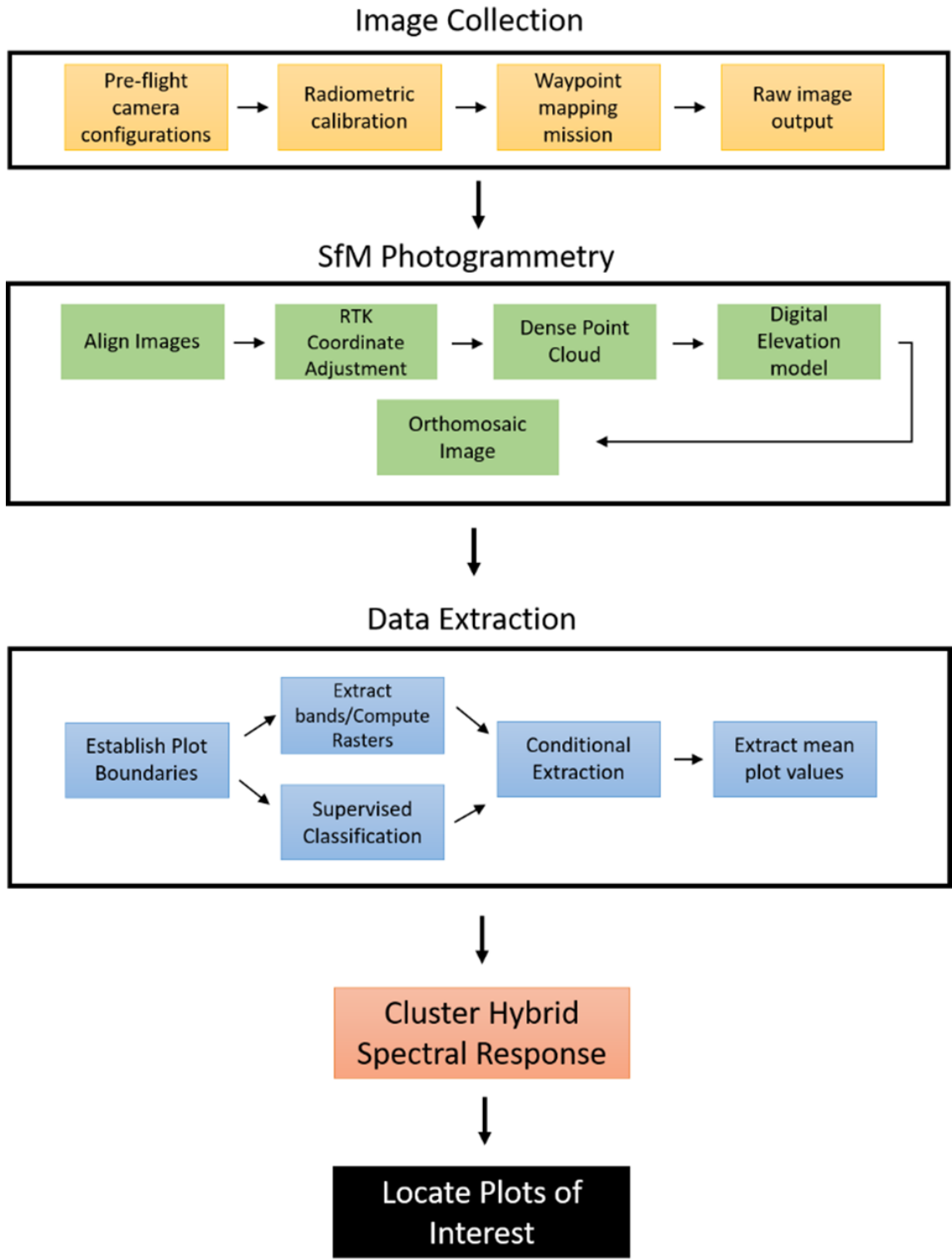


Figure 3.2 Workflow diagram of image collection, image processing, data extraction, and statistical analysis.

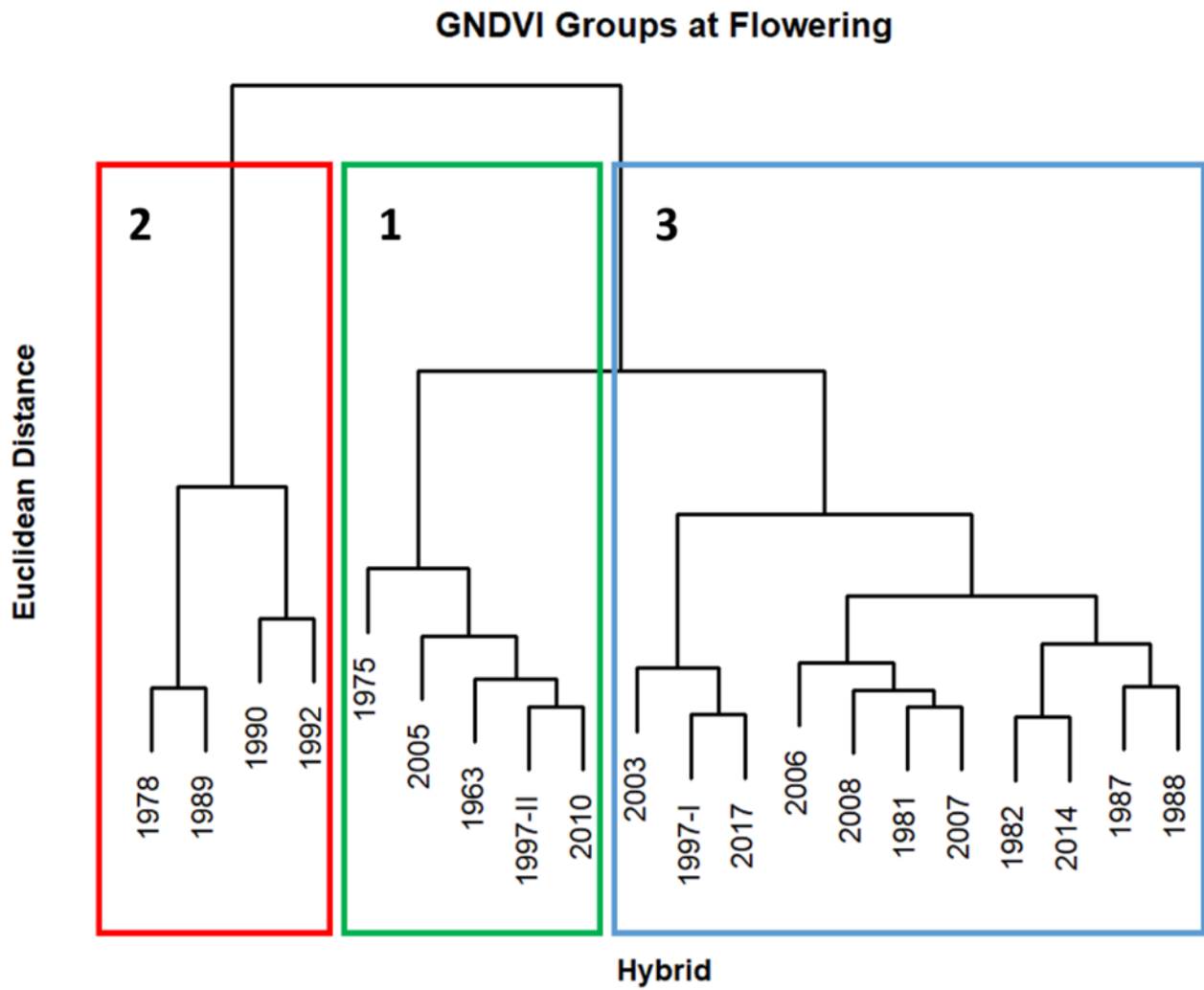


Figure 3.3 Dendrogram produced by hierarchical clustering the mean GNDVI data for each of the genotypes, resulting in the formation of three distinct cluster groups. Hybrids are denoted by year of release.

Tables

Table 3.1 Correlation and Regression Coefficients for spectral bands and sampled biomass traits, LAI, and grain yield.

Trait	Flowering																	
	Blue			Green			Red			Red Edge			NIR					
	r	r ²	RMSE	r	r ²	RMSE	r	r ²	RMSE	r	r ²	RMSE	r	r ²	RMSE	r	r ²	RMSE
Fresh Whole Plant Biomass	0.47	0.22 ***	0.01	0.07	0.00	0.01	0.26	0.07	0.01	0.01	0.01	-0.10	0.01	0.01	0.01	0.49	0.24 ***	0.02
Fresh Stem Biomass	0.42	0.18 **	0.01	-0.03	0.00	0.01	0.25	0.06	0.01	0.01	0.01	-0.19	0.03	0.01	0.01	0.36	0.13 **	0.02
Fresh Leaf Biomass	0.46	0.22 ***	0.01	0.13	0.02	0.01	0.26	0.07	0.01	0.01	0.01	-0.01	0.00	0.02	0.02	0.61	0.37 ***	0.02
LAI	0.38	0.14 **	0.01	0.08	0.01	0.01	0.25	0.06	0.01	0.01	0.01	-0.06	0.00	0.02	0.02	0.31	0.10 *	0.02
Dry Whole Plant Biomass	-0.04	0.00	0.01	0.10	0.01	0.01	-0.16	0.03	0.01	0.01	0.01	0.11	0.01	0.01	0.01	-0.03	0.00	0.02
Dry Leaf Biomass	0.14	0.02	0.01	0.31	0.09 *	0.01	-0.13	0.02	0.01	0.01	0.01	0.28	0.08 *	0.01	0.01	0.35	0.12 *	0.02
Dry Stem Biomass	0.02	0.00	0.02	0.12	0.02	0.02	-0.14	0.02	0.02	0.02	0.02	0.11	0.01	0.02	0.02	0.09	0.01	0.02
Yield	-0.04	0.00	0.01	-0.34	0.12 *	0.01	-0.18	0.03	0.01	0.01	0.01	-0.42	0.18 **	0.01	0.01	0.32	0.10 *	0.02

Trait	Soft Dough																	
	Blue			Green			Red			Red Edge			NIR					
	r	r ²	RMSE	r	r ²	RMSE	r	r ²	RMSE	r	r ²	RMSE	r	r ²	RMSE	r	r ²	RMSE
Fresh Whole Plant Biomass	0.43	0.17 ***	0.01	0.25	0.06	0.01	0.33	0.11 *	0.00	0.01	0.03	0.00	0.00	0.01	0.01	0.45	0.20 ***	0.01
Fresh Stem Biomass	0.38	0.15 **	0.01	0.16	0.03	0.01	0.28	0.09 *	0.00	0.01	-0.07	0.00	0.00	0.01	0.01	0.40	0.16 **	0.01
Fresh Leaf Biomass	0.47	0.22 ***	0.01	0.43	0.19 ***	0.01	0.39	0.15 ***	0.00	0.00	0.25	0.07	0.01	0.01	0.01	0.51	0.26 ***	0.01
LAI	0.05	0.00	0.01	-0.08	0.01	0.01	0.12	0.01	0.01	0.01	-0.13	0.01	0.01	0.01	0.01	0.09	0.01	0.01
Dry Whole Plant Biomass	0.32	0.10 *	0.01	0.29	0.08 *	0.01	0.17	0.03	0.01	0.01	0.10	0.01	0.01	0.01	0.01	0.31	0.09 *	0.01
Dry Leaf Biomass	0.52	0.27 ***	0.01	0.34	0.12 *	0.01	0.49	0.24 ***	0.00	0.00	0.16	0.03	0.01	0.01	0.01	0.46	0.21 ***	0.01
Dry Stem Biomass	0.25	0.06	0.01	-0.02	0.00	0.01	0.24	0.06	0.00	0.00	-0.20	0.04	0.01	0.01	0.01	0.39	0.15 **	0.01
Yield	-0.13	0.02	0.01	-0.26	0.07	0.01	-0.18	0.03	0.01	0.01	-0.36	0.13 **	0.01	0.01	0.01	0.35	0.12 **	0.01

Trait	Physiological maturity																	
	Blue			Green			Red			Red Edge			NIR					
	r	r ²	RMSE	r	r ²	RMSE	r	r ²	RMSE	r	r ²	RMSE	r	r ²	RMSE	r	r ²	RMSE
Fresh Whole Plant Biomass	0.07	0.00	0.01	0.06	0.00	0.01	-0.12	0.01	0.01	0.01	0.01	0.00	0.00	0.02	0.02	0.43	0.18 ***	0.02
Fresh Stem Biomass	0.08	0.01	0.01	0.04	0.00	0.01	-0.10	0.01	0.01	0.01	-0.02	0.00	0.00	0.02	0.02	0.37	0.14 **	0.02
Fresh Leaf Biomass	0.00	0.00	0.01	0.12	0.02	0.01	-0.14	0.02	0.01	0.01	0.10	0.01	0.01	0.02	0.02	0.51	0.26 ***	0.01
LAI	-0.03	0.00	0.01	-0.20	0.04	0.01	-0.08	0.01	0.01	0.01	-0.27	0.07	0.01	0.01	0.01	0.26	0.07	0.02
Dry Whole Plant Biomass	0.02	0.00	0.01	0.06	0.00	0.01	-0.17	0.03	0.01	0.01	0.06	0.00	0.00	0.02	0.02	0.30	0.09 *	0.02
Dry Leaf Biomass	0.06	0.00	0.01	0.17	0.03	0.01	-0.08	0.01	0.01	0.01	0.14	0.02	0.02	0.02	0.02	0.42	0.18 **	0.02
Dry Stem Biomass	-0.13	0.02	0.01	-0.07	0.00	0.01	-0.28	0.08 *	0.01	0.01	-0.01	0.00	0.00	0.02	0.02	0.31	0.10 *	0.02
Yield	-0.15	0.02	0.01	-0.37	0.14 **	0.01	-0.26	0.07	0.01	0.01	-0.42	0.17 **	0.01	0.01	0.01	0.21	0.04	0.02

*, **, ***, significant at $p < 0.05, 0.01, 0.001$. RMSE, root mean square error.

Table 3.2 Vegetation indices computed for biomass, LAI, and yield comparison.

Vegetation Index	Formula	Reference
BNDVI	$\frac{\rho_{\text{NIR}} - \rho_{\text{B}}}{\rho_{\text{NIR}} + \rho_{\text{B}}}$	[57]
GNDVI	$\frac{\rho_{\text{NIR}} - \rho_{\text{G}}}{\rho_{\text{NIR}} + \rho_{\text{G}}}$	[37, 58]
NDVI	$\frac{\rho_{\text{NIR}} - \rho_{\text{R}}}{\rho_{\text{NIR}} + \rho_{\text{R}}}$	[59]
SR	$\frac{\rho_{\text{NIR}}}{\rho_{\text{R}}}$	[60]
EVI	$2.5 \times \frac{\rho_{\text{NIR}} - \rho_{\text{R}}}{\rho_{\text{NIR}} + 6 \times \rho_{\text{R}} - 7.5 \times \rho_{\text{B}} + 1}$	[37, 61]

Acronyms: BNDVI, blue normalized difference vegetation index; GNDVI, green normalized difference vegetation index; NDVI, normalized difference vegetation index; SR, simple ratio, EVI, enhanced vegetation index. ρ denotes spectral reflectance

Table 3.3 Correlation and regression coefficients for VIs and ground sampled biomass traits, LAI, and grain yield.

Trait	Flowering														
	BNDVI			GNDVI			NDVI			SR			EVI		
	r	r ²	RMSE	r	r ²	RMSE	r	r ²	RMSE	r	r ²	RMSE	r	r ²	RMSE
Whole Plant Fresh Biomass	0.00	0.00	0.01	0.39	0.15 **	0.01	0.21	0.04	0.01	0.30	0.09 *	0.52	0.45	0.21 ***	0.04
Stem Fresh Biomass	-0.05	0.00	0.01	0.39	0.16 **	0.01	0.13	0.02	0.01	0.22	0.05	0.54	0.34	0.12 **	0.04
Leaf Fresh Biomass	0.07	0.01	0.01	0.39	0.15 **	0.01	0.24	0.06	0.01	0.33	0.11 *	0.53	0.50	0.25 ***	0.04
LAI	-0.07	0.00	0.01	0.24	0.06	0.02	0.09	0.01	0.01	0.20	0.04	0.54	0.27	0.07	0.04
Leaf Dry Biomass	0.14	0.02	0.01	-0.02	0.00	0.02	0.35	0.12 *	0.01	0.26	0.07	0.52	0.50	0.25 ***	0.04
Whole Plant Dry Biomass	0.02	0.00	0.01	-0.12	0.01	0.02	0.12	0.01	0.01	0.03	0.00	0.55	0.15	0.02	0.04
Stem Dry Biomass	0.05	0.00	0.01	-0.05	0.00	0.02	0.18	0.03	0.01	0.10	0.01	0.57	0.23	0.05	0.05
Yield	0.38	0.14 **	0.01	0.56	0.31 ***	0.01	0.41	0.17 **	0.01	0.48	0.23 ***	0.48	0.34	0.11 *	0.04

Trait	Soft Dough														
	BNDVI			GNDVI			NDVI			SR			EVI		
	r	r ²	RMSE	r	r ²	RMSE	r	r ²	RMSE	r	r ²	RMSE	r	r ²	RMSE
Whole Plant Fresh Biomass	-0.29	0.08 *	0.01	-0.08	0.01	0.01	-0.17	0.03	0.01	0.30	0.09 *	0.57	0.28	0.08 *	0.02
Stem Fresh Biomass	-0.25	0.07	0.01	0.00	0.00	0.01	-0.13	0.02	0.01	0.35	0.13 **	0.56	0.28	0.08 *	0.02
Leaf Fresh Biomass	-0.34	0.11 *	0.01	-0.27	0.08 *	0.01	-0.24	0.06	0.01	0.12	0.02	0.59	0.22	0.05	0.02
LAI	0.02	0.00	0.01	0.16	0.03	0.01	-0.06	0.00	0.01	0.15	0.02	0.60	-0.01	0.00	0.02
Leaf Dry Biomass	-0.41	0.16 **	0.01	-0.19	0.04	0.01	-0.36	0.13 *	0.01	0.07	0.01	0.59	0.03	0.00	0.03
Whole Plant Dry Biomass	-0.25	0.07	0.01	-0.20	0.04	0.01	-0.08	0.01	0.01	0.15	0.02	0.59	0.32	0.10 *	0.02
Stem Dry Biomass	-0.11	0.01	0.01	0.18	0.03	0.01	-0.08	0.01	0.01	0.35	0.13 *	0.57	0.23	0.05	0.02
Yield	0.25	0.06	0.01	0.39	0.15 **	0.01	0.30	0.09 *	0.01	0.56	0.32 ***	0.48	0.15	0.02	0.02

Trait	Maturity														
	BNDVI			GNDVI			NDVI			SR			EVI		
	r	r ²	RMSE	r	r ²	RMSE	r	r ²	RMSE	r	r ²	RMSE	r	r ²	RMSE
Whole Plant Fresh Biomass	0.09	0.01	0.01	0.09	0.01	0.02	0.26	0.07 *	0.01	0.32	0.10 *	0.43	0.41	0.17 *	0.03
Stem Fresh Biomass	0.02	0.00	0.01	0.08	0.01	0.02	0.21	0.04	0.01	0.29	0.09 *	0.44	0.37	0.14 *	0.03
Leaf Fresh Biomass	0.26	0.07	0.01	0.13	0.02	0.02	0.36	0.13 **	0.01	0.34	0.11 *	0.43	0.42	0.18 *	0.03
LAI	0.15	0.03	0.01	0.33	0.11 *	0.02	0.20	0.04	0.01	0.21	0.05	0.45	0.21	0.04	0.03
Leaf Dry Biomass	0.17	0.03	0.01	0.05	0.00	0.02	0.30	0.09 *	0.01	0.30	0.09 *	0.43	0.39	0.15 ***	0.03
Whole Plant Dry Biomass	0.06	0.00	0.01	0.00	0.00	0.02	0.23	0.05	0.01	0.31	0.09 *	0.43	0.35	0.12 **	0.03
Stem Dry Biomass	0.15	0.02	0.01	0.10	0.01	0.02	0.27	0.07	0.01	0.33	0.11 *	0.44	0.31	0.10 *	0.03
Yield	0.18	0.03	0.01	0.44	0.20 ***	0.02	0.26	0.07	0.01	0.30	0.09 *	0.44	0.24	0.06	0.03

*, **, ***, significant at p < 0.05, 0.01, 0.001, respectively. RMSE, root mean square error.

Table 3.4 Results of ANOVA and Tukey HSD test for significant differences in biomass traits, LAI, and grain yield in clusters defined by hybrid NIR spectral responses.

Trait	Cluster	Flowering Mean ^{1,2}	Flowering SEM ³	Soft Dough Mean	Soft Dough SEM	Maturity Mean	Maturity SEM
Total Fresh Biomass	1	4326 ^a	154	4811 ^a	140	4874 ^a	169
	2	4184 ^a	160	4913 ^a	291	4687 ^{ab}	184
	3	3775 ^a	126	4304 ^a	247	3987 ^b	130
Fresh Leaf Biomass	1	1195 ^a	44	1428 ^{ab}	45	1224 ^a	46
	2	1097 ^{ab}	45	1565 ^a	92	1151 ^a	49
	3	997 ^b	48	1231 ^b	60	932 ^b	34
Fresh Stem Biomass	1	2665 ^a	101	3381 ^a	102	3703 ^a	148
	2	2653 ^a	106	3348 ^a	219	3536 ^{ab}	139
	3	2476 ^a	109	3073 ^a	192	3054 ^b	124
Total Dry Biomass	1	N/A	N/A	1863 ^a	65	2941 ^a	124
	2	N/A	N/A	1797 ^a	154	2878 ^a	126
	3	N/A	N/A	1612 ^a	111	2627 ^a	112
Dry Leaf Biomass	1	345 ^a	14	397 ^{ab}	11	353 ^a	12
	2	306 ^{ab}	18	347 ^a	37	333 ^{ab}	15
	3	272 ^b	15	318 ^b	13	291 ^b	17
Dry Stem Biomass	1	N/A	N/A	763 ^a	53	912 ^a	51
	2	N/A	N/A	840 ^a	153	870 ^a	37
	3	N/A	N/A	687 ^a	57	761 ^a	38
LAI	1	4.8 ^a	0.38	N/A	N/A	N/A	N/A
	2	4.0 ^a	0.37	N/A	N/A	N/A	N/A
	3	3.7 ^a	0.29	N/A	N/A	N/A	N/A

¹ Units for biomass, LAI, and yield adjusted for g m²⁻¹, leaf area m²⁻¹, and kg ha⁻¹, respectively

² Letters denote Tukey HSD mean separation at p < 0.05 significance level

³ Standard error of the mean

Table 3.5 RGB VIs computed for comparison with ground-measured senescence scores.

Vegetation Index	Formula	Reference
ExG	$2\rho_G - \rho_R - \rho_B$	[63-65]
NDI	$\frac{\rho_G - \rho_R}{\rho_G + \rho_R}$	[63, 65]
ExGR	$3\rho_G - 2.4\rho_R - \rho_B$	[63]
VARI	$\frac{\rho_G - \rho_R}{\rho_G + \rho_R - \rho_B}$	[66-67]
GLI	$\frac{2\rho_G - \rho_R - \rho_B}{2\rho_G + \rho_R + \rho_B}$	[63]

ExG, excess green; NDI, normalized difference index; ExGR, excess green red; VARI, visible atmospherically resistant index; GLI, green leaf index. ρ denotes spectral reflectance.

Table 3.6 Correlation and regression coefficients for RGB VIs and senescence scores.

Growth Stage	ExG			NDI			ExGR			VARI			GLI		
	r	r ²	RMSE												
SD	0.31	0.10 *	0.02	0.33	0.11 *	0.02	0.34	0.11 **	0.03	0.35	0.12 **	0.03	0.23	0.05	0.02
HD	0.22	0.05	0.02	0.26	0.07 *	0.03	0.24	0.06	0.03	0.29	0.09 *	0.04	0.21	0.04	0.02
M	0.28	0.08 *	0.03	0.57	0.33 ***	0.03	0.35	0.12 **	0.04	0.60	0.36 ***	0.05	0.48	0.23 ***	0.03

ExG, excess green; NDI, normalized difference index; ExGR, excess green red; VARI, visible atmospherically resistant index; GLI, green leaf index; SD, soft dough; HD, hard dough; M, maturity

*, **, ***, significant at $p < 0.05, 0.01, 0.001$, respectively

Chapter 4 - Conclusions and Further Direction

Conclusions

The rising global population presents farmers and crop breeders with unprecedented challenges of increasing crop yields. With a growing human population comes the need for increased food, fiber, fuel, and forage production to sustain life as we know it. As a changing climate is forecasted to produce unfavorable growing conditions for traditional crops, it is thought that grain sorghum will become even more vital to food security around the world. Therefore, breeding cultivars of stress-resistant sorghum is crucial to increasing the world food supply in the future.

To accomplish this feat, new technologies must be utilized for the rapid screening and selection of sorghum cultivars, depending on the trait of interest. In a breeding operation with thousands of plots, manual evaluation of these plots can be very time consuming and can delay the entire process. However, with unmanned aerial systems (UAS) and high-resolution multispectral imaging, new opportunities arise for more efficient evaluation, screening, and pinpointing genotypes containing traits of interest. In as little as 20-30 minutes, potentially thousands of plots can be mapped with a single aircraft, as opposed to evaluating each plot manually. In addition, if methodologies are established that are user-friendly and easy to comprehend, sorghum breeders beginning to use multispectral imaging will be greatly assisted in this transition. In this study, methodologies were optimized specifically for breeders looking for herbicide tolerant traits and stay green (SG) traits, and the results indicate potential use of high-resolution UAS imagery greatly aiding in the sorghum cultivar selection process.

Chapter one is a literature review of information related to sorghum herbicide tolerance breeding, SG breeding, and remote sensing being used for cultivar selection in these areas.

Through a thorough examination of the literature on these topics, it was found that UAS remote sensing showed potential to aid in trait-selection for various breeding operations. Although there were some studies that had been conducted for herbicide tolerance and SG analysis in grain sorghum, it was also found that there is still scope for improvement. This Chapter essentially focused specifically at the development of methodologies for sorghum breeders to extract data from UAS imagery, and to validate these newly-developed methodologies with small-scale sorghum experiments.

Chapter two was an investigation of the relation of vegetative indices (VIs) with ground-measured mesotrione visual injury scores. Critical to this experiment was the development of a methodology in which sorghum breeders can extract data for identification of traits of interest. Within this methodology, a comparison was made between supervised classification algorithms to determine significant differences between them in terms of overall accuracies. Because vegetation extraction is crucial for breeders to determining spectral differences between cultivars, determining a proper vegetation extraction method is important for future use. Results demonstrated no significant differences between the overall accuracy scores of support vector machine (SVM) and maximum likelihood (ML), but the random forest (RF) classifier was significantly less accurate than both algorithms. In addition, the SVM algorithm was the most consistent across all measurement days, indicating that it was the most robust algorithm within the course of this study. The SVM was therefore chosen to extract the data for comparison with ground-measured herbicide injury. With two genotypes and one hybrid being sprayed with 4 different rates of mesotrione, it was discovered that there was a strong correlation between VI data and injury ratings. The strongest correlations were seen within the first 15 days after treatment (DAT); these results are not surprising given that herbicide injury was more visible to

the camera during these dates than the following dates. Out of four VIs tested, the normalized difference vegetation index (NDVI) was observed to have the highest correlation to injury scores. Based on a two-way analysis of variance (ANOVA) testing the effects of genotype and rate on NDVI scores, we were able to detect significant differences between genotypes and rates when looking at the main effects models. We therefore, concluded that assisted by machine learning image classification techniques, high resolution UAS imagery shows potential to assist sorghum breeders with selecting for herbicide-tolerance to provide more post-emergence weed control for sorghum growers.

Chapter three focused specifically on creating a methodology for sorghum breeders to investigate post-flowering drought tolerance (in the form of the SG trait). As the SG trait can help sorghum growers continue to produce grain for human consumption, forage for animal consumption, and above-ground biomass for biofuel production in precipitation-limited environments, it is a highly sought-after trait in sorghum breeding operations worldwide. If sorghum cultivars are able to be rapidly screened and selected, it may be possible to introduce improved sorghum hybrids for dry-land sorghum farmers, providing a means of food and income security for millions worldwide. In this study, the methodology created for data extraction was tested with 20 sorghum hybrids, with an emphasis on characterizing senescence patterns, plant biomass, and final grain yield of 20 different sorghum hybrids. Biomass samples were taken at the flowering (F), soft dough (SD), and physiological maturity (M) growth stages, and senescence ratings were taken at F, SD, hard dough (HD), and M stages. The NIR band was seen as the most related to sorghum biomass characteristics, and hierarchical clustering was used to form three distinct cluster groups. An ANOVA was conducted to determine ground-truth differences between these groups, and depending on the trait and stage, certain differences were

able to be detected. For final grain yield, the green normalized difference vegetation index (GNDVI) was seen to be the most significant vegetative index at F, and a subsequent cluster analysis revealed three groups that showed no statistical differences in grain yield among hybrids. As there was a very high level of NIR saturation on the plants designated for senescence measurements, VIs from the visible electromagnetic spectrum were constructed, with the visible atmospherically resistant index (VARI) being the most highly related to ground-measured senescence scores. As previously, the data was clustered into three groups, and no statistical differences were discovered between cluster groups in regards to senescence scores. For this particular study, the hybrids were not selected specifically due to differences in biomass, senescence, or yield, so these results do not invalidate the methodology. In conclusion, the methodology that was developed as a result of this study shows potential to assist sorghum breeders in locating and selecting for traits related to SG in sorghum in large-scale breeding trials.

Further Direction

Future studies involving this technology for cultivar selection should focus on broadening the scope of investigation in various geographic regions. Currently, each study has been completed over one growing season in one specific region; in order to explore the robustness of these methodologies, more extensive analyses must be conducted. These suggestions for further research are elaborated on in the following paragraphs.

For the herbicide tolerance experiment, more modes of action must be explored in multiple geographic regions. It was easy to see a response from mesotrione application, as the end result of application was a reduction of chlorophyll due to lipid peroxidation. However, for

other modes of action such as auxinic herbicides, photosystem-II inhibitors, etc., the resulting injury to susceptible plants may not result in drastic spectral changes and thus may not be as visible to multispectral cameras. However, if it is found that UAS imaging is able to detect significant differences among tolerant and susceptible cultivars, UAS could be even more useful in grain sorghum herbicide tolerance breeding operations than originally presumed. It is important to note that in these future studies, it is important to ensure that spectral fluctuations are due to differing levels of herbicide injury and not external factors such as water stress, weed pressure, insect pressure, etc. Such factors would complicate data analysis, and would make it difficult to separate levels of herbicide injury in the analysis.

In addition, image classification can be further explored for vegetation separation in herbicide-tolerance studies. As this study focused on supervised classification because of the control it allows users to exercise over the classification, there are many other means of image classification that have been accepted for vegetation discrimination. Future studies should compare the aforementioned supervised pixel-based algorithms with unsupervised pixel classification, object based classification (supervised and unsupervised), and binary image thresholding. These algorithms have yet to be compared to one another for herbicide tolerance studies, so such an evaluation is warranted to determine the most accurate method of vegetation extraction for this purpose.

For the SG study, future studies should use the developed methodology to examine if spectral differences can be detected amongst hybrids with known differences in senescence rates, above-ground biomass, and grain yield. As previously mentioned, the hybrids in this study were not chosen for significant differences among the studied traits, and although there were some significant differences among biomass at varying stages, there were no significant differences

among grain yield and senescence scores (at M). In a breeding trial with thousands of plots, it is very likely that significant differences would exist for these different traits, so such a procedure would help to validate this methodology. To add, it would be beneficial to increase the number of geographic locations in such a study, which would help to determine the methodology's robustness in detecting significant differences in different locations.

It would also benefit if future SG studies can investigate cameras with differing resolutions, as well as including a calibration technique that will not saturate out the NIR band. The calibration panel that we used was very highly reflective, which led to problems with NIR saturation in bright sunlight. Future radiometric calibration procedures should be made with a darker panel, which is hypothesized to reduce saturation in the invisible electromagnetic spectrum. In addition, if higher resolution images are obtained whether by differing sensor or flight altitude, the optimum equipment/flight parameters could be determined for future use by sorghum breeders in pursuit of the SG trait.